THE CONSISTENCY OF DIFFERENTIAL AND INTEGRAL THERMONUCLEAR NEUTRONICS DATA

A DISSERTATION

Presented to

The Faculty of the Division of Graduate Studies

By

William Albert Reupke

In Partial Fulfillment

of the Requirements for the Degree

Doctor of Philosophy

in the School of Nuclear Engineering

Georgia Institute of Technology

December, 1977

THE CONSISTENCY OF DIFFERENTIAL AND INTEGRAL THERMONUCLEAR NEUTRONICS DATA

Approved:

J. Karl Davidson, Chairman

Douglas W. Muir

Joseph D. Clement

M. Jonathan Haire

John W. Poston

Date approved by Chairman Nov. 17, 1977

TABLE OF CONTENTS

ACKNOWLEDGMENTS

Among the community of people throughout the world who recognize the research enterprise, I wish to thank the citizens of the State of Georgia for making possible the preparatory phases of this research and the citizens of the United States of America for their support, particularly during the latter stages of this work. My friends in the Federal Republic of Germany, who - during turbulent times in the States - spurred on my interest in resuming the formal quest for knowledge, must be thanked tenfold.

Amongst those who maintain the pathways of research, the Division of Graduate Studies and the School of Nuclear Engineering at the Georgia Institute of Technology, and the Los Alamos Scientific Laboratory, operated for the U.S. Department of Energy by the University of California, have provided essential support, with coordination provided by the Associated Western Universities. Here I wish to acknowledge the central role of my adviser at Georgia Tech, J. Narl Davidson. In addition, I must acknowledge the equally crucial, invisible network maintained by my fellow students and by others who have so ably served on short notice.

Finally, I wish to thank the handful who accompanied me to the threshold: the members of the Applied Nuclear Data Group at Los Alamos, who provided a congenial atmosphere for research; my adviser at Los Alamos, Douglas W. Muir, for his constant advice and counsel; my late mother, Mrs. Albert Reupke, for her infinite patience; and finally, my wife Karen, for her constant support and assistance with the typing.

LIST OF TABLES

LIST OF ILLUSTRATIONS

CHAPTER I

INTRODUCTION

To increase the accuracy of the neutronics analysis of nuclear reactors, physicists and engineers have employed a variety of techniques, including the adjustment of multigroup differential data to improve consistency with integral data. Of the various adjustment strategies, a generalized least-squares procedure which adjusts the combined differential and integral data can significantly improve the accuracy of neutronics calculations compared to calculations employing only differential data. This investigation analyzes 14 MeV neutron-driven integral experiments, using a more extensively developed methodology and a newly developed computer code, to extend the domain of adjustment from the energy range of fission reactors to the energy range of fusion reactors.

Neutronics Analysis of Fusion Reactor Blankets and Shields

A classical test of engineering design analysis is the agreement of calculation and experiment within prescribed limits of error. The present state-of-the-art in calculation methods and integral experiments, as applied to fusion reactor neutronics design, is reviewed here. In a subsequent section of this chapter the principles of consistency analysis and data adjustment are introduced.

State-of-the-Art in Calculation Methods

Cornerstones of neutronics calculations are evaluated nuclear data and methods of solving the neutron transport equation, together with the sensitivity calculation technique of relating changes in nuclear data to changes in the results of neutron transport calculations. This subsection reviews the state of the present art in these basic components of neutronics calculation.

Status of Evaluated Nuclear Data. In the earliest controlled fusion reactor designs investigators at Princeton performed their own evaluations even on the most basic nuclear data.[1] In subsequent years, nuclear data initially evaluated for weapons applications became more widely disseminated and was combined with evaluations undertaken for fission reactor applications to permit controlled fusion reactor calculations on a somewhat firmer data base. The emergence of organized nuclear data evaluation for controlled fusion reactors may be traced to the 1970 International Atomic Energy Agency Helsinki conference on nuclear data, where both British and Soviet reviewers noted continuing serious deficiencies.[2] For example, it was noted by V. S. Crocker et al that the important ^{7}Li(n,xt) reaction remained 25% uncertain throughout the range of interest. In some energy regions, namely 8-13 MeV, no measurements were available. At the most recent critical review of evaluated nuclear data needs for the near-term requirements of the United States' fusion reactor program,[3] the Neutronics Working Group concluded that new

experimental data and more accurate representations of secondary neutron spectra for ^{7}Li should be incorporated in the ENDF/B-V evaluation. A number of other improvements were suggested, including the organized evaluation of cross section uncertainties.

This introduction emphasizes that the utility of the existing data is limited in most cases by the continuing absence of quantitative uncertainty estimates. Sensitivity theory has, in large measure, provided new incentive for organized cross section error evaluation. However, in most cases, and in the present work, the designer must still provide his own evaluation, just as in former years the designer was faced with evaluation of the cross sections proper. This remark applies particularly to secondary energy and angular distribution uncertainties. Since the wealth of possible cross section data far exceeds the data of immediate interest, the evaluation of uncertainties must be guided by the larger context of engineering significance. Since this same context also guides the selection and design of integral experiments, one may expect an appropriate base of evaluated cross section uncertainty data will evolve in parallel with the requirements of consistency analysis.

Status of Neutron Transport Calculation Methods. Reactor physicists and engineers have applied the neutron transport equation to 1)

fusion reactor scoping studies, 2) analysis of particular design features, such as shield ducts, and 3) the analysis of integral experiments. To date, the bulk of the calculations have been applied in the first two areas and the experimental confirmation of fusion reactor neutronics design methodology remains at an embryonic stage.

From the earliest design sketches to modern scoping studies, the uncertainty in calculational results due to error in the solution of the transport equation often has been small compared to the effects of uncertainty in the nuclear data, particularly in certain ideal cases where the problem geometry is chosen to satisfy analytical requirements. For realistic engineering configurations, where multidimensional discrete ordinates and Monte Carlo computations become necessary,[4,5] practical limitations in computing machinery and the increasing chance of human error make solution of the transport equation more uncertain. Thus, experimental verification becomes a necessity. Even for clean experimental geometries it is not obvious that in a given case the transport solution errors will be small compared to the effects of cross section errors.[6] To quantitatively resolve this question it is necessary to utilize cross section sensitivity methods.

Status of Cross Section Sensitivity Analysis. Perturbation methods for calculating the change in an integral transport result due to group cross section change are a comparatively recent development in the evolution of fusion reactor design analysis. First applied in

one-dimensional, discrete-ordinates, multigroup form,[7] Bartine et al extended the method to two dimensions.[8] The method is applied presently to fusion reactor neutronics in one dimension only. Sensitivity calculations have also been attempted in a Monte Carlo setting.[9] In the sensitivity profile, the sensitivity is calculated for fixed secondary neutron energy and angular distributions but the method is more general.[10] Such sensitivity profiles imply which of the cross sections in a given nuclear design are most important and, therefore, which cross sections should be known most accurately.

When the sensitivity data are multiplied by statistical estimates of the cross section uncertainties in an appropriate way, the product gives the uncertainty in the integral transport quantity which is due to the cross section uncertainty. This result is useful in two ways. First, the designer may determine whether the uncertainty in calculated results lies within allowable design margins. Gerstl et al have recently used the technique for the TFTR controlled fusion device.[11] Second, sensitivities help to determine whether differences between calculation and experiment are statistically consistent with the estimated cross section uncertainties. Thus, the techniques of sensitivity analysis have set the stage for statistical consistency analysis.

State-of-the-Art in Integral Experiments

Early 14 MeV neutron-driven integral experiments afforded rough confirmation of the relatively crude nuclear data and calculational

tools then in use. In recent years an increasing number and variety of such experiments have been performed and modern calculation-experiment comparisons have been undertaken. Thus in the 1950's, -60's, and -70's the number of new 14 MeV neutron-driven integral experiments has increased as roughly one, two, and eight, respectively.[12,13] As the number of available experiments increases certain advantages accrue: the calculational base is tested over a wider range of conditions, learning processes lead to experiments of improved quality as well as improved quantity, and greater opportunity for realistic error evaluation is provided by the consideration of discrepancies amongst the results of similar experiments. While such proliferation of experiments generally accompanies advancement in the state-of-the-art, calculational understanding is not keeping pace with experimental results. This work attempts, in part, to place a sharper focus on the analysis of existing experiments to extract the maximum information content and to improve the usefulness of future experiments by exposing weaknesses in present experiment design.

Systematic efforts to evaluate cross sections and cross section uncertainties have not been accompanied by parallel developments in the realm of integral experiments. In principle, one may imagine several measurements - by various investigators - of a given integral quantity. The comparison of such results would lead to an integral experiment evaluation, including realistic estimates of the uncertainties in the

evaluated integral results. That this development has not occurred is not a reflection of greater confidence placed in the results of single integral experiments and their published uncertainties but of a less systematic utilization of integral data than cross section data. If and when integral data are used systematically in nuclear design, then more critical evaluation of integral experiments and their uncertainties will ensue. For the present, it is again the nuclear designer who must perform his own evaluation of integral experiments and their uncertainties. This evaluation technique is developed in the present work as an important component of consistency analysis.

In addition to the role of the clean integral experiments just discussed, the strategy of current fusion reactor neutronics design calls for generic-design experiments and, ultimately, mockup experiments. The latter more closely simulate the full complexity of a reactor shield. Although the present work uses clean experiments, the history of fast fission reactor integral experiments suggests also the utility of at least the generic-design experiment in formulating optimal cross sections for design purposes.[14] Thus, the techniques developed here may, with additional effort, be extended to the emerging generic-design experiments for fusion reactors.

Quantitative Consistency Analysis in Nuclear Design

Introduced here is qualitative consistency analysis as it is presently practiced in the United States nuclear design community. The

present practice is contrasted with quantitative consistency analysis used elsewhere in the world. Current efforts to infuse United States consistency analysis with quantitative technique are reviewed.

Status of Consistency Analysis in the United States Nuclear Design Community

As practiced in the United States today the consistency of calculated and experimental integral quantities is approached in a qualitative way. The interpretation of discrepancies may consist of numerical experiments designed to expose the part of the discrepancy which may be attributed to calculation error. When calculation error is reduced to low levels by use of more precise numerical methods the residue of discrepancy — assumed to be due to nuclear data error — is examined by trial and error. The qualitative procedures that are used consist of recalculating the experiment with an alternative data set. This set may consist of data evaluated by an alternative evaluating body or of data evaluated with an alternative base of experimental data, as in the comparison of calculations from nationally evaluated cross sections and locally evaluated cross sections. Thus, the ENDF/B data base may be compared with the Lawrence Livermore Laboratory data set ENDL. In any case, the techniques developed overseas for adjusting the data set systematically and deterministically for purposes of nuclear design have not been exploited in this country.

Criticism in this country has greeted trial and error methods in the application of integral results to cross section evaluation.

S. Pearlstein describes the trial and error approach:

> The third version of ENDF/B appeared in February 1972. Within the experimental errors of the best microscopic cross section measurements, data were chosen that gave results consistent with carefully performed and documented integral experiments.[15]

And R. A. Karam responds:

> The work of the Cross-Section Evaluation Working Group (CSEWG) on cross-section data files is well-known and commendable. Of late, however, their practice to adjust cross sections (ENDF/B-II→III) to make the discrepancy between calculated and measured integral reactor parameters less embarrassing, is neither scientific nor warranted. The difficulty with this approach is that it assumes *a priori* that the methods of calculating integral parameters are valid. There is no basis for this assumption and the recommendation of our European colleagues [author refers to comments of J. Rowlands] to abandon the practice of cross-section fudging is highly endorsed here. Integral measurements do provide important checks and occasionally may point out the need for remeasuring and/or rechecking the accuracy of cross-section data. At this time, such measurements should have no consideration in the makeup of evaluated data files.[16]

Indeed, United States interest in the use of integral experiments for cross section evaluation has been tentative, at best. This result owes, in large measure, to the uneven performance of data sets adjusted by trial and error methods.

The Role of Quantitative Consistency Analysis

Quantitative, statistical techniques in calculation-experiment comparison were initially explored by A. V. Campise in the United States,[17,18] in 1961. The first least-squares formulations were advanced at the 1964 Geneva conference by C. Cecchini, V. Farinelli,

A. Gandini, and M. Salvatores of Italy,[19] and by M. Humi, J. Wagschal, and T. Yeivin of Israel.[20] In subsequent years numerous overseas investigators developed the techniques further. These techniques use least-squares algorithms, wherein changes in integral values are related to changes in cross section values by sensitivity theory. The least squares technique defines a set of new, or adjusted, cross sections and integral data which maximize consistency in a well-defined statistical sense. Although the initial conditions or input data are subject to judgment and evaluation as in the use of most other algorithms, the input data are at least explicitly stated. Unlike the trial and error results criticized above, least squares results are reproducible.

In spite of the relatively mature development of statistical consistency analysis outside of the United States, a spectrum of opinion remains. A skeptic argues:

> One of the best weapons, to promote the development, in the hands of the nuclear or reactor physicist is the disagreement between calculated and measured data. By adjusting data, sometimes arbitrarily, there is the danger of blunting this important weapon by the doubtful aesthetic satisfaction of a better agreement too quickly obtained sometimes by, to put it bluntly, juggling data.[21]

This criticism, aimed directly at trial-and-error adjustment but also obliquely at the more sophisticated methods, seems, when carried to its logical conclusion, to reject the statistical approach entirely. All discrepancies are analyzed in terms of systematic, as opposed to random, sources of error.

A more restrained criticism of some applications is set forth by a conservative practitioner of data adjustment:

> I am disappointed with the approach which is being adopted in ENDF/B [Version 3] of taking account of integral experiments when selecting data. In my view this procedure does not lead to an improvement in accuracy of individual items of data because the items of data changed to fit the integral experiments are not unique. It is only the combined set of data which gives the improved performance. For this reason I think that it would be preferable to produce two versions of ENDF/B, one which takes account only of the direct cross section measurements and the second which takes account of the integral experiments. The second set would only be of interest to people making calculations for the reactor type corresponding to the integral experiments used in the cross section refinement.[22]

Although directed at the qualitative United States approach in evidence in ENDF/B-III, this criticism is more general. It draws a sharp line of demarcation between the use of integral experiments in 1) the evaluation of nuclear data for a specific design and 2) the evaluation of nuclear data for a general purpose file. Indeed, it seems reasonable that, since design data are usually adjusted in multigroup format and hence involve a particular within-group flux-weighting scheme, uncritical extension to the unweighted, general purpose evaluation would be methodologically unfounded if not in outright numerical error.

In response to this limitation, Pazy et al have developed a continuous-energy formulation of quantitative consistency analysis. The method is more difficult to apply in practice and is still somewhat restrictive. But the continous energy method may not even be necessary.

In the words of the developers:

> ...with the progressing perfection of computation facilities and the ensuing practicability of increasingly higher multigroup approximations, the distinction between a step function and a continuous correction factor tends to vanish, group-constant adjustment effectively reduces to microscopic cross-section modification, and the problem of the one approach versus the other becomes purely academic and loses its relevance.[23]

It is not the principal purpose of this work to prove the use of quantitative consistency analysis for the general purpose of cross section evaluation but to focus on nuclear design applications. Thus, an important aspect of the work is the first use of the technique in an energy group structure as fine as one hundred energy groups. This choice of energy group structure is characteristic of the trend in fusion reactor blanket and shield analysis to use more energy groups than in fission reactor core design. At the same time it points toward the use of quantitative consistency analysis in cross section evaluation.

Current United States Efforts in Quantitative Consistency Analysis

After the work of Campise, United States efforts continued with investigations by Ott, Pond, and Kallfelz[24] and by Kallfelz and Chow[25] at Georgia Institute of Technology. These studies of least-squares techniques as a method of error identification form part of the background of the present work. In addition, statistical data adjustment for purposes of nuclear design has been addressed by D. R. Harris of the Los Alamos Scientific Laboratory[26] and by F. G. Perey of Oak Ridge National Laboratory.[27] In collaboration with W. B. Wilson and the

present author, Harris developed the first United States code for consistency analysis, as detailed in Chapter III of this work. The emphasis in this work, as distinguished from previous efforts, is to place the consistency analysis implications of least-squares methods before the data adjustment implications. In particular, the calculation of the initial chi-square is taken as an important quantitative measure of consistency which is lacking in the qualitative calculation-experiment comparisons and in many of the quantitative comparisons. Moreover, the system final chi-square is taken as a measure of the consistency of the combined network of calculation, experiment, and uncertainty estimation. Particular items of cross section adjustment required to maximize the statistical consistency are considered significant only if the final consistency is judged acceptable. Thus a data adjustment is only a contingent result of the more fundamental consistency analysis.

In a parallel development at Oak Ridge National Laboratory, Weisbin et al[28] have adapted an Italian data adjustment code and applied it to reactor core design analysis. However, the work falls short of the present work in several respects: 1) the consistency analysis aspects of the problem are subordinate; that is, no chi-square analysis is performed, 2) the analysis of a two-dimensional integral experiment is attempted with one-dimensional methods, 3) statistical correlations among integral data are neglected, 4) output uncertainties do not take the external consistency of calculated and experimental integral results

into account, and 5) only two integral data are used. The importance of these considerations is detailed later in this work.

Quantitative Consistency Analysis in the Design of Fusion Reactor Blankets and Shields

This work represents the confluence of two recent streams of development in nuclear engineering research: 1) the emergence of fusion reactor technology as a major subject of research, including blanket and shield neutronics research, and 2) recent progress in cross section adjustment techniques. The general problem attacked in the present work is to implement an improved method for the construction of an adjusted library of group cross sections suitable for neutronics design and to apply the method to a particular class of problems in fusion reactor neutronics design. To reduce the problem to manageable proportions it was early decided to limit the number of integral experiments considered. Of the United States integral experiments, only two were judged to be of suitable quality, namely the Los Alamos tritium production experiment and the Livermore pulsed sphere experiment. Both experiments evolved in the United States weapons program. Since the techniques of quantitative cross section adjustment had not previously been applied to such experiments, the territory under investigation remained essentially unexplored.

The choice of the Wyman experiment was based on several additional considerations. The only known attempt at cross section adjustment in

this energy regime had been applied to this experiment. Second, the experiment is considered to be relatively free of uncertainties in calculational method. In particular, the geometry is closely one-dimensional. Third, it was anticipated that reevaluation of the experimental results and their statistical errors would go beyond the published data and in this case the experimenter was personally known to the author. Moreover, the timely availability of an Associated Western Universities fellowship held in residence at the Los Alamos Scientific Laboratory would permit closer scrutiny of the original experimental data and of archival material pertaining to the experiment. Finally, a major consideration was the availability of sufficient computing resources at the Los Alamos Scientific Laboratory to permit an extensive program of computer code development.

The choice of the Livermore pulsed spheres was based on the following considerations. A substantial body of qualitative cross section analysis and studies for this experiment already exists. The geometry is — apart from certain two-dimensional effects — relatively clean and the measurements are well documented. Finally, the measurement of a family of spheres differing only in nuclear thickness affords a unique opportunity to analyze important questions that could not otherwise be so readily studied.

In the higher energy regime of the fusion reactor, several problems in the application of consistency analysis were expected.

Because of the higher energies involved, a larger number of cross section energy groups would be used. Moreover, the effects of the secondary neutron energy distribution and angular distribution should be more pronounced. Thus, the number of effective cross sections could be vastly larger and the programming of special subroutines would be required to handle the associated matrix inversion problems. The cross sections would pose further problems: for the principal nuclides of interest, ^{6}Li and ^{7}Li, evaluated error data, including correlated errors, were not available. Of further significance would be the problem of assessing and formatting the uncertainties in the integral data. In particular, a unique feature of the integral data selected was that, unlike the classical core-physics adjustment problem, in which the data are taken from numerous different assemblies and have a weaker degree of correlation, the present work would draw a large number of data from a single assembly or two. Thus, integral data correlations could not be neglected as in previous studies. For the pulsed spheres, questions concerning dimensionality and time-resolution were anticipated.

In the course of the work some of the anticipated problems proved inconsequential while yet other, unanticipated problems arose. In the material to follow it is hoped that the reader will gain perspective on the use of quantitative consistency analysis techniques in fusion reactor neutronics design and will at the same time uncover new areas of investigation.

In the course of the work some of the anticipated problems proved inconsequential, while yet other, unanticipated problems arose. In the material to follow, it is hoped that the reader will gain perspective on the use of quantitative consistency analysis techniques in fusion reactor neutronics design and will, at the same time, uncover new areas of investigation.

REFERENCES

1. L. Spitzer, Jr., D.J. Grove, W.E. Johnson, L. Tonks, and W.F. Westendorp, Problems of the Stellarator as a Useful Power Source, NYO-6047, U.S. Atomic Energy Commission (Secret, 1954; declassified 1959).

2. Proc. 2nd Int. Conf. Nuclear Data for Reactors, 15-19 June 1970, Helsinki, Vol. 1, p. 67, International Atomic Energy Agency, Vienna (1970).

3. J.R. Powell, J.A. Fillo, B.G. Twining, and J.J. Dorning, Proc. Magnetic Fusion Energy Blanket and Shield Workshop, Vol. 1, ERDA-76/117/1, U.S. Energy Research and Development Administration (1975).

4. Y. Gohar, C.W. Maynard, and E.T. Cheng, Proc. 2nd Topical Mtg. Technology of Controlled Nuclear Fusion, Vol. 3, p. 833, CONF-760935, U.S. Energy Research and Development Administration (1977).

5. M.A. Abdou, L.J. Milton, J.C. Jung, and E.M. Gelbard, loc. cit., Vol. 2, p. 398.

6. R. Herzing, L. Kuypers, P. Cloth, D. Filges, R. Hecker, and N. Kirch, Nucl. Sci. Eng., 60, 169 (1975).

7. D.E. Bartine, R.G. Alsmiller, Jr., E.M. Oblow, and F.R. Mynatt, Cross-Section Sensitivity of Breeding Ratio in a Fusion Reactor Blanket, ORNL TM-4208, U.S. Atomic Energy Commission (1973).

8. R.L. Childs, D.E. Bartine, and W.W. Engle, Jr., Trans. Am. Nucl. Soc., 21, 543 (1975).

9. H. Rief, Sensitivity Studies and Shielding Benchmarks, p. 68, Organization for Economic Cooperation and Development, Paris (1975).

10. S.A.W. Gerstl, Sensitivity Profiles for Secondary Energy and Angular Distributions, presented at the 5th Int. Conf. Reactor Shielding, 18-22 April 1977, Knoxville, Tenn. (to be published).

11. S.A.W. Gerstl, D.J. Dudziak, and D.W. Muir, Nucl. Sci. Eng., 62, 137 (1977).

12. B.R. Leonard, Proc. Magnetic Fusion Energy Blanket and Shield Workshop, ERDA-76/117/1, p. 66, U.S. Energy Research and Development Administration (1975).

13. A.E. Profio, Trans. Amer. Nucl. Soc., 26, 486 (1977).

14. W.G. Davey, in: E.L. Draper, ed., Technology of Controlled Thermonuclear Fusion Experiments, CONF-72111, p. 668, U.S. Atomic Energy Commission (1974).

15. S. Pearlstein, Proc. Int. Symp. Physics of Fast Reactors, Tokyo, 16-19 October 1973, Vol. 2, p. 603, Power Reactor and Fuel Development Corporation, Tokyo (1973).

16. R.A. Karam, Trans. Am. Nucl. Soc., 19, 389 (1974).

17. A.V. Campise, Proc. Sem. Physics of Fast and Intermediate Reactors, Vol. 3, p. 335, International Atomic Energy Agency, Vienna (1961).

18. A.V. Campise, Trans. Am. Nucl. Soc., 5, 69 (1962).

19. C. Cecchini, V. Farinelli, A. Gandini, and M. Salvatores, Proc. 3rd U.N. Conf. Peaceful Uses of Atomic Energy, Vol. 2, p. 388, United Nations, New York (1965).

20. M. Humi, J.J. Wagschal, and Y. Yeivin, loc. cit., Vol. 2, 398.

21. S. Yiftah, Panel Discussion, Int. Conf. Physics of Fast Reactor Operation and Design, 24-26 June 1969, London. Quoted in H. Kuroi and H. Mitani, J. Nucl. Sci. Technol., 12, 663 (1975).

22. J. Rowlands, Discussion, Proc. Int. Symp. Physics of Fast Reactors, Tokyo, 16-19 October 1973, Vol. 2, p. 610, Power Reactor and Fuel Development Corporation, Tokyo (1973).

23. A. Pazy, G. Rakavy, I. Reiss, J.J. Wagschal, and Atara Ya'ari, Nucl. Sci. Eng., 55, 280 (1974).

24. K.O. Ott, R.B. Pond, and J.M. Kallfelz, A Study of Methods of Cross-Section Error Identification Utilizing Integral Data from Fast Critical Assemblies, ZPR-TM-87, Argonne National Laboratory (1972).

25. E.T.Y. Chow, An Investigation of Methods for Neutron Cross Section Error Identification Utilizing Integral Data, Ph.D. Dissertation, Georgia Institute of Technology (1974).

26. D.R. Harris, Trans. Am. Nucl. Soc., 18, 340 (1974).

27. F.G. Perey, Remarks on Nuclear Data Adjustment, American Committee for Reactor Physics, Spring Meeting, 1975.

28. C.R. Weisbin, J.H. Marable, J.L. Lucius, E.M. Oblow, F.R. Mynatt, R.W. Peelle, and F.G. Perey, Application of FORSS Sensitivity and Uncertainty Methodology to Fast Reactor Benchmark Analysis, ORNL/TM-5563, Oak Ridge National Laboratory (1976).

CHAPTER II

THEORY OF QUANTITATIVE CONSISTENCY ANALYSIS

The previous chapter reviewed the role of consistency analysis in the neutronics design of fusion reactor blankets and shields. Introduced in the present chapter are methodological considerations in consistency analysis, consistency algorithms, and considerations in the use of the algorithms. The numerical implementation of these methods of consistency analysis is treated in the following chapter.

Methodological Considerations

Methodological considerations arise at three levels. They are, in order of increasing specificity: data consistency in general, data consistency in neutronics applications, and data consistency in thermonuclear neutronics applications.

General Data Consistency Analysis

The Nature of Consistency. In its simplest form, the consistency relationship is a logical relationship between simple propositions. For example, the logically contradictory statements, "Snow is white" and "Snow is not white" are inconsistent. Generally, two sets of propositions which together imply a logical contradiction are inconsistent. Otherwise they are consistent. For example, Euclidean geometry is inconsistent

with non-Euclidean geometry of non-zero curvature. Statements which are logically consistent are sometimes physically inconsistent, such as, "Peter is in the United States now," and "Peter is in Europe now." Or, statements may be inconsistent in a sense which is not purely a matter of formal logic or of physical plausibility, such as, "Peter is lying," and "Peter does not know he is lying."

In a different class reside statements like, "The length of the pin is 3 cm." The consistency of such statements is dependent on the implied precision. The lengths 3.0 $\pm$ 0.1 cm and 3.3 $\pm$ 0.1 appear plainly inconsistent, 3.05 $\pm$ 0.1 and 3.07 $\pm$ 0.1 appear consistent, but 3.0 $\pm$ 0.1 and 3.2 $\pm$ 0.1 appear in-between. Thus, a quantitative measure of consistency must be applied to such statements.

Measures of Consistency. The consistency of statements such as the above may be assessed by methods of statistical hypothesis testing. Following J. Neyman and E. S. Pearson, a given hypothesis is formulated in probabalistic terms and compared with a set of observation data by computing a statistic, or function of the observation data. The value of the statistic is compared with the value the statistic would have if the hypothesis were true. This comparison is known as a test of the hypothesis. For example, one may wish to test whether the observed incidence of colds among 1000 persons taking Vitamin C is a result of chance (the so-called null hypothesis: Vitamin C has no effect). Four possibilities occur:

a) Ho is true, test accepts Ho.

b) Ho is true, test rejects Ho.

c) Ho is false, test accepts Ho.

d) Ho is false, test rejects Ho.

In cases a) and d) the test performs as desired, but in b) and c) it fails. Letting P(a) denote the probability that statement "a" is true, suppose $P(b) = \alpha$ and $P(c) = \beta$. Then α is called the significance level of the test and $1-\beta$ is the power of the test. In a good test α should be as small as possible and $1-\beta$ should be as large as possible. However, in some cases no single test may be found which best satisfies both criteria. Thus, the measure of consistency between hypothesis and data may be test-dependent.

A classical hypthesis test is the K. Pearson goodness-of-fit test. This test measures the consistency of a given probability distribution with a sample which is supposed to be drawn from the distribution. Thus, the result of N measurements of the length of a pin may be divided into K equal-length intervals and the number of measurements n_i in each interval may be compared with the number p_i expected from a specified normal distribution (or from any other distribution of specified character). Let $\sigma(p_i)$ be the expected standard deviation of p_i for many repetitions of the N measurements. Then the goodness-of-fit statistic is:

$$D^2 = \sum_{i=1}^{K} \frac{(n_i - p_i)^2}{\sigma^2(p_i)} \qquad (2\text{-}1)$$

If the number of measurements is increased without limit, D^2 approaches the χ^2 distribution with K-1 degrees of freedom.[2] The test consists of rejecting Ho at the α level of significance if the probability that D^2 equals or exceeds χ^2 is α. That is, if the observed quantity D^2 has a poor chance of exceeding χ^2, but D^2, in fact, exceeds χ^2, then the rejection is highly significant. Using similar tests, one may measure the consistency of statements of the form, "The length of the pin is 3.0 ± 0.1 cm" and "The length of the pin is 3.2 ± 0.1 cm." In particular, one may test whether both samples are drawn from the same distribution.

Maximum Consistency Principles. Several principles for maximizing the consistency of a hypothesis are in use: 1) the principle of best fit or minimum χ^2, 2) the principle of maximum likelihood, and 3) the principle of minimum variance. Under appropriate conditions each of the three principles lead to the same set of equations, the so-called normal equations, for the most consistent population parameters.

The principle of best fit or minimum χ^2 (see, for example, Bevington) flows from the goodness-of-fit statistic D^2 described previously. Thus, the optimum values of the population parameters of an assumed distribution consist of those parameters which minimize D^2. To the extent that the goodness-of-fit test is valid only in the limit of large samples, so too is the principle of best fit limited in its validity. This drawback must be weighed against the conceptual simplicity of deriving an algorithm for maximum consistency from the general notion of a statistical test

as the measure of consistency.

The principle of maximum likelihood derives from the mathematical function which gives the joint probability that all of the observations are sampled from the hypothetical distribution. The parameters of the distribution are sought such that this joint probability, or likelihood function, is a maximum. For a normal distribition with mean μ and standard deviation σ, the function has the form

$$P(\mu,\sigma) = \prod_{i=1}^{N} \frac{1}{\sigma\sqrt{2\pi}} \exp\left[-\frac{1}{2}\left(\frac{x_i-\mu}{\sigma}\right)^2\right] \qquad (2\text{-}2)$$

where x_i are the discrete observations. Since P is maximized by minimizing the exponential, the solution is formally the same as that of the best fit method. Both may be described as least-squares methods for obtaining the normal equations. For a complete discussion of the connection between the method of best fit and the method of maximum likelihood, the reader is referred to the literature of theoretical statistics.[4]

The minimum-variance principle expresses the fact that the normal equations may be derived[5] by seeking population parameters, expressed as a linear function of the observations, such that the resulting population possesses least variance and is also unbiased. The normal equations are obtained by this method whether the population has a normal distribution or not. Thus, if one appeals directly to a criterion of minimum variance one may arrive at the normal equations apart from considerations of consistency.

Can minimum variance be justified? One may imagine a situation in which a population parameter is sought such that the penalty of deriving a result other than the population parameter increases in proportion to the magnitude of the error. Under such circumstances it appears desirable to obtain as narrow and as unbiased a distribution as possible. However, a minimum penalty strategy may or may not lead to a least-squares or minimum variance solution, depending on the particular form of the penalty function. The strongest argument that might be introduced is that for a wide variety of penalty functions the minimum variance solution will yield, in some average sense, the minimum penalty. Indeed, such considerations may be approached from the standpoint of formal statistical decision-making theory.[6] However, this approach involves additional complications which are not central to the theme of the present work.

Hierarchy of Observations. Table 2-1 shows the emergence of additional methodological considerations at various stages in a hierarchy of observation statements. The hierarchy does not reflect the historical evolution of actual observation statements and is used here for purposes of logical analysis only. A tabulated methodological consideration arises in assessing the consistenty of two observation statements at the tabulated level and is emergent at that level. The methodological consideration appearing at one level also applies at all subsequent levels. When the consistency of two observation statements at different levels is evaluated

Table 2-1. Hierarchy of Observation Statements

Datum	Example	Methodology
Elementary Observation	Single reading of a mass, length, count value, etc. A pointer reading.	Error, random and systematic.
Evaluated elementary observation	Combination of elementary observations to yield a mass, length, etc.	Estimating. Weighting. Consistency. Ratio of external-to-internal consistency.
Derived observation	Combination of evaluated elementary observations to yield a derived quantity, e.g., a cross section at a particular energy, a critical mass, etc.	Confirmed theoretical relations among observands. Propagation of errors. Covariance estimation.
Parameter estimate	Combination of evaluated, derived observations with arbitrary function or with physical model to yield parameter estimate and to permit interpolation, extrapolation. E.g., combination of several secondary-neutron measurements at discrete energies to yield a nuclear temperature.	Model confirmation.
Community-recommended value	Combination of independently reported observations and/or parameterizations to give a recommended value, e.g., ENDF/B cross section, Particle Properties Group mass of rho meson, etc.	Standardization.

the applicable methodological considerations extend to the higher level.

Elementary Observation. Random error is probabilistic, systematic error is deterministic. That is, the magnitude and sign of a particular random error in a particular elementary observation cannot be predicted, even in principle, but the magnitude and sign of a particular systematic error in a particular elementary observation is, at least in principle, predictable. For example, the effect of quantum noise in a reading of a sensitive electrometer is not predictable in principle, but the effect of an improperly set decade selector is predictable. In a symmetric way, it is not possible, even in principle, to correct a given random error, but it is quite possible to correct a given systematic error. For example, if it is realized after the fact that the decade selector is set a factor of ten too high, leading to a reading ten times too small, the original reading may be multiplied by ten and it is not necessary to repeat the measurement. The random error may be reduced only by taking additional readings.

In fact quantum indeterminism on the one hand,and the procedural blunder on the other, serve better to illustrate the classical textbook distinction between random and systematic error than they do to clarify these types of error as they arise in practice. It is often the case that correctable-in-principle errors are not correctable-in-fact, if only for reasons of time and budget. In such circumstances, a systematic error is treated as if it were a random error and is combined statistically

with true random error.

Evaluated Elementary Observation. Because of the role of random and systematic error at the elementary observation level, it is customary to repeat observations before estimating the value of the observand. The result is the evaluated elementary observation. Distinctions which operate at the level of the elementary observation also operate at the present level. In particular, error may exist in the estimation process itself, and this error may be random or systematic. Thus, round-off error may be significant in an estimation calculation and calculational blunders may occur. In this subsection only methodological considerations which are emergent at the level of the evaluated elementary observation are considered.

Although a particular random error cannot be predicted, a definite distribution of such errors usually exists and the mean or expectation of this distribution may be estimated given the weight of individual observations. Normally, the elementary observations are assigned equal weight, but the common practice of rejecting suspect readings altogether amounts to assigning zero weight to some. Here the role of bias and subjective judgment is apparent as a higher level of systematic error.

Let us suppose that N corrected elementary observations x_i of equal weight are performed. An estimate of the mean of the distribution from which the observations are sampled is the sample mean:

$$\bar{x} = \frac{1}{N} \sum_{i=1}^{N} x_i \qquad (2\text{-}3)$$

To estimate the spread or variance of the distribution of observations the so-called sample variance is calculated:

$$s^2(x) = \frac{1}{N-1} \sum_{i=1}^{N} (x_i - \bar{x})^2 \quad . \tag{2-4}$$

Finally, the variance of the sample mean is estimated by:

$$s^2(\bar{x}) = \frac{1}{N(N-1)} \sum_{i=1}^{N} (x_i - \bar{x})^2 \quad . \tag{2-5}$$

Thus, the evaluated elementary observation $\bar{x}$ and an estimate of the variance of $\bar{x}$ are obtained.

In the foregoing discussion of the estimation of the mean and the variance of the mean, all elementary observations were assigned unit weight and were lumped together. This is a natural procedure when all N observations are performed on a single occasion, i.e., by a single investigator, using a given procedure, and at a definite time and place. Suppose that the entire set of N observations is repeated on M different occasions. The M means $\bar{x}_i$ may be separately calculated, and in turn the variance of these individual means may be calculated:

$$s^2_{ext} = \frac{1}{M-1} \sum_{i=1}^{M} (\bar{x}_i - \bar{\bar{x}})^2, \tag{2-6}$$

where $\bar{\bar{x}}$ is the mean of the means. The subscript "ext" is used to indicate that the variance of the mean here is obtained by a new set of observations external to the original N observations. If the M occasions of observation

are consistent the $s^2(\bar{x})$ should approximately equal s^2_{ext}. Birge, an American physicist, denoted the ratio $s^2_{ext}/s^2(\bar{x})$ as the ratio of external-to-internal consistency.[7] Birge argued that when the ratio is excessive, say five, it is likely sources of systematic error perturb some of the observations. For example, if the occasion of the N observations is repeated once a day for one week and some, but not all, of the observations are performed in the afternoon, when a temperature increase lowers (by a correctable amount) the numerical result of all observations performed that afternoon, then the ratio of external-to-internal consistency may be too high. In such an event, one of two courses of action is open. The source of systematic error may be correctable, in which case the usually smaller variance by internal consistency should apply. If the error is not correctable, Birge argued that the larger variance by external consistency should apply.

Derived Observation. For some high-precision, fundamental work, the evaluated elementary observation is the final experimental result. Usually, however, the evaluated elementary observation is combined with other such observations, using confirmed theoretical relationships between the observands, to yield a derived observation. For example, evaluated elementary observations of currents and thicknesses may be combined to yield a cross section observation.

In combining the evaluated elementary observations the confirmed theoretical relationship is used in two ways: to estimate the observand

corresponding to the derived observation and to estimate the associated variance. In estimating the variance the confirmed theoretical relationship and the variance estimates obtained previously for the evaluated elementary observations may be combined in a simple, exact way when the theoretical relationship is linear in the elementary observands. This rule of combination, the so-called law of propagation of errors, is derived in a later section. The covariance concept does not operate at the level of elementary observations on a single observand. The concept arises from the fact that when the random error in an elementary observation of x is of one sign there may be a significant probability that the random error in an elementary observation of y is of the same sign. In such a case the errors are said to be positively correlated. If the errors are of opposite sign they are negatively correlated. Although they are superficially similar in effect, positively correlated errors are conceptually distinct from systematic errors.

Parameter Estimate. When the observand is an ordered pair, e.g. a cross section at a particular incident particle energy, the investigator may summarize tables of evaluated, derived observations of many different, ordered-pair observands in a graph. The curve may be constructed by educated sketching, by fitting an arbitrary function such as a polynomial or spline, or by fitting to a function suggested by a plausible theoretical model. The function is prescribed by the fitted values of parameters, such as a polynomial coefficient or a nuclear temperature. Suppose, for

simplicity, that one member x_i^o of each ordered pair observation (x_i^o, y_i^o) is known accurately, such as incident particle energy. One may wish to find L parameter estimates $\bar{a}_k$ such that $\bar{y}_i = f(\bar{a}_k, x_i^o)$, $1 \leq i \leq N$, and $L < N$, minimizes the sum of the squares of the inverse-variance weighted residuals:

$$s^2 = \sum_{i=1}^{N} \sum_{j=1}^{N} (y_i^o - \bar{y}_i) \left[\text{cov}^{-1} (y_i^o, y_j^o) \right] (y_j^o - \bar{y}_j). \qquad (2\text{-}7)$$

The estimation scheme is related to the scheme considered previously. The former univariate probability distribution from which the observation is sampled is here replaced by a multivariate distribution in the N derived observations. Elementary observations on a given variate are replaced by a single derived observation on each variate. The single derived observation is, in principle, derived ultimately from compounded evaluated elementary observations and, in turn, the evaluated elementary observations are derived from many elementary observations.

When the form of the fitting function is chosen merely for mathematical convenience, the quantity s^2 is no more than a formal goodness-of-fit parameter. On the other hand, when the form of the fitting function is chosen on plausible theoretical grounds, s^2 is not only a formal goodness-of-fit parameter but is a measure of the mutual consistency of the observations and corresponding covariance estimates and the theoretical model. In the sense that the theoretical model provides an external criteria of consistency which is crudely analogous to the external criteria

provided by additional occasions of observation, s^2 is a ratio of external-to-internal consistency.

In the event that the fit is poor, one or a number of factors may be at fault. The theoretical model may be poor, the variances and covariances may have been poorly assessed, or previously unsuspected and therefore uncompensated systematic error may be involved. Finally, the fit may be poor only because a particularly unfortunate combination of extreme fluctuations in the statistical sampling of errors occurred. It is normally not possible to identify conclusively the source of inconsistency by examination of the data alone and recourse must be had to additional data or additional theory. However, certain trends may be suggestive. For example, the fitted data may lie consistently above the theoretical model in one region of parameter space, and consistently below in another region. If the theoretical model is well-confirmed, such a situation may be accounted for in terms of unidentified skew-type, or negative, correlations in the data. In this way, external consistency at the level of parameter estimation is analogous to external consistency at lower levels in the observation hierarchy.

Community-recommended value. The determination of community-recommended values by consistency analysis is illustrated by applications in elementary particle physics,[8] nuclear physics,[9] nuclear reactor physics,[10-12] and atomic physics.[13-15] Methodological considerations have been treated in the literature,[16,17] but consist largely of problems

which have already been discussed at lower levels in the observation hierarchy.

It often happens that despite the most careful work by experimental investigators, the use of ostensibly identical methods gives rise to external inconsistencies which cannot be resolved by additional laboratory investigation. When the best of investigators disagree, progress can grind to a halt until it is agreed which procedure shall in the interim be used as a standard. Thus, inconsistencies can be resolved, if not removed altogether, by community action. While rational principles play a major role in such deliberations there exists in the final analysis an element of arbitrariness which is involved in achieving consistency.

Neutronic Data Consistency Analysis

Critical reviews of neutronics consistency analysis have appeared in the recent literature.[18-21] To a large extent the considerations involved in previous critiques are applicable to consistency analysis and least-squares estimation in general. Treated in the present subsection are those methodological considerations which are unique to neutronic data consistency analysis.

In the language of the foregoing section neutronic data consistency analysis is a higher-level parameterization. A linearized form of the Boltzmann transport equation, with multigroup neutron cross sections as parameters, is fit to both derived observations, namely certain integral experiments, and to community-recommended parameter observations, namely

evaluations of neutron cross sections. From a hierarchical point of view, the analysis is cross level. It is further characterized by the inclusion of parameter observations as a subset of the observations.

Although the evaluation of neutron cross sections is more formally developed than the evaluation of integral experiments, it is not as developed as the evaluation of other community-recommended quantities such as the atomic constants. The additional complexity of the theoretical relations among observands in the case of neutron cross sections accounts in part for this disparity. A weakness which has only recently received formal consideration is the lack of evaluation and compilation of neutron cross-section variances and covariances.[22] Compared to the evaluation of particle properties data and atomic constants evaluation there is at present no unified approach to the evaluation of neutron cross sections.[23]

If neutron cross section evaluation is poorly systematized, integral experiment evaluation is even more so. No evaluated compendia of integral experiments comparable to ENDF/B exist, although evaluations or compilations of key integral experiments have been[24,25] - and are presently[26] - under development. The task of critical evaluation of integral experiments, which properly involves the comparison of a given experiment with related integral experiments and the critical evaluation of errors and their correlations, falls largely on the particular data user. When this critical evaluation has been performed, then some

measure of symmetry is restored between the two hierarchies of derived observations and community-recommended values.

Another way to achieve symmetry is to attempt to resolve the cross section evaluation into the originally-reported observations of the cross sections. If, in fact, the evaluation is resolvable into more primitive observations, then the result of the entire consistency analysis should be just the same whether the primitive cross-section observations are used separately or are lumped into the evaluated quantity. In this case, such resolution confers no practical benefit and is unduly cumbersome. On the other hand, if the cross section evaluation is not precisely expandable into cross section observations, then to attempt to do so is to attempt a re-evaluation.

Note that a cross-level consistency analysis of evaluated cross sections and individual integral experiments is similar to a cross-level analysis in which a newly available derived observation of a particular cross section is used to update an existing cross-section evaluation. In this light, the difference between neutron cross-section consistency analysis and neutronic data consistency analysis is narrowed.

A conspicuous feature of neutronic data consistency analysis is the role of the Boltzmann transport equation as the major theoretical relation among the cross-section observands and the integral observands. The solution of this integro-differential equation, even in simple geometries, is considerably more expensive, or considerably more approx-

imate at a given cost level, than the solution of the theoretical relations among observands in much of data consistency analysis in other disciplines. The approximations which are introduced in the solution of the Boltzmann equation, for example, the cross-section multigrouping process, the finite spatial mesh and angular quadrature, etc., all lead to a high-level source of systematic error in the solution of the theoretical relations among observands. It is a basic methodological principle of consistency analysis that the systematic error in such calculations should be reduced significantly below that of the random errors in the observations. This objective is compromised by finite calculational resources. Hence the validity of the consistency analysis is also compromised. The problem is compounded by the non-linear nature of the relationship between neutron cross sections and the integral responses obtained from the transport equation. Thus recourse must be made to linearization about some small neighborhood in cross-section space.

Although the computational requirements for a rigorous statistical consistency analysis are generally more demanding in neutronic data consistency analysis than in the application of statistical consistency analysis in many other disciplines, it must at the same time be recognized that the computational requirements are not necessarily more severe than those involved in the consistency analysis of cross-section measurements proper. To be sure, the analysis and evaluation of several measurements

of a 14.1 MeV neutron cross section may be relatively uncomplicated, but the analysis of an energy-dependent cross section using a sophisticated and detailed statistical model of the nucleus or an R-matrix fit may involve computer resources on the order of those required for the solution of the Boltzmann transport equation in simple geometry. To take an extreme case, measurements of a Maxwellian-averaged 1/v thermal capture cross section, when viewed as a very simple kind of integral experiment, are more cheaply fitted with the 2200 meter-per-second cross section, than are measurements of the energy dependent cross section fitted with the Briet-Wigner parameters.

Thus, the range of calculational difficulty in both nuclear model assisted cross section evaluation and in neutronic data consistency analysis is so wide that calculational error is no more an argument against the use of integral data in consistency analysis than it is against the use of nuclear models in cross section evaluation. It is not uncommon in the observation of cross sections to introduce thick-target or multiple scattering corrections requiring solution of the neutron transport equation itself. In this respect, the distinction between consistency analysis among differential data alone and that including integral data is again narrowed.

In conclusion, our examination of the methodological considerations of neutronic data consistency analysis support the view that such considerations for the most part arise at the level of general data consistency analysis.

Thermonuclear Neutronic Data Consistency Analysis

If the distinction between general data consistency analysis and neutronic data consistency analysis is more a distinction of degree than of kind, much the same is true of the distinction between neutronic data consistency analysis in general and thermonuclear neutronics consistency analysis. Quantitative distinctions may be drawn in the nature of the cross-section data base, the integral data base, and the calculational framework. For example, neutron cross sections in the range 2-20 MeV have been less thoroughly measured and evaluated,[27] there exist notably fewer 14 MeV integral experiments of interest, and the calculational complexity in the 14 MeV regime due to higher-order angular approximations is notable.[28] However, there appear to be no qualitatively new methodological considerations in the extension of neutronics data consistency analysis techniques to thermonuclear applications.

Algorithms Used in the Present Work

In the preceding sections methodological considerations in the implementation of consistency analysis were discussed. Here the algorithms used in consistency analysis are presented. First a summary of useful concepts is presented and some notational considerations are given.

The expectation of a function of a random variable $f(x)$ with probability distribution $P(x)$ is given by:

$$E[f(x)] = \int_{-\infty}^{\infty} f(x)P(x)dx, \tag{2-8}$$

and the expectation of x itself is defined as the mean. The variance of x is defined by:

$$\text{var } x = s^2 = E[x-E(x)]^2, \tag{2-9}$$

where s is the standard deviation.

Given N random variables $x_1,\ldots x_N$ with joint probability distributions $P(x_i,x_j)$ defined between any two of them, the covariance of x_i,x_j is defined as:

$$\text{cov}(x_i,x_j) = \int_{-\infty}^{\infty}\int_{-\infty}^{\infty} [x_i-E(x_i)][x_j-E(x_j)]P(x_i,x_j)dx_i dx_j, \tag{2-10}$$

or:

$$\text{cov}(x_i,x_j) = E\left\{[x_i-E(x_i)][x_j-E(x_j)]\right\}. \tag{2-11}$$

Let a sequence of variables $x_1,\ldots x_N$ be denoted by the N x 1 vector,

$$X = \begin{bmatrix} x_1 \\ . \\ . \\ . \\ x_N \end{bmatrix} = \{x_n\}, \tag{2-12}$$

then

$$E(X) = \left\{E(x_n)\right\} \tag{2-13}$$

The dispersion matrix (or covariance matrix) of X is defined by:

$$D(X) = \begin{bmatrix} \mathrm{cov}(x_1,x_1) & \cdots & \mathrm{cov}(x_1,x_N) \\ & & \\ \mathrm{cov}(x_N,x_1) & \cdots & \mathrm{cov}(x_N,x_N) \end{bmatrix} \quad . \tag{2-14}$$

Note that Equations 2-11 to 2-14 imply:

$$D(X) = E\{[X-E(X)][X-E(X)]^T\}, \tag{2-15}$$

where "T" denotes the matrix transposition operator. Note also that the diagonal of the dispersion matrix consists of the variances $s_1^2,\ldots s_N^2$.

The correlation coefficient between x_i and x_j is given by

$$\rho_{ij} = \mathrm{cov}(x_i,x_j)/s_i s_j \tag{2-16}$$

and the correlation coefficient matrix is defined analogously. Note that the diagonal elements of the correlation coefficient matrix are ones.

Several useful theorems are stated here without rigorous proof. The reader is referred to several references in statistics and measurement theory for further details.[5,29-31]

The change in a linear function $y_k = y_k\ (x_1,\ldots x_N)$, due to changes in the x_n is given by:

$$\Delta y_k = \sum_{i=1}^{N} \frac{\partial y_k}{\partial x_i}\ \Delta x_i. \tag{2-17}$$

If the x_i represent random errors sampled from probability distributions with zero means, and if the Δx_i are mutually independent, the law of propagation of errors is given by:

$$\text{var } y_k = \sum_{i=1}^{N} \left(\frac{\partial y_k}{\partial x_i}\right)^2 \text{var } x_i. \tag{2-18}$$

If the x_i are statistically correlated one obtains the more general expression:

$$\text{var } y_k = \sum_{i=1}^{N} \sum_{j=1}^{N} \frac{\partial y_k}{\partial x_i} \frac{\partial y_k}{\partial x_i} \text{cov}(x_i, x_j). \tag{2-19}$$

In other words, the evaluation of the uncertainty in a linear function of various parameters with correlated errors is dependent not on the variances of the parameters but rather the entire dispersion matrix.

An even more general form is obtained as follows. Consider two linear functions y_k and y_ℓ of random variables $x_1, \ldots x_N$. By Equation 2-11:

$$\text{cov}(y_k, y_\ell) = E\left\{[y_k - E(y_k)][y_\ell - E(y_\ell)]\right\}. \tag{2-20}$$

But from Equation 2-17:

$$y_k - E(y_k) = \sum_{i=1}^{N} \frac{\partial y_k}{\partial x_i} [x_i - E(x_i)], \tag{2-21}$$

and

$$y_\ell - E(y_\ell) = \sum_{j=1}^{N} \frac{\partial y_\ell}{\partial x_j} [x_j - E(x_j)], \tag{2-22}$$

hence:

$$\operatorname{cov}(y_k,y_\ell) = E\left\{ \sum_{i=1}^{N} \sum_{j=1}^{N} \frac{\partial y_k}{\partial x_i} \frac{\partial y_\ell}{\partial x_j} \; [x_i - E(x_i)][x_j - E(x_j)] \right\} \qquad (2\text{-}23)$$

Since y_k and y_ℓ are linear, the derivatives may be removed from the expectation integral and one obtains:

$$\operatorname{cov}(y_k,y_\ell) = \sum_{i=1}^{N} \sum_{j=1}^{N} \frac{\partial y_k}{\partial x_i} \frac{\partial y_\ell}{\partial x_j} \; \operatorname{cov}(x_i,x_j). \qquad (2\text{-}24)$$

Moreover, Equation 2-24 is conveniently generalized to M functions $y_1,\ldots y_M$ of $x_1,\ldots x_N$ by writing y and x as column vectors Y and X, and expressing the derivatives as an M x N matrix P such that Y = PX. Then, from Equation 2-15, one has:

$$D(Y) = E\left\{[PX-E(PX)][PX-E(PX)]\right\}^T \qquad (2\text{-}25a)$$

$$= E\left\{P[X-E(X)][X-E(X)]^T P^T\right\} \qquad (2\text{-}25b)$$

$$= PE\left\{[X-E(X)][X-E(X)]^T\right\} P^T \qquad (2\text{-}25c)$$

$$= PD(X)P^T. \qquad (2\text{-}25d)$$

It may be shown further that if PX is of the special form $P_\alpha X_\alpha + P_\beta X_\beta$ and X_α and X_β are uncorrelated, then

$$D(Y) = P_\alpha D(X_\alpha) P_\alpha^T + P_\beta D(X_\beta) P_\beta^T. \qquad (2\text{-}26)$$

It was assumed in the preceding discussion that the variable y_k is linear in the $x_1,\ldots x_N$. For non-linear functions $Y_k(X_1,\ldots X_N)$, which are linear in some small region about $Y_k^\circ(X_1^\circ,\ldots X_N^\circ)$, one defines:

$$x_i = (X_i - X_i^\circ)/X_i^\circ. \tag{2-27}$$

(The symbol "X_i" is not to be confused with the vector symbol "X".)

Taylor expansion of Y_k for small variations about the reference values X_i° yields to first order:

$$Y_k - Y_k^\circ = \sum_{i=1}^{N} \frac{\partial Y_k}{\partial X_i} \Bigg|_o (X_i - X_i^\circ). \tag{2-28}$$

Dividing by Y_k°, and multiplying the right hand side by X_i°/X_i°, one obtains:

$$\frac{Y_k - Y_k^\circ}{Y_k^\circ} = \sum_{i=1}^{N} \frac{\partial Y_k/\partial X_i}{Y_k/X_i} \Bigg|_o \frac{X_i - X_i^\circ}{X_i^\circ}, \tag{2-29}$$

or:

$$y_k = \sum_{i=1}^{N} P_{ki} x_i \tag{2-30}$$

where $y_k = (Y_k - Y_k^\circ)/Y_k^\circ$, $P_{ki} = (\partial Y_k/\partial X_i)/(Y_k/X_i)\,|_o$, and $x_i = (X_i - X_i^\circ)/X_i^\circ$. The quantities y_k are identified with the linear function of the preceding discussion, $y_k = y_k(x_1, \ldots x_N)$, in the small region about the reference point. By using Equation 2-25 it may be shown that the dispersion matrix element normalization is expressed as:

$$\text{cov}\,(x_i, x_j) = \text{cov}\,(X_i, X_j)/X_i^\circ X_j^\circ, \tag{2-31}$$

$$\text{cov}\,(y_k, y_\ell) = \text{cov}\,(Y_k, Y_\ell)/Y_k^\circ Y_\ell^\circ. \tag{2-32}$$

A generalization of these results, useful when Monte Carlo calculations introduce statistical uncertainty in the neutron transport operator, is presented in Appendix IV.

With the establishment of these preliminary concepts and notational conventions, the consistency analysis algorithms used in this work[32] are now summarized. The standard least-squares algorithm is presented, the algorithm is compared with certain variants implemented in the present work, and the use and interpretation of the algorithm is discussed.

Standard Least Squares Procedure

Consider the linear model

$$O(AX) = AX + \varepsilon, \tag{2-33}$$

where the vector O(AX) represents an observation of the linear function AX defined on the parameter vector X and perturbed by random errors ε. (All symbols denote matrices unless otherwise noted.) The errors are sampled from a normal, multivariate probability distribution with finite second moments and zero means. An initial estimate of the dispersion matrix for the observations, D[O(AX)], need only be known to within a scalar factor s^2. This factor will be estimated on the basis of consistency requirements. Let the number of elements L in O(AX) exceed the number of elements N in X. Then maximum likelihood estimates, $\hat{X}$, of X are obtained by minimizing the exponential in the likelihood function of the normal distribution. By generalization from Equation 2-2 the function to be minimized is:

$$S^2 = [O(AX)-A\hat{X}]^T s^2 D^{-1} [O(AX)][O(AX)-A\hat{X}]. \tag{2-34}$$

Expand the above equation, giving:

$$\begin{aligned} S^2 = {} & [O(AX)]^T s^2 D^{-1} [O(AX)]\, O(AX) \\ & + \hat{X} A^T s^2 D^{-1} [O(AX)] A\hat{X} \\ & - [O(AX)]^T s^2 D^{-1} [O(AX)] A\hat{X} \\ & - \hat{X}^T A s^2 D^{-1} [O(AX)] O(AX), \end{aligned} \tag{2-35}$$

and differentiate with respect to X to find the minimum. After regrouping terms one finds:

$$2(\delta\hat{X})^T \left\{ A^T s^2 D^{-1} [O(AX)] A\hat{X} - A^T s^2 D^{-1} [O(AX)] O(AX) \right\} = 0. \tag{2-36}$$

This result leads directly to a linear system in $\hat{X}$:

$$\left\{ A^T D^{-1} [O(AX)] A \right\} \hat{X} = A^T D^{-1} [O(AX)] O(AX), \tag{2-37}$$

These are the normal equations referred to previously. Note that the solution is independent of the scale factor s^2. The maximum likelihood estimates of the observands are then:

$$\hat{O}(AX) = A\hat{X} . \tag{2-38}$$

The dispersion matrix of the parameter estimate is obtained as follows: Rewrite Equation 2-37 as:

$$\hat{X} = B^{-1} A^T D^{-1} [O(AX)] O(AX), \tag{2-39}$$

where $B = A^T D^{-1} [O(AX)] A$. Then using Equation 2-25d, one finds:

$$D(\hat{X}) = B^{-1}A^{T}D^{-1}[O(AX)]s^{2}D[O(AX)]D^{-1}[O(AX)]AB^{-1} \qquad (2\text{-}40a)$$

$$= s^{2}B^{-1}A^{T}D^{-1}[O(AX)]AB^{-1} \qquad (2\text{-}40b)$$

$$= s^{2}(A^{T}D^{-1}A)^{-1}. \qquad (2\text{-}40c)$$

An unbiased estimate of the scalar factor s^2 is required to estimate $D(\hat{X})$. For an exact derivation of this estimate the reader is referred to the statistics literature.[31] The result is given here:

$$\hat{s^2} = \frac{1}{L-N}\,[O(AX)-\hat{O}(AX)]^{T}D^{-1}[O(AX)][O(AX)-\hat{O}(AX)], \qquad (2\text{-}41)$$

where the variance of the estimate is estimated by:

$$\text{var}\,\hat{s^2} = \hat{s^2}/2(L-N). \qquad (2\text{-}42)$$

The numerator of Equation 2-41 is just the inverse covariance-weighted sum of squares of the residuals after the minimization, using the initially estimated dispersion matrix. The denominator, L-N, is the expected value of the sum of squares when weighted with the unknown parent distribution. For example, if D[O(AX)] is initially underestimated the numerator will be larger than expected and $\hat{s^2}$ will be larger than unity. The interpretation of the scale factor is discussed further below.

Note that the inversion of matrices of order L x L is required in the standard algorithm above.

Parameters a Subset of the Observands: No Cross Type Correlations

In the special case that the observation vector O(AX) is a partitioned vector of N + M elements consisting of an N-element subvector O(X) of observations on X and an M-element subvector O(SX) of observations on a linear function S of X, Equation 2-33 may be written:

$$\begin{bmatrix} O(X) \\ O(SX) \end{bmatrix} = \begin{bmatrix} I \\ S \end{bmatrix} X + \epsilon \qquad (2\text{-}43)$$

X will ultimately be interpreted as a multigroup cross-section vector and SX will be interpreted as an integral quantity related to the multigroup cross sections by a matrix S of sensitivity coefficients. In a more general sense, O(X) is interpreted as a direct observation of X and O(SX) is interpreted as an indirect observation of X.

If it is now assumed that the observations of X are not statistically correlated with the observations of SX, then:

$$D[O(AX)] = \begin{bmatrix} D[O(X)] & 0 \\ 0 & D[O(SX)] \end{bmatrix} . \qquad (2\text{-}44)$$

Note that observations on X alone, and the resulting dispersion matrix D[O(X)], imply by Equation 2-25 a dispersion matrix D[SO(X)]. However, the result of a direct observation of SX may or may not be correlated in error space with an observation of X. It is one of the purposes of the consistency algorithm to combine D[O(X)] and D[O(SX)] in a consistent manner. This combination may introduce correlations between the new

estimates $\hat{X}$ and $\hat{SX}$ of X and SX, respectively, as detailed immediately below, but it is quite possible that the errors in the initial observations of X are not correlated with the errors in the initial observations of SX. It is then easily shown that:

$$\begin{bmatrix} D[O(X)] & 0 \\ 0 & D[O(SX)] \end{bmatrix}^{-1} = \begin{bmatrix} D^{-1}[O(X)] & 0 \\ 0 & D^{-1}[O(SX)] \end{bmatrix}. \tag{2-45}$$

When the above equation is inserted with Equation 2-44 into the standard least-squares algorithm, one obtains in a straightforward manner the partitioned forms of the data adjustment relations:

$$\left\{D^{-1}[O(X)] + S^T D^{-1}[O(SX)]S\right\}\hat{X} = D^{-1}[O(X)]O(X) + S^T D^{-1}[O(SX)]O(SX), \tag{2-46}$$

$$\begin{bmatrix} \hat{O}(X) \\ \hat{O}(SX) \end{bmatrix} = \begin{bmatrix} \hat{X} \\ S\hat{X} \end{bmatrix}, \tag{2-47}$$

$$\hat{D}(\hat{X}) = \hat{s^2}\left\{D^{-1}O(X) + S^T D^{-1}[O(SX)]S\right\}^{-1}, \tag{2-48}$$

$$\hat{D}\begin{bmatrix} \hat{O}(X) \\ \hat{O}(SX) \end{bmatrix} = \begin{bmatrix} \hat{D}(\hat{X}) & \hat{D}(\hat{X})S^T \\ S\hat{D}(\hat{X}) & S\hat{D}(\hat{X})S^T \end{bmatrix}, \tag{2-49}$$

$$\begin{aligned} \hat{s^2} = \frac{1}{M}\Big\{&[O(X)-\hat{O}(X)]^T D^{-1}[O(X)][O(X)-\hat{O}(X)] \\ &+ [O(SX)-\hat{O}(SX)]^T D^{-1}[O(SX)][O(SX)-\hat{O}(SX)]\Big\}, \end{aligned} \tag{2-50}$$

and:

$$\text{var } \hat{s}^2 = \hat{s}^2/2M. \qquad (2\text{-}51)$$

Note the appearance of the cross-type correlation terms, $\hat{SD}(\hat{X})$ and its transpose $\hat{D}(\hat{X})S^T$ as discussed immediately above.

While the matrix inversions required in the standard least-squares prescription are of order (M+N) x (M+N), the present case requires only the easier inversion of matrices of order (MxM) and (NxN). When there are no cross-type correlations between the observations of X and SX and when M is approximately equal to N, this derivative of the least-squares algorithm may be particularly useful.

The algorithm is also useful as an intermediary in the derivation of a more specialized algorithm presented below.

Number of Indirect Observations Less than Number of Direct Observations

A further economy in the matrix inversion[33,34] is possible if the number of indirect observations M is less than the number of direct observations N. The general approach is to use Equation 2-47 to transform the N x N system of Equation 2-46 into an intermediate M x M system in $O(\hat{SX})$ and to follow with a transformation of the intermediate system into an M x M system in $\hat{X}$.

The first transformation begins with use of the distributive law on Equation 2-46:

$$D^{-1}[O(X)]\hat{X} + S^TD^{-1}[O(SX)]\hat{SX} = D^{-1}[O(X)]O(X) + S^TD^{-1}[O(SX)]O(SX), \qquad (2\text{-}52)$$

or:

$$D^{-1}[O(X)]\hat{X} = D^{-1}[O(X)]O(X)-S^{T}D^{-1}[O(SX)]S\hat{X} + S^{T}D^{-1}[O(SX)]O(SX) \quad (2\text{-}53a)$$

$$= D^{-1}[O(X)]O(X)-S^{T}D^{-1}[O(SX)][S\hat{X}-O(SX)]. \quad (2\text{-}53b)$$

That is,

$$D^{-1}[O(X)]\hat{X} = D^{-1}[O(X)]O(X)-S^{T}D^{-1}[O(SX)][\hat{O}(SX)-O(SX)]. \quad (2\text{-}54)$$

Both sides are multiplied by $SD[O(X)]$:

$$S\hat{X} = \hat{O}(SX) = SO(X)-SD[O(X)]S^{T}D^{-1}[O(SX)][\hat{O}(SX)-O(SX)]. \quad (2\text{-}55)$$

Equation 2-46 in $\hat{X}$ is thus replaced by the above equations in $S\hat{X}$.

The desired intermediate system is readily obtained by subtracting $\hat{O}(SX)-O(SX)$ from both sides of Equation 2-50:

$$O(SX) = SO(X)-\left\{SD[O(X)]S^{T}D^{-1}[O(SX)]+I\right\}[\hat{O}(SX)-O(SX)], \quad (2\text{-}56)$$

or:

$$O(SX)-SO(X) = -\left\{S[DO(X)]S^{T}+D[O(SX)]\right\}D^{-1}[O(SX)]\left\{\hat{O}(SX)-O(SX)\right\}. \quad (2\text{-}57)$$

Equation 2-57 represents an MxM linear system which could be solved for $\hat{O}(SX)-O(SX)$; indeed, the form:

$$\hat{O}(SX)-O(SX) = - D[O(SX)]\left\{SD[O(X)]S^{T}+D[O(SX)]\right\}^{-1}[O(SX)-SO(X)] \quad (2\text{-}58)$$

is used in a subsequent derivation.

The intermediate system, Equation 2-57, is re-expressed in terms of X by multiplying the equation from the left by

$$S^T\left\{SD[O(X)]S^T + D[O(SX)]\right\}^{-1}, \text{ or:}$$

$$S^T\left\{SD[O(X)]S^T + D[O(SX)]\right\}^{-1}[O(SX)-SO(X)] =$$

$$-S^TD^{-1}[O(SX)][\hat{O}(SX)-O(SX)]. \qquad (2\text{-}59)$$

The form $S^TD^{-1}[O(SX)][\hat{O}(SX)-O(SX)]$ is eliminated by the use of Equation 2-54:

$$D^{-1}[O(SX)]\hat{X}-D^{-1}[O(SX)][O(SX)] =$$

$$S^T\left\{SD[O(X)]S^T + D[O(SX)]\right\}^{-1}[O(SX)-SO(X)]. \qquad (2\text{-}60)$$

Thus:

$$\hat{X} = O(X) + D[O(X)]S^TG[O(SX)-SO(X)], \qquad (2\text{-}61a)$$

where:

$$G = \left\{SD[O(X)]S^T + D[O(SX)]\right\}^{-1}. \qquad (2\text{-}61b)$$

Equation 2-61 is the desired result.

Note that the only matrix to be inverted to obtain $\hat{X}$ is G, which is of order equal to the number of indirect observations M. As before, the estimate of the complete observation vector is obtained from $\hat{X}$ by Equation 2-47.

The analog of Equation 2-48, giving the new estimate of the dispersion matrix of $\hat{X}$, is obtained as follows. Equation 2-61 is rewritten in the form:

$$\hat{X} = \left\{I-D[O(X)]S^TGS\right\}O(X) + D[O(X)]S^TGO(X), \tag{2-62}$$

and using Equation 2-26 one obtains:

$$\begin{aligned} D(\hat{X}) = &\left\{I-D[O(X)]S^TGS\right\}D[O(X)]\left\{I-D[O(X)]S^TGS\right\}^T \\ &+ \left\{D[O(X)]S^TG\right\}D[O(SX)]\left\{D[O(X)]S^TG\right\}^T. \end{aligned} \tag{2-63}$$

This equation is expanded and $D[O(X)]S^T \ldots SD[O(X)]$ is factored out of the last three terms. Upon introducing the scalar factor $\hat{s^2}$ there results:

$$\hat{D}(\hat{X}) = \hat{s^2}\left\{D[O(X)]-D[O(X)]S^TGSD[O(X)]\right\}. \tag{2-64}$$

As before, Equation 2-49 gives the dispersion matrix of the complete observation vector.

The estimate of the scalar factor $\hat{s^2}$ is obtained explicitly by substituting into Equation 2-50, using Equations 2-54, 2-58, and 2-61:

$$\hat{s^2} = \frac{1}{M}\left\{[\hat{O}(SX)-SO(X)]^TG[\hat{O}(SX)-SO(X)]\right\}. \tag{2-65}$$

The variance of $\hat{s^2}$ is estimated by Equation 2-42 as before.

As a result of this transformation the largest matrix inversion required is of order equal to the number of indirect observations M. When M is significantly less than N, the present derivation of the standard algorithm is most useful. In the multigroup cross-section interpretation of the direct observations, in particular, the present algorithm permits the extension of consistency analysis to very fine multigroup structures without prohibitive increase in execution time. In a fine energy group structure, the dependence of the group cross section on the choice of flux-weighting function is less severe. Thus, the generality and utility of the newly-estimated group cross sections is increased correspondingly. However, it must be remembered that the present algorithm requires that no correlations be present between the direct (cross section) and indirect (integral quantity) observations. Fortunately, this condition is frequently realized in practice.

Considerations in the Use of the Algorithms

In applying any algorithm it seems obvious that the input data should conform reasonably well to the assumptions in the algorithm and that the output data be properly interpreted. These requirements are discussed below.

The Evaluation of Input Data

The evaluation of input data comprises the bulk of the effort in the application of consistency analysis. Several preliminary applications of the algorithm may be involved in the process. Specific consid-

erations in the evaluation of the observation vector O(AX), the design matrix A, and the dispersion matrix D[O(AX)] are discussed here.

The Observation Vector. This section discusses a particular form of the component O(X) in the partitioned observation vector O[X/SX], proceeds to considerations of observation vector selection, and concludes with a remark concerning the evaluation of the observation vector which has been selected.

Consider that O(X) is an observation of the dimensionless form of the parameter as given by Equation 2-27:

$$x_i = (X_i - X_i^\circ)/X_i^\circ.$$

At $X_i = X_i^\circ$, O(X) is identically zero. In this case, an obvious simplification of the equations results. In fact, it is initially convenient to equate the observation value of X_i with its reference value (say the ENDF/B value of a cross section). But this need not always be the case. For example, in a non-linear, iterative problem, the second application of the algorithm will operate on the output of the first, namely $\hat{O}(X)$. This output value of X will, in general, no longer be equal to X_i°.

In selecting the elements of the observation vector it is usually necessary for practical reasons to limit the number of direct observations which participate in the analysis. Thus one excludes parameters which are so accurately known in relation to the others that a new, slightly different estimate would have relatively little effect on the results.

Observations of a direct or indirect nature which possess uncertainties or dispersion matrix elements which are so large as to give negligible statistical weight in the analysis are similarly rejected. Finally, one excludes parameters which do not contribute significantly to the matrix S.

When the obviously unimportant parameters have been excluded, it may be the case that the remaining parameters are still too numerous. In this event, one must begin with those parameters known to be significant and select from the borderline cases by performing trial adjustments with a single borderline parameter added at a time to test the effect of the parameter.

Once the identity of the observations to be included in the analysis has been determined, it remains to consider the best values to be used in the analysis. While the paradigm of the observation in the physical sciences is the simple instrument reading, it is often the case that the observation summarizes the result of prior statistical processing, as reviewed earlier. For example, an element of the observation vector may itself represent some average of a number of measurements. This average may consist of a simple, equal-weighted scheme applied to all readings, may involve the rejection of certain suspect readings, or may even involve a more sophisticated form of weighted average. Even at this primitive level, the evaluation of input data is not entirely algorithmic.

The Design Matrix. The matrix operator S must be linear in the range of interest. This requirement may be demonstrated either by directly calculating SX and examining its behavior in the region of interest or by estimating the magnitude of second-order terms using higher-order perturbation theory or variational theory. The range of interest may be estimated by performing a trial consistency analysis, assuming linearity, to determine the range within which the newly estimated quantities fall. In practice, the calculation and validation of the matrix S in a neutronic consistency analysis may consume a large portion of the computer budget.

The Dispersion Matrix. The evaluation of the relative magnitudes of the dispersion matrix elements constitutes an indispensable part of the application of the estimation algorithms. To the extent that published error estimates are credible, the estimator may be concerned primarily with the correctness of his implementation of the algorithms. Experience shows that frequently published error estimates are only a beginning step in an iterative process of identifying or quantifying overlooked systematic and random errors. The physical basis of an error source may not be entirely clear, but the overall magnitude of the random errors can sometimes be estimated by statistical methods including the specialized use of the preceding algorithms.

The Interpretation of Output Data

The essential output data are the newly estimated or adjusted vector of direct and indirect observations, $\hat{O}(X)$ and $\hat{O}(SX)$, and the dispersion matrix of the newly estimated observations, $\hat{D}$. This section presents certain formal considerations in the interpretation of the output data and additional considerations which arise in practical application.

Output Observations. Note that in the case of direct and indirect partitions in the observation vector, Equation 2-47 implies that $\hat{O}(SX) = S\hat{O}(X)$. The form of this relationship is similar to that between the observands, namely, (indirect observand) = (S) x (direct observand). It is unlike the relationship between the corresponding input observations, where the error vector mediates. Thus, the relationship between the input estimates of the observands is statistical in nature, but the relationship between output estimates is deterministic. An interesting consequence of this fact is treated below.

Output Dispersion Matrix. It has been noted that an arbitrary scale factor may be applied to the input dispersion matrix D without changing the value of the output observation vector. The significance of the term $\hat{s}^2$ is discussed below.

Note the formal appearance of the cross-type correlation terms, $S\hat{D}(\hat{X})$ and $\hat{D}(\hat{X})S^T$, in the output dispersion matrix (Equation 2-49). No correlation was assumed initially. These terms appear because of an

essential asymmetry in the relationship of O(X) and O(SX) on the one hand, and of $\hat{O}(X)$ and $\hat{O}(SX)$ on the other. Although in the linear model the two observands X and SX are deterministically related, the relationship between the random variables O(X) and O(SX) is just the statistical relationship between two error vectors as given in the cross-type partition of the initial dispersion matrix. On the other hand, the relationship between the output values of the random variables, $\hat{O}(X)$ and $\hat{O}(SX)$, is apparent in Equation 2-47. That is, $\hat{O}(SX) = S\hat{O}(X)$. By Equation 2-25 this deterministic relationship between the output values of the random variables dictates the form of the indirect matrix $\hat{D}[\hat{O}(SX)] = S\hat{D}(\hat{X})S^T$ in Equation 2-49, as well as the cross-type terms $S\hat{D}(\hat{X})$ and $\hat{D}(\hat{X})S^T$. The appearance of the cross terms in the dispersion matrix of the newly estimated quantities should not be construed as new evidence for a statistical correlation between the errors in the input observations but as a statement of a necessary correlation between the residual errors in the output estimates.

Interpretation of $\hat{s}^2$. The quantity $\hat{s}^2$ in Equations 2-41, 2-51, or 2-65 may be interpreted heuristically.

Consider the simple case of N equal-weight observations $x_{i,n}$ of the x_i-th element of X. Estimate the variance of the distribution from which the $x_{i,n}$ are sampled by computing the arithmetic mean x_i and evaluating:

$$\text{var } x_{i,n} = \frac{1}{N-1} \sum_{n=1}^{N} (x_{i,n} - x_i)^2. \qquad (2\text{-}66)$$

Postulate some *a priori* value of the variance, namely $(\text{var } x_{i,n})_o$. This value represents the variance within some unknown factor s^2. That is, (variance) = $(s^2)x\ (\text{var } x_{i,n})_o$. Then an estimate of s^2 may be obtained by the use of the estimate of the variance obtained from the observations to give:

$$\hat{s^2} = \frac{1}{N-1}\ (\text{var } x_{i,n})_o^{-1} \sum_{n=1}^{N} (x_{i,n} - x_i)^2. \qquad (2\text{-}67)$$

This expression corresponds precisely to Equation 2-41, where the *a priori* variance estimate corresponds to the input dispersion matrix and the mean of the equal-weighted observations corresponds to the output observations.

Note that the input dispersion matrix is evaluated by considerations internal to the variables represented. For example, the dispersion matrix element of an evaluated cross section X_i is initially estimated by considering the spread in reported individual measurements of X_i, without reference to indirect measurements of X_i. On the other hand, the output dispersion matrix element is derived by reference to the entire network of direct and indirect measurements of X_i. Thus $\hat{s^2}$ is related to the ratio of external-to-internal consistency.

When the errors are sampled from a normal distribution, the quadratic form of $\hat{s^2}$ is distributed as the chi-square statistic with L-N degrees of freedom and a quantitative significance level is attached to the ratio of external-to-internal consistency. This significance level is stated in terms of the probability that a random sample of

observations would yield a value of chi-square per degree of freedom (χ^2/DF), or reduced chi-square, equal to or greater than the given value, in this case $\hat{s}^2$.

The chi-square statistic may also be considered as a test of the general hypothesis that the observations are sampled from distributions with means other than the least-squares solution of the algorithm. In the second and third algorithms consider the hypothesis that the means of the direct observations are just the input values O(X) and the means of the indirect observations are just the implied means SO(X). Then, the goodness-of-fit statistic assumes the form:

$$D^2 = \frac{1}{M}\left\{[O(SX)-SO(X)]^T D^{-1}[O(SX)][O(SX)-SO(X)]\right\} . \qquad (2\text{-}68)$$

Here the dispersion matrix of the direct observations has disappeared along with the zero elements of the observation vector. This degenerate form arises in neutronic application, where the existence of standard cross-section data (as in ENDF/B) favors a certain choice of input values for the direct observations. In this event, it is natural to think of Equation 2-68 as giving an initial chi-square and Equation 2-41 as giving a final chi-square. However, the absence of the cross-section data dispersion matrix in the initial chi-square renders the initial chi-square alone a poor measure of consistency.

REFERENCES

1. J. Neyman and E.S. Pearson, Phil. Trans. Roy. Soc., 231, 289 (1933).

2. P.L. Meyer, Introductory Probability and Statistical Applications, Addison-Wesley (1965).

3. P.R. Bevington, Data Reduction and Error Analysis for the Physical Sciences, McGraw-Hill (1969).

4. R.A. Fisher, Contributions to Mathematical Statistics, Paper No. 8, Wiley (1950).

5. W.C. Hamilton, Statistics in Physical Science, Ronald Press, New York (1964).

6. L.J. Savage, The Foundations of Statistics, Wiley (1954).

7. R.T. Birge, Phys. Rev., 40, 207 (1932).

8. T.G. Trippe et al, Rev. Mod. Phys., 48, No. 2, Part 2 (1976).

9. L.A. Koenig, J.H.E. Mattauch, and A.H. Wapstra, Nucl. Phys., 31, 1-17 (1962).

10. S. Pearlstein, Nuclear Cross Sections and Technology, NBS Special Publication 425, Vol. 1, p. 332, U.S. National Bureau of Standards (1975).

11. B.R. Leonard, Jr., D.A. Kottwitz, and J.K. Thompson, Evaluation of the Neutron Cross Sections of ^{235}U in the Thermal Energy Region, NP-167, Electric Power Research Institute (1976).

12. D.C. Dodder, G.M. Hale, R.A. Nisley, K. Witte, and P.G. Young, in T. Fuketa, Proc. EANDC Topical Disc. Critique of Nuclear Models and their Validity in the Evaluation of Nuclear Data, JAERI-M-5984, Japan Atomic Energy Research Institute (1975).

13. J.W. DuMond and E.R. Cohen, Rev. Mod. Phys., 25, 691-708 (1953).

14. E.R. Cohen, Rev. Mod. Phys., 25, 709-713 (1953).

15. E.R. Cohen and B.N. Taylor, J. Phys. Chem. Ref. Data, 2, 663-734 (1973).

16. D.N. Langenberg and B.N. Taylor, Precision Measurement and Fundamental Constants, NBS Special Publication 343, Panel Discussion, 493-526, National Bureau of Standards (1971).

17. M. Roos, M. Hietanen, and J. Luoma, Physica Fennica, 10, 21-33 (1975).

18. A. Gandini, M. Petilli, and M. Salvatores, Proc. Symp. Physics of Fast Reactors, Tokyo, October 16-19, 1973, Vol. 2, p. 612, Power Reactor and Fuel Development Corporation, Tokyo (1973).

19. H. Kuroi and H. Mitani, J. Nucl. Sci. Technol., 12, 663 (1975).

20. E.T.Y. Chow, An Investigation of Methods of Neutron Cross Section Error Identification Utilizing Integral Data, Ph.D. Dissertation, Georgia Institute of Technology (1974).

21. D.R. Harris, Trans. Am. Nucl. Soc., 18, 340 (1974).

22. F.G. Perey, G. De Saussure, and R.B. Perez, in J.M. Kallfelz and R.A. Karam, Advanced Reactors: Physics, Design, and Economics, p. 578 (Pergamon Press, 1975).

23. Yu.I. Grigoryan, L.L. Sokolovski, and F.E. Chukreev, The Evaluation of Nuclear Data, INDC (CCP) - 75/LN, I.V. Kurchatov Institute for Atomic Energy (1976).

24. Reactor Physics Constants, ANL-5800, Argonne National Laboratory (1963).

25. G.E. Hansen and H.C. Paxton, Reevaluated Critical Specifications of Some Los Alamos Fast Neutron Systems, LA-4208, Los Alamos Scientific Laboratory (1969).

26. E.M. Bohn et al, Benchmark Testing of ENDF/B-IV (ENDF-230), Brookhaven National Laboratory (1976).

27. D. Steiner et al, The Status of Neutron-Induced Nuclear Data for Controlled Thermonuclear Research Applications: Critical Reviews of Current Evaluations, USNDC-CTR-1, Oak Ridge National Laboratory (1974).

28. D.J. Dudziak, 2nd Topical Mtg. Technology of Controlled Nuclear Fusion, CONF-760935, Vol. 3, p. 819, U.S. Energy Research and Development Administration (1977).

29. T.W. Anderson, An Introduction to Multivariate Statistical Analysis, Wiley, New York (1957).

30. Y.F. Linnik, The Method of Least Squares and Principles of the Theory of Observations, Pergamon, New York (1961).

31. M.G. Kendall and M. Stuart, The Advanced Theory of Statistics, Hafner, New York (1973).

32. W.A. Reupke, Matrix Formulation of Data Adjustment Methods, in D.W. Muir and P.G. Young, Applied Nuclear Data Research and Development, April 1-June 30, 1975, LA-6123-PR, p. 12, Los Alamos Scientific Laboratory (1975).

33. J.B. Dragt, in STEK-The Fast Thermal Coupled Facility at RCN at Petten, RCN-122, Reactor Center of the Netherlands (1970).

34. H. Häggblom, Adjustment of Neutron Cross-Section Data by a Least-Squares Fit of Calculated Quantities to Experimental Results, Part I, Theory, AE-422, Aktiebologet Atomenergi (1971).

CHAPTER III

DEVELOPMENT OF A COMPUTER PROGRAM FOR CONSISTENCY ANALYSIS

Newly-developed computer programs, ALVIN and ALVIN2, implement the consistency algorithms discussed in the previous chapter. The present chapter summarizes the nature of existing programs for consistency analysis, develops the rationale for the new codes, outlines the basis of the sensitivity calculation modules, reviews the code structure and, finally, discusses the validation of the programs.

Rationale for a New Code

In Table 3-1 are listed several previously documented programs for neutronic data consistency analysis and their typical application, grouped according to the three algorithms presented previously. The most extensively used algorithm is the third. This algorithm exploits the absence of covariances between neutron multigroup data and integral data and the numerical dominance of neutron data over integral data, to reduce the matrix to be inverted to an order equal to the number of integral data only. However, only Dragt et al provide in their code for covariances amongst the integral data and use these covariances in practice. In the present perspective, failure to provide for integral data covariances in the mathematical formulation of the consistency

Table 3-1. Consistency Analysis Codes and their Applications

Reference	Program	Typical Application: Neutron Data	Typical Application: Integral Data	Remarks
Standard Least Squares Method				
Barré et al[1]	BARRACA	Fissile and structural, 70 data, 5 groups.	Fast criticals, 116 data. Covariances not used.	Observation vector contains only integral data.
Hemment and Pendlebury[2]	PENICUIK	Fissile and structural, 134 data, 8 groups. Covariances not used.	25 fast criticals, 25 data. Covariances not used.	Covariances allowed in special forms only.
Observations on Parameters a Subset of Observation Vector. No Cross-type Correlations				
Häggblom[3]	JOHN	Fissile and structural, 156 data, 6 groups. Covariances used.	19 fast criticals, 58 data. Covariances, if any used, not stated.	Number of neutron data covariance elements limited to 29 because of computer time limitations.
Number of Indirect Observations Less than Number of Direct Observations				
Pazy et al[4]	--	Fissile materials, 520 data, 40 groups.	15 fast criticals, 15 data.	Continuous and discrete mathematical formulations. Implemented in discrete form.
Campbell and Rowlands[5]		Fissile and structural, 220 data, 10 groups. Covariances used.	17 fast criticals, 107 data. Covariances used.	Covariances allowed in special forms only.

Table 3-1. (Cont'd)

Reference	Program	Typical Application: Neutron Data	Typical Application: Integral Data	Remarks
Number of Indirect Observations Less than Number of Direct Observations				
Mitani and Kuroi[6]	LEAST	Fissile and structural. 330 data, 15 groups. Covariances used.	Fast criticals, 56 data.	Covariances in integral data not in formulation.
Gandini et al[7]	AMARA	Fissile materials, 27 data, 27 groups. Covariances used.	3 fast criticals, 12 data.	Covariances in integral data not accepted by code.
Dragt et al[8,9]	ADJ3	^{101,102,104}Ru capture cross section in variously-weighted group averages, 234 data, 26 groups. Covariances used.	^{101,102,104}Ru sample reactivity worths, 6 samples each in 5 fast cores, 30 data total. Covariances used.	Adjustment of mixed nuclear model parameters and group cross sections. Adjusted cumulatively using 26 neutron data per computer run.

analysis, failure to allow for such covariances in the code structure, or failure to evaluate such covariances in practice, is a major defect of most efforts to date.

An additional limitation of the listed programs is the need to obtain sensitivity coefficients by an independent computer program which is at best coupled to the consistency analysis code by tape, disc, cards, or other media. Such an independent mode of operation is acceptable in the linear case, since the sensitivity coefficients need be calculated only once. However, the mode is tedious and error-prone in the non-linear case, since the sensitivity coefficients must be iterated. For the non-linear analyses required to extend the techniques of consistency analysis to a wider class of problems, it is more efficient to develop a computer program with integral modules for both the sensitivity calculation and the consistency calculation.

Prototypes of such a unitary program fit thermal cross section data and neutronic data for the fissile nuclides. One such program, DAFT1,[10] authored by D. R. Harris, served as the prototype of ALVIN. Initially, the consistency or least-squares module of ALVIN, DAFT2, was based on the standard least-squares algorithm given in Chapter II. Subsequently, Harris added a second module, DAFT3, to exploit the reduced matrix inversion requirements of the third algorithm.[11] However, the initial version of DAFT3 allowed no covariances. This restriction was removed in a collaborative effort[12] between Harris and D. W. Muir and

the present author. The resulting code is documented elsewhere,[13] but to introduce a framework for the discussion of the additional programming developments in ALVIN2, this chapter presents additional background.

Sensitivity Model

ALVIN calculates the sensitivity matrix elements with the first-order perturbation theory[14] and normalizes them as required in Equation 2-29 of the linear model. The interpretation used in ALVIN and in ALVIN2 is similar to an earlier formulation.[15] This section reviews the perturbation theory and discusses modifications and extensions of the theory required in ALVIN2.

Sensitivities

A time-independent inhomogeneous operator equation has the form:

$$L\psi = S, \tag{3-1}$$

and its adjoint counterpart has the form:

$$L^{+}\psi^{+} = S^{+}. \tag{3-2}$$

Here the forward and adjoint solutions ψ and ψ^{+} satisfy certain boundary conditions. The adjoint operator L^{+}, satisfies the general condition of adjointness:

$$(\chi^{+},L\phi) = (L^{+}\chi^{+},\phi), \tag{3-3}$$

and specifically:

$$(\psi^{+},L\psi) = (L^{+}\psi^{+},\psi). \tag{3-4}$$

The inner product (ϕ,χ) denotes the integral of $\phi(\xi)\chi(\xi)$ over all phase space ξ.

It is desirable at this point to derive a lemma for future use as follows. From Equation 3-2 and the adjoint relation, Equation 3-3:

$$(S^+,\psi) = (L^+\psi^+,\psi) = (\psi^+,L\psi), \tag{3-5}$$

but by Equation 3-1:

$$(\psi^+,L\psi) = (\psi^+,S), \tag{3-6}$$

hence the lemma:

$$(S^+,\psi) = (\psi^+,S). \tag{3-7}$$

The inner products in Equation 3-7 are subsequently identified with the integral transport quantities of interest in the consistency analysis.

For perturbations in L, L^+, S, and S^+, Equations 3-1 and 3-2 become

$$(L+\delta L)(\psi+\delta\psi) = S + \delta S, \tag{3-8}$$

and:

$$(L^+ + \delta L^+)(\psi^+ + \delta\psi^+) = S^+ + \delta S^+. \tag{3-9}$$

The change in an inner product, say (S^+,ψ), is obtained, in terms of the changes in the operators and in the sources, as follows.

By definition:

$$\delta(S^+,\psi) = (S^+ + \delta S^+, \psi+\delta\psi) - (S^+,\psi). \tag{3-10}$$

The expression is expanded as follows:

$$\begin{aligned}\delta(S^+,\psi) &= (S^+,\psi+\delta\psi) + (\delta S^+,\psi+\delta\psi) - (S^+,\psi) \\ &= (S^+,\psi) + (S^+,\delta\psi) - (S^+,\psi) + (\delta S^+,\psi+\delta\psi) \\ &= (S^+,\delta\psi) + (\delta S^+,\psi+\delta\psi).\end{aligned} \tag{3-11}$$

Eliminate S^+ on the r.h.s. by using Equation 3-2:

$$\delta(S^+,\psi) = (L^+\psi^+,\delta\psi) + (\delta S^+,\psi+\delta\psi). \tag{3-12}$$

The general adjoint condition, Equation 3-3, is used:

$$\delta(S^+,\psi) = (\psi^+,L\delta\psi) + (\delta S^+,\psi+\delta\psi), \tag{3-13}$$

and $L\delta\psi$ is eliminated by expanding Equation 3-8.

Finally, the change in (S^+,ψ) is obtained in terms of the changes in the operators and in the sources by using Equation 3-1 to give:

$$\delta(S^+,\psi) = -[\psi^+,\delta L\ (\psi+\delta\psi)] + (\psi^+,\delta S) + (\delta S^+,\psi+\delta\psi). \tag{3-14}$$

Note that Equation 3-14 is exact and is valid for large perturbations in the operators and sources. In this exact equation the perturbed function ψ is required. Since the exact solution of the perturbed equation is as costly as calculating $\delta(S^+,\psi)$ by direct successive calculations, the classical first-order perturbation theory assumption of small changes is invoked. It is assumed that the changes L, L^+, S, and S^+ are sufficiently small that $\psi+\delta\psi\simeq\psi$. In this case, Equation 3-14 becomes:

$$\delta(S^+,\psi) = -(\psi^+,\delta L\psi) + (\psi^+,\delta S) + (\delta S^+,\psi). \tag{3-15}$$

For the case of no change in the forward-equation source δS, a simpler form results:

$$\delta(S^+,\psi) = -(\psi^+,\delta L\psi) + (\delta S^+,\psi). \tag{3-16}$$

From the above approximate expression for $\delta(S^+,\psi)$ in $\delta L\psi$ and δS^+, a more useful expression is obtained by identifying Equation 3-1 with the Boltzmann transport equation. In a one-dimensional multigroup represen-

tation the angular variables are expanded in spherical harmonics. In the case of azimuthal symmetry, i.e. for plane and spherical geometry, expansion in the simpler Legendre polynomials is possible. The angular flux ψ, for example, is expanded as follows:

$$\psi_g(\underline{r},\underline{\Omega}) = \sum_{j=0}^{\infty} \frac{2j+1}{4\pi} \psi_{gj}(\underline{r}) P_j(\mu), \tag{3-17}$$

and:

$$\psi_g^+(\underline{r},\underline{\Omega}) = \sum_{j=0}^{\infty} \frac{2j+1}{4\pi} \psi_{gj}^+(\underline{r}) P_j(\mu), \tag{3-18}$$

where g represents the g-th energy group, $\underline{r}$ and $\underline{\Omega}$ denote the particle position and direction vectors, and P_j represents the j-th Legendre polynomial.

Thus $L\psi=S$ assumes the form:

$$(\dot{\nabla}\cdot\underline{\Omega}+\Sigma_g) \sum_{j=0}^{\infty} \frac{2j+1}{4\pi} \psi_{gj}(\underline{r}) P_j(\mu) \tag{3-19}$$

$$- \sum_{g'=1}^{\hat{g}} \sum_{j=0}^{\infty} \frac{2j+1}{4\pi} \Sigma^j_{g'\to g} \psi_{g'j}(\underline{r}) P_j(\mu) = \sum_{j=0}^{\infty} \frac{2j+1}{4\pi} S_{gj}(\underline{r}) P_j(\mu),$$

where Σ_g is the macroscopic cross section in group g, and $\Sigma^j_{g'\to g}$ is the j-th component of the scattering cross section from group g' to group g. The perturbation of $L\psi$ is then:

$$\delta L\psi = (\delta\Sigma^x_g) \sum_j \frac{2j+1}{4\pi} \psi_{gj} P_j(\mu) - \sum_{g'=1}^{\hat{g}} \sum_j \frac{2j+1}{4\pi} (\delta\Sigma^{x,j}_{g'\to g}) \psi_{g'j} P_j(\mu), \tag{3-20}$$

where "x" denotes the perturbed nuclide and partial reaction type, the j-summation is carried out over all Legendre moments, and the spatial

variable is now implicit. Similarly, the perturbation of S^+ is given by:

$$\delta S^+ = \sum_j \frac{2j+1}{4\pi} (\delta S^+_{gj}) P_j(\hat{\mu}) . \tag{3-21}$$

Insert the above expressions for $\delta L\psi$ and δS^+ into Equation 3-17 and expand ψ and ψ^+. By using the orthogonality condition:

$$\int_{-1}^{+1} P_j(\mu) P_\ell(\mu) d\mu = \frac{2\delta_{j\ell}}{2j+1} ,$$

$$\delta_{j\ell} = \begin{cases} 0, j \neq \ell \\ 1, j = \ell, \end{cases} \tag{3-22}$$

one obtains in a straightforward manner:

$$\delta(S^+,\psi) = -\int \underline{dr} \sum_g \sum_j \frac{2j+1}{4\pi} [(\delta\Sigma^x_g)\psi_{gj} - \sum_{g'=1}^{\hat{g}} (\delta\Sigma^{x,j}_{g'\to g})\psi_{g'j}]\psi^+_{gj}$$

$$+ \int \underline{dr} \sum_g \sum_j \frac{2j+1}{4\pi} (\delta S^+_{gj})\psi_{gj} . \tag{3-23}$$

Here the volume element relation, $\int \underline{d\Omega} = 2\pi \int_{-1}^{+1} d\mu = 4\pi$, has been used to eliminate Ω.

The above equation contains the general angle-dependent adjoint source in the form of Legendre expansion coefficients S^+_{gj}.

$$S^+_{gj} = 2\pi \int_{-1}^{+1} S^+_g(\mu) P_j(\mu) d\mu . \tag{3-24}$$

Although these coefficients may be obtained for any order of angular anisotropy in S^+_g, all of the applications in this work identify S^+_g with the angle-integrated cross section Σ^x_g. In particular,

$$S^{+}_{g,0} = 2\pi \int_{-1}^{+1} \Sigma^{x}_{g} \cdot 1 \cdot d\mu = 4\pi\Sigma^{x}_{g}, \tag{3-25}$$

and $S^{+}_{gj} = 0$ for $j > 0$. Then Equation 3-23 becomes

$$\delta(S^{+},\psi) = -\int_{T} \underline{dr} \sum_{g}\sum_{j} \frac{2j+1}{4\pi} [(\delta\Sigma^{x}_{g})\psi_{gj} - \sum_{g'=1}^{\hat{g}} (\delta\Sigma^{x,j}_{g'\to g})\psi_{g'j}]\psi^{+}_{gj}$$
$$+ \int_{R} \underline{dr} \sum_{g} (\delta\Sigma^{x}_{g}) \frac{n_R}{n_T} \psi_{gj}. \tag{3-26}$$

The $(\delta S^{+},\psi)$ term allows for the fact that the number density n_R and the spatial region R of the cross section identified with the integral quantity of interest may be different than the number density n_T and spatial region T for the transport medium cross section. The latter situation occurs, for example, when the integral quantity of interest is the fission rate in a thin foil of enriched ^{238}U which is embedded in a slab of natural UO_2 and the ^{238}U (n,f) reaction is perturbed. Then R extends over the foil only and T extends over the slab.

Equation 3-26 gives the total variation in(S^{+},ψ) for given changes in Σ^{x}_{g} and in the various $\Sigma^{x,j}_{g'\to g}$. Note that the first integral, i.e., the transport contribution, consists of a loss term, due to the importance-weighted removal of neutrons when the within-group cross section is increased, and a gain term, which represents the importance-weighted arrival of neutrons when the in-scattering cross section from other groups is increased. The second integral, i.e., the detector contribu-

tion, represents a gain in the response which is directly due to the increase in the detector cross section itself. It is not importance-weighted. This second term is calculated by ALVIN2 but not by ALVIN.

By taking the partial derivatives the sensitivity coefficients are obtained:

$$\frac{\partial(S^+,\psi)}{\partial\Sigma_g^x} = -\int_T \underline{dr} \sum_j \frac{2j+1}{4\pi} \psi_{gj} \psi_{gj}^+ + \int_R \underline{dr} \frac{n_R}{n_T} \psi_{gj}, \tag{3-27}$$

and:

$$\frac{\partial(S^+,\psi)}{\partial\Sigma_{g'\to g}^{x,j}} = \int_T \underline{dr} \frac{2j+1}{4\pi} \psi_{g'j} \psi_{gj}^+ \tag{3-28}$$

Alternatively, these equations may be placed on a microscopic basis:

$$\frac{\partial(S^+,\psi)}{\partial\sigma_g^x} = -\int_T \underline{dr}\, n_T \sum_j \frac{2j+1}{4\pi} \psi_{gj} \psi_{gj}^+ + \int_R \underline{dr}\, n_R \psi_{gj}, \tag{3-29}$$

and:

$$\frac{\partial(S^+,\psi)}{\partial\sigma_{g'\to g}^{x,j}} = \int_T \underline{dr}\, n_T \frac{2j+1}{4\pi} \psi_{g'j} \psi_{gj}^+ \tag{3-30}$$

Sensitivity Profile. In principle, all of the group transfer cross sections and their Legendre expansions may vary in consistency analysis. That is, the shapes of the secondary neutron energy-angle

distributions may vary. In a hundred-group problem the number of cross section variables in the consistency analysis then becomes of order 10^4 per nuclide per reaction type and this number, particularly for initial scoping calculations, is inconveniently large. Instead, one may define a perturbation in which the secondary neutron energy-angle distributions are fixed. Then, for the perturbed group g:

$$\frac{\delta\Sigma^{x,j}_{g\to g'}}{\Sigma^{j}_{g\to g'}} = \frac{\delta\Sigma^{x}_{g}}{\Sigma^{x}_{g}}, \tag{3-31}$$

for all j. For the unperturbed groups, $g' \neq g$:

$$\frac{\delta\Sigma^{x,j}_{g'\to g}}{\Sigma^{x,j}_{g'\to g}} = 0. \tag{3-32}$$

Then the variation in (S^+,ψ) is:

$$\delta(S^+,\psi) = \frac{\partial(S^+,\psi)}{\partial\Sigma^{x}_{g}}\,\delta\Sigma^{x}_{g} + \sum_{j=0}^{\infty}\sum_{g'}\frac{\partial(S^+,\psi)}{\partial\Sigma^{x,j}_{g\to g'}}\,\delta\Sigma^{x,j}_{g\to g'}. \tag{3-33}$$

and from Equation 3-31:

$$\delta(S^+,\psi) = \frac{\partial(S^+,\psi)}{\partial\Sigma^{x}_{g}}\,\delta\Sigma^{x}_{g} + \sum_{j=0}^{\infty}\sum_{g'}\frac{\partial(S^+,\psi)}{\partial\Sigma^{x,j}_{g\to g'}}\,\frac{\delta\Sigma^{x}_{g}}{\Sigma^{x,j}_{g\to g'}}\,\Sigma^{x,j}_{g\to g'}. \tag{3-34}$$

The following form represents Equation 3-34 as a dimensionless derivative:

$$\frac{\partial(S^+,\psi)}{(S^+,\psi)}\Big/\frac{\partial\Sigma^{x}_{g}}{\Sigma^{x}_{g}} = \frac{1}{(S^+,\psi)}\left\{\frac{\partial(S^+,\psi)}{\partial\Sigma^{x}_{g}}\,\Sigma^{x}_{g}\right.$$

$$+ \sum_{j=0}^{\infty} \sum_{g'} \frac{\partial(S^{+},\psi)}{\partial \Sigma^{x,j}_{g\to g'}} \Sigma^{x,j}_{g\to g'} \Big\} \equiv P^{x}_{g} \,. \qquad (3\text{-}35)$$

A plot of P^{x}_{g} vs. g is known as a sensitivity profile.[15] It conveniently characterizes a simple class of cross section sensitivities which are useful in consistency analysis.

Extensions of Sensitivity Theory

To permit the application of ALVIN to a wider class of problems and to effect certain economies in storage requirements, new features were developed for the present work. This section treats extensions of the sensitivity theory.

Detector Contribution

An important sensitivity calculation not addressed in the original version of ALVIN treats cross section perturbations which affect not only the transport of neutrons from source to detector but the detector response as well. For compactness of presentation the previous section already includes the additional theoretical expressions.

Sensitivity Profile for Constant Total Cross Section. While the value of a given partial cross section, such as elastic scattering, may be rather uncertain, relatively little uncertainty may be associated with the more easily measured total cross section. One could formulate the consistency analysis problem in 2*NG cross section variables, where NG is the number of energy groups, and where the invariance of the total

cross section is treated by means of negative covariances. But it is more convenient to use only NG variables of one partial cross section, e.g., the elastic, and to use a sensitivity coefficient which represents the change in the integral quantity when the one reaction is varied but the total cross section is held constant. Thus the number of cross section variables is halved and the storage requirements and execution time are reduced.

The reaction, x, and its complement, y, are defined by the relation:

$$\sigma_g^t = \sigma_g^x + \sigma_g^y, \tag{3-36}$$

where σ^t is the total cross section. Let the uncertainty in σ_g^t be sufficiently small that for practical purposes σ_g^t is constant. Then:

$$d\sigma_g^x = -d\sigma_g^y \tag{3-37}$$

Introduce the partial sensitivity profile elements under the condition that the secondary neutron energy and angular distributions are constant. Thus:

$$p_g^z = \frac{\partial(S^+,\psi)}{\partial\sigma_g^z} \Big/ \frac{(S^+,\psi)}{\sigma_g^z}, \tag{3-38}$$

for z = x, y. The total derivative is given by the equation:

$$d(S^+,\psi) = \frac{\partial(S^+,\psi)}{\partial\sigma_g^x}\, d\sigma_g^x + \frac{\partial(S^+,\psi)}{\partial\sigma_g^y}\, d\sigma_g^y, \tag{3-39}$$

But Equation 3-37 and 3-39 imply:

$$d(S^+,\psi) = \frac{\partial(S^+,\psi)}{\partial\sigma_g^x}\, d\sigma_g^x - \frac{\partial(S^+,\psi)}{\partial\sigma_g^y}\, d\sigma_g^x, \tag{3-40}$$

and:

$$\frac{d(S^+,\psi)}{d\sigma_g^x} = \frac{\partial(S^+,\psi)}{\partial\sigma_g^x} - \frac{\partial(S^+,\psi)}{\partial\sigma_g^y} . \qquad (3\text{-}41)$$

Insertion of Equation 3-38 into Equation 3-41 leads to the desired compound sensitivity profile:

$$p_{xy}^g = \frac{d(S^+,\psi)}{(S^+,\psi)} \Bigg/ \frac{d\sigma_g^x}{\sigma_g^x} \Bigg|_{\sigma^t=\text{const.}} = p_g^x - \frac{\sigma_g^x}{\sigma_g^y} p_g^y . \qquad (3\text{-}42)$$

Programming of Consistency Algorithms

The present section summarizes programming features of the consistency analysis algorithms developed in Chapter I. Both the original ALVIN code and the modifications and extensions implemented in ALVIN2 are treated. Sensitivity programming features are discussed in a later section.

ALVIN

D. R. Harris programmed the bulk of the consistency analyses features of the original code. This subsection highlights those features which are of immediate interest. Additional detail is provided by Reference 13.

Internal Features. The standard least-squares method and the case of no cross-type correlations with the number of indirect observations less than the number of direct observations are implemented in subroutines DAFT2 and DAFT3, respectively. Two departures from the

format of Chapter II are of interest. First, the dimensionless forms of the variables in ALVIN differ slightly from those given in Chapter II. The former refer to the evaluated cross section data or to the integral data: the latter refer to the arbitrary cross section reference point or to the integral quantities calculated at this reference point. It is easily shown that both algorithms give identical results when these dimensionless quantities are interpreted consistently within their respective algorithms.

Second, in both DAFT2 and DAFT3 the ratio of external-to-internal consistency, $\hat{s}^2$, is not always applied to the output dispersion matrix, as indicated in Chapter II. When the initially computed value falls below unity, it is reset to unity. This procedure implements Birge's recommendation that the errors should be assigned according to internal consistency or according to external consistency, whichever is worse. However, the value of the reduced final chi-square, which is numerically equal to $\hat{s}^2$, is printed for reference purposes.

Input/Output Features. Input features of interest are the input observation vector, the input design or sensitivity matrix, and the input dispersion matrix. Output features include the basic output observation vector and output dispersion matrix, as well as certain diagnostic features.

An input subroutine, INFO, supplies the input observation vector and input dispersion matrix to both DAFT2 and DAFT3. Similarly, the input design or sensitivity matrix is supplied from cards by an input

routine, SENSRD, and/or by the sensitivity calculation subroutine, SENSI. INFO presets the reference values of the cross sections at their initial values, that is, O(X) = 0 in the linearized form. Thus, INFO does not yet permit iterative, non-linear operation, where O(X) may be non-zero on the first iteration.

The dispersion matrix input to INFO may be either a vector of relative standard deviations of differential and integral data, or may be a full relative dispersion matrix. If DAFT3 is used, cross-type partitions are ignored. SENSRD permits the reading of an externally prepared sensitivity matrix S of order equal to the number of integral data by the number of differential data. Alternatively, a partition of this matrix is used if the balance of S is to be calculated by SENSI. For DAFT2, which uses the full design matrix A of the general least-squares method, DAFT2 internally supplies the identity partition. To use DAFT2 as a general least-squares algorithm the I-setting function of DAFT2 must be replaced by more general coding, or a dummy vector of cross-section variables must be supplied.

Outputs include the adjusted observation vector and the adjusted dispersion matrix, as well as various diagnostics. These are supplied by both DAFT2 and DAFT3 using similar, internally coded output formats. The output observation vector is a relative cross section or integral value. After rescaling by $\hat{s}^2$, the output dispersion matrix is available as the subset of relative standard deviations, the full relative disper-

sion matrix, or the full correlation coefficient matrix. In addition, the dispersion matrix partitions of adjusted differential alone and of adjusted integral data alone are printed.

Output diagnostics include chi-square diagnostics, the dispersion multiplier or scale factor, and the matrix inversion determinants. Chi-square diagnostics give the contributions of the individual diagonal elements which represent cross-section residuals and integral-value residuals, the diagonal sum for the cross-section residuals, and the diagonal sum for the integral-value residuals. Also printed is the reduced chi-square of the entire system before and after adjustment.

ALVIN2

For increased utility the consistency analysis routines in ALVIN have been modified and extended. In ALVIN2 the matrix multiplication operations of DAFT3 have been greatly speeded by saving intermediate matrix products in otherwise redundant arrays. As originally coded, DAFT3 calculated directly the general element of the final product. The output format has been expanded to include the relative standard deviations of the calculated integral quantities which are due to the input cross section errors. Thus, it is possible to examine the uncertainty of the integral quantity before, as well as after, adjustment. Output diagnostics have been increased by supplementing the matrix inversion determinant check with a direct multiplication check on the matrix and its calculated inverse. If any element of the product matrix

differs from the identity matrix by more than a predetermined amount, the element in question is printed.

Programming of Sensitivity Model

Summarized in this section are features of interest in the sensitivity programming. Both the original code and modifications and extensions implemented for ALVIN2 are treated here. A later section treats the interaction of the consistency and sensitivity features.

ALVIN

W. B. Wilson programmed the bulk of the original sensitivity modules. The heart of the sensitivity calculations, Equations 3-29 and 3-30, are implemented by subroutine SENSI, using geometry data and density data read in by SENSI and fluxes and adjoints read in by subroutine REDFLX. Discrete ordinates directed fluxes are converted by REDFLX to Legendre fluxes. SENSI normalizes, stores, and transmits through labeled commons selected sensitivities for use in the consistency algorithms. For this purpose integral data are read in by SENSI and cross section data are read in by subroutine CROSEC. Sensitivity profiles are in turn compounded by subroutine PROFIL from data supplied by SENSI and CROSEC. In ALVIN, sensitivity profiles are printed but are not passed to the consistency algorithms.

ALVIN2

Modifications and extensions of the sensitivity model discussed previously have been implemented in ALVIN2 by the present author. In addi-

tion, certain improvements were made to render the code more flexible when applied to a wider class of problems.

Additional terms representing the detector response in Equation 3-29 have been added to SENSI, and input statements have been provided which prescribe the detector integration region and the corresponding nuclide number density.

The compound sensitivity profile given in Equation 3-42 may be implemented in several ways. In the present work, a small auxiliary program was written to perform the indicated sum, using P_g^x and P_g^y from two previous PROFIL calculations.

ALVIN requires that the order of Legendre expansion of the input cross section transfer matrix $\sigma_{g\to g'}^{x,j}$ be equal to the order of expansion of the fluxes. It is occasionally found that the anisotropy of inelastic partial cross sections is not processed at the multigroup stage. Hence, provision has been made in ALVIN2 to separately stipulate the order of expansion of the perturbed cross section and the order of the fluxes.

It has been mentioned previously that sensitivities calculated according to Equations 3-29 and 3-30 in SENSI may be normalized and stored in a sensitivity array for use in the subsequent process of consistency analysis. In ALVIN no provision has been made for the storage of sensitivity profiles in the consistency analysis sensitivity arrays. This limitation has been removed in ALVIN2 by means of a new subroutine, PROSAV.

To simplify the solution of shielding problems and breeding blanket problems, where the integral quantities may consist of various detectors located at several depths in the same assembly, ALVIN2 includes a coding option which requires only the reading of a single forward flux file and several adjoint flux files instead of several pairs of forward and adjoint flux files.

ALVIN2 Graphics Features

ALVIN2 generates additional output files for use by two post-processing graphics codes, ALPLOT and HIST3D. ALPLOT generates input and output observation vector data, error vector data, and selected sensitivity data in a format for use by the proprietary interactive graphics package DISSPLA. HIST3D prepares sensitivity matrix and dispersion matrix input data for the LASL three-dimensional graphics program PICTURA.

Program Architecture

ALVIN contains two main functions as previously described: the consistency analysis and the sensitivity coefficient calculation. The two functions are coordinated by an executive function, or main program. The main program reads the problem size and two basic control parameters, KSENS and KADJST, from the input stream. KSENS and KADJST determine the detailed mode of operation of the sensitivity functions and of the data adjustment functions, respectively, as shown in Figure 3-1. Depending

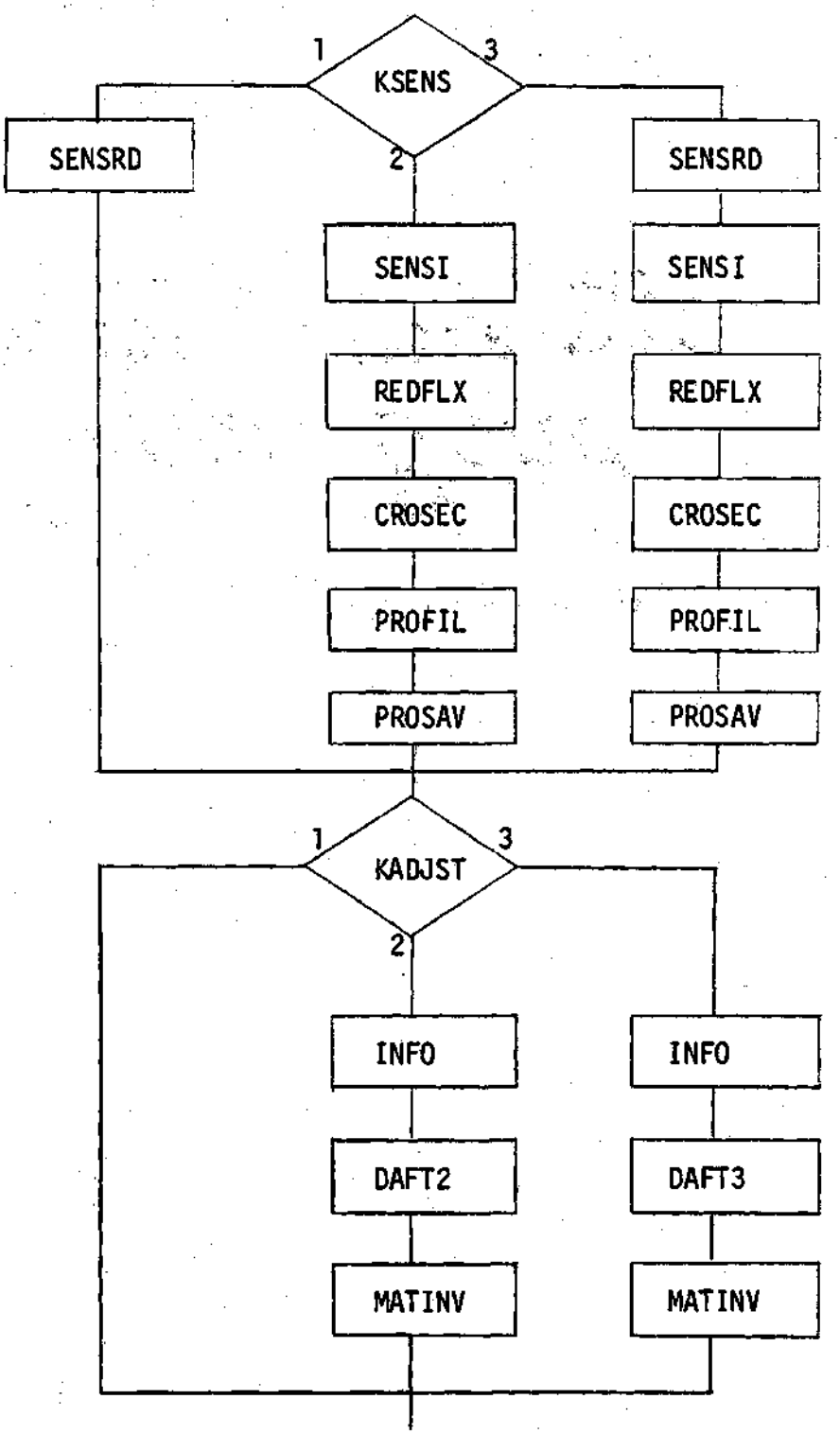

Figure 3-1. ALVIN2 Flowchart.

on the value of KSENS, the program reads externally prepared sensitivities using subroutine SENSI and its subroutine, or both reads in sensitivities and calculates sensitivities. Depending on the value of KADJST, ALVIN terminates with the sensitivity function or combines the sensitivities with DAFT2 or DAFT3. The order of subroutine calls for the various paths is also shown, and includes the ALVIN2 subroutine PROSAV for the storing of calculated sensitivity profiles. As presently operated at the Los Alamos Scientific Laboratory Central Computing Facility, the 1100 statement lines of the ALVIN program are maintained on an IBM photostore memory. The program is edited on-line, using the CDC UPDATE software package, to implement ALVIN2. Further details are provided in a technical report,[13] in program-package documentation at the Argonne Code Center, and in Appendix I of the present work.

Code Validation

The ALVIN codes have been validated by separate tests in the adjustment mode, in the sensitivity mode, and in the present work, in the combined mode.

Previous Work

D. R. Harris used DAFT2 and DAFT3 to solve a small test problem for comparison with desk-calculator results. Harris also performed a larger, preliminary adjustment of 19 differential data and 24 fast, critical assembly integral data, without correlations, using both DAFT2 and DAFT3. Identical adjustments were obtained with each module.[13]

W. B. Wilson validated the sensitivity modules by comparing ALVIN results with sensitivities which were directly calculated from successive runs by using unperturbed and perturbed cross section libraries. Results for absorbed dose in air at the edge of a 70-cm radius iron sphere driven by a D-Be neutron source and calculated by $S_{16}P_5$ discrete-ordinates with 41 energy groups were in satisfactory agreement for perturbations in the Fe total group cross section up to 10%.[13]

Present Work

Further validation of the sensitivity modules and the first linkage of the sensitivity and adjustment modules of ALVIN and ALVIN2 were performed by this author. The sensitivity module validation differs from the previous validation by perturbing a partial cross section instead of a total reaction cross section, by testing the capability of the sensitivity module to calculate several sets of sensitivity profiles in a single run, and by testing the detector response $(\delta S^{+},\psi)$ added to ALVIN2. Further details of the sensitivity matrix validation used in the computations of the present work are given in Appendix III. Combined use of the sensitivity and adjustment modules validated the sensitivity storing functions and tested the error correlation features of ALVIN2.

REFERENCES

1. J.P. Chaudat, J.Y. Barré, and A. Khairaillah. Proc. Int. Symp. Physics of Fast Reactors, Tokyo, October 16-19, 1973, Vol. 1, p.1207, Power Reactor and Fuel Development Corporation, Tokyo (1973).

2. P.C.E. Hemment and E.D. Pendlebury. Proc. Int. Conf. Fast Critical Experiments and their Analysis, Argonne, Illinois, October 10-13, 1966. ANL-7320, p. 88, Argonne National Laboratory (1966).

3. H. Häggblom. Adjustments to Neutron Data from ENDF/B-III by Using Integral Data in a Least-Squares Fit. AE-RF-74-3037, Aktiebolaget Atomenergi (1974).

4. C.G. Campbell and J.L. Rowlands. The Relationship of Microscopic and Integral Data. 2nd Int. Conf. Nuclear Data for Reactors, Helsinki, 15-19 June 1970, Vol. 2, p. 391. International Atomic Energy Agency, Vienna (1970).

5. A. Pazy, G. Rakavy, I. Reiss, J.J. Wagschal, and Atara Ya'ari. Nucl. Sci. Eng.,55, 280 (1974).

6. H. Mitani and H. Kuroi. J. Nucl. Sci. Technol.,9, 642 (1972).

7. A. Gandini, M. Petilli, and M. Salvatores. Proc. Int. Symp. Physics of Fast Reactors, Tokyo, October 16-19, 1973, Vol. 2, p. 629. Power Reactor and Fuel Development Corporation, Tokyo (1973).

8. H. Gruppelaar, J.B. Dragt, A.J. Janssen, and J.W.M. Dekker. Nuclear Cross Sections and Technology, Vol. 1, p. 165. NBS Special Publication 425, U.S. National Bureau of Standards (1975).

9. J.B. Dragt, J.W.M. Dekker, H. Gruppelaar, and A.J. Janssen. Nucl. Sci. Eng.,62, 117 (1977).

10. D.R. Harris. DAFT1 - A Fortran Program for Least Squares Fitting of 0.0253 eV Neutron Data for Fissile Nuclides, WAPD-TM-761. Bettis Atomic Power Laboratory (1968).

11. D.R. Harris and W.B. Wilson. Technique for Simultaneous Adjustment of Large Nuclear Data Libraries, in G.M. Hale, D.R. Harris, and R.E. MacFarlane, Applied Nuclear Data Research and Development Quarterly Progress Report, Oct. 1-Dec. 31, 1974, p. 11, LA-5944-PR, Los Alamos Scientific Laboratory (1975).

12. W.A. Reupke, D.R. Harris, and D.W. Muir. Techniques for Simultaneous Adjustment of Large Nuclear Data Libraries (II), in D.W. Muir and P.G. Young, Applied Nuclear Data Research and Development, Apr. 1-June 30, 1975, p. 12, LA-6123-PR, Los Alamos Scientific Laboratory (1975).

13. D.R. Harris, W.A. Reupke, and W.B. Wilson. Consistency Among Differential Nuclear Data and Integral Observations: The ALVIN Code for Data Adjustment, for Sensitivity Calculations, and for Identification of Inconsistent Data, LA-5987, Los Alamos Scientific Laboratory (1975).

14. G.I. Bell. Nuclear Reactor Theory, Van Nostrand Reinhold Company, New York (1970).

15. D.E. Bartine, F.R. Mynatt, and E.M. Oblow. SWANLAKE, A Computer Code Utilizing ANISN Radiation Transport Calculations for Cross Section Sensitivity Analysis, ORNL-TM-3809, Oak Ridge National Laboratory (1973).

CHAPTER IV

COMPUTATIONAL PROCEDURE

Chapter IV presents a method of attack suitable for most computational tasks in consistency analysis, it describes the selection of a specific problem in fusion reactor neutronics consistency analysis, and it sets forth the calculational procedure for this selected problem in sufficient detail to permit the replication of results. These results are then presented in Chapter V.

Method of Attack

The first task in consistency analysis is the choice of suitable neutronics data, including the integral experiments proper. As indicated in Chapter II, the choice of problem and selection of data may involve considerably more effort than the calculation itself. Once suitable data have been identified, the computational procedure may be broken down into two areas: determination of the consistency of the data prior to, and after, the adjustment. Tasks pertaining to the consistency of the data before adjustment include the calculation of the integral quantities from the unadjusted cross-section data, the evaluation of the experimental integral results and the associated error matrix, and the calculation of the chi-square of the system at the reference point corres-

ponding to the initially evaluated cross sections. Tasks pertaining to the consistency of the data after adjustment include the evaluation of the cross section error matrix and the calculation of the sensitivity matrix.

Selection of Data for Analysis

General

Neutronics data selection criteria may be divided into two general kinds: 1) purpose-dependent criteria, and 2) purpose-independent criteria. These are briefly summarized as follows:

Purpose-dependent Criteria. Broadly speaking, neutronic data consistency analysis serves one of two purposes: 1) to facilitate neutronic design, and 2) to improve basic cross section data. The selection criteria for integral experiments in neutronic data consistency analysis depend in some measure on which of these two objectives is to be emphasized.

For the purpose of aiding neutronic design, the basic criterion is that the integral experiment approximate reasonably well, in a neutronics sense, the engineering design of interest. Obviously, the integral experiment should not duplicate the design (otherwise the design prototype itself would serve as the experiment). Similarity of design is desirable for two reasons. One is to guarantee that the governing, or sensitive, cross sections are similar. This requirement is illustrated in extreme form when the consistency analysis is carried out in a broad

energy group environment. In this case, similarity-of-spectrum must be assured in order that the adjusted group cross sections from the consistency analysis be applicable to the engineering design of interest. The second reason for seeking neutronic similarity arises from a peculiar feature of systematic error in consistency analysis. When systematic error in the transport calculation is unduly large relative to statistical error, the minimization may be thought of as yielding a set of fictitious cross sections that will tend to minimize the discrepancy between calculation and experiment for all systems with a sufficiently similar calculational bias, but which will tend to worsen the agreement when the calculational bias is reversed. Thus, the criterion of neutronic similarity in integral experiment selection represents a cushion against the normally undesirable effects of uncorrected or unidentified systematic error in the transport calculation.

The criteria for general cross section improvement are rather different. Here, reduction of calculation-vs.-experiment discrepancies over the widest possible applications range is desired. For this purpose, utmost emphasis must be placed on the reduction of calculational systematic error. The latter, in turn, favors experiments expressly designed to ease calculational difficulties. Such clean integral experiments should also encompass a wide range of neutron spectra and should incorporate a variety of response function spectra in order to minimize the effects of unidentified bias. While constituent nuclides will be

those of practical interest, it is desirable to limit the number of nuclides to reduce data storage requirements and to permit analysis in a fine energy group structure with fine angular resolution.

Historically, the primary purpose of most data adjustment efforts is to facilitate neutronic design. In certain cases, the conditions warrant a secondary objective of general cross-section improvement. That is, the two purposes need not be mutually exclusive.

Purpose-independent Criteria. A number of important criteria in neutronics data selection are common to both of the previously enumerated purposes of consistency analysis. These include the following: 1) A reasonably well evaluated set of reference cross sections should exist. In particular, it should be free of unidentified systematic error. 2) The chosen integral quantities and their cross-section sensitivities should be economically calculable without a large residue of calculational systematic error. 3) The integral data should be sufficiently well understood to permit an evaluation which is reasonably free of uncorrected systematic error. 4) The statistical errors on the integral data should be sufficiently small, and the cross-section sensitivities sufficiently high that the integral data has significant effect on the overall data consistency. 5) A good cross-section error evaluation, including evaluated covariances, should exist or be readily obtainable. 6) For a linear analysis, the cross-section sensitivities should be constant within the evaluated uncertainty limits of the cross sections.

Since it is usually not possible to know in advance whether the above general criteria are satisfied by a given set of integral data, a certain amount of trial-and-error is necessary in practice. However, even in such cases as prove unpromising after preliminary analysis, the way is often found thereby to the development of new integral experiments which satisfy the desired criteria.

Present Work

The purpose of the present work is to develop and to implement a method of statistical consistency analysis, with application to specific neutronics design problems, namely thermonuclear neutronics design problems. Integral experiments for this application lie in the historical area of thermonuclear weapons design, and in the more recently active area of fusion power reactor blanket design. A targeted consistency analysis for design purposes would concentrate in one area, while a comprehensive program of cross-section improvement for the energy range 14 MeV and below would encompass integral experiments of both weapon and reactor orientation.

Since, in the present investigation, primary emphasis was placed on methods development and demonstration, and secondary emphasis was placed on the particular design application, the choice of design application was dictated primarily by convenience. By historical accident, the opportunity was presented to continue D. W. Muir's and M. E. Wyman's analysis[1] of an earlier, weapons-oriented Los Alamos experiment,[2] which

was well-suited for methods demonstration. In this experiment, Wyman measured the production of tritium in an ^{n}LiD sphere driven by 14 MeV neutrons. Note that were it not for the spectrum softening effects of the deuterium, the experiment would also be suitable for power reactor design application. See Table 4-1.

In addition, early consideration was given to the Livermore leakage spectrum experiments.[3] However, preliminary analyses of the pulsed sphere experiments uncovered complications in the geometrical treatment which suggested deferral of this integral data to an entirely separate work (see Appendix IV).

Description of Integral Data: The Wyman Experiment

The balance of this section highlights the neutronics features of the Wyman experiment. These features are described in the previously-cited Los Alamos Scientific Laboratory report and, in greater detail, in unpublished notebooks.[4-6] The present description includes specifications of 1) the source, 2) the transport medium and boundary conditions, and 3) the detector.

The nominal source is an isotropic point source of 14.1 MeV neutrons, the transport medium is a 30-cm radius sphere composed of natural lithium deuteride of specific gravity 0.836, the outer boundary condition is a vacuum, and the detector response is the triton production (per source neutron per Li atom) in small samples of natural lithium and lithium-7 metal positioned at various radii in the sphere.

Table 4-1. Consistency Analysis Criteria: Wyman Experiment

Criteria satisfied	Criteria unsatisfied
1. 14 MeV source approximates D-T plasma neutron spectrum reasonably well.	1. ENDF/B Li cross-section error matrix not yet available.
2. Geometry is readily calculable.	2. Large D content gives softer spectrum than in most reactor blankets of interest.
3. Nuclear thickness (3.4 mfp) of system is comparable to that of reactor breeding zone.	
4. Small number of nuclides is compatible with relatively fine energy group structure.	
5. Tritium breeding in Li metal closely resembles reactor parameter of interest.	
6. Integral result errors comparable to cross-section errors.	

The actual source is a Cockroft-Walton 240 keV deuteron beam which impinges on an air-cooled tritium-loaded zirconium target at a 45° angle of incidence. The departure from nominal specifications results from 1) simple D-T reaction kinematic effects, and 2) target holder structure effects. The simple kinematic effects are well understood and permit analytic calculation of an angular distribution of yield and energy. The target structure effects are twofold: 1) those due to the deceleration of deuterons in the target structure prior to nuclear reaction, and 2) those due to the interaction of the freshly-produced neutrons with the target structure. J. D. Seagrave et al have combined the analytically represented kinematic effects with computer calculations of the first-listed target holder effects to give tabulations of neutron yield, neutron average energy, and neutron energy distribution width, as a function of azimuthal angle for targets of the type used in the Wyman experiment.[7] The neutron target interaction effects produce an alteration in total neutron yield at a given azimuthal and polar angle, as well as an alteration in neutron energy distribution. A. Hemmindinger et al have measured the yield variation, due to all effects, in azimuthal and polar angles, using a ^{238}U counter and a scintillation counter for a target similar to that used in the Wyman experiment.[8]

The actual transport medium consists of a 30-cm radius sphere of ^{n}LiD powder of specific gravity 0.836, with holes for the source assembly, including beam tube, alpha particle recoil counter, and cooling tube. A 2-cm spherical void exists at the center. The balance

of void representing the source penetrations is less than 1% of the sphere volume. As indicated in Reference 1, the deuteride may be contaminated with about 3% H_2O. The segments of the sphere are fastened together at the periphery with two aluminum rings. These represent a negligibly small fraction of the total material. The entire assembly is located within a meter or two of the laboratory floor and within a similar distance of at least one laboratory wall. However, compositions and thicknesses of these reflecting regions is unreported.

The actual detectors consist of copper-encapsulated natural lithium and 99.2% ^{7}Li-enriched lithium positioned at radii varying from 2.5 cm to 27.5 cm. Because of the possibility of flux distortion near the target structure and the possibility of room-return effects at the periphery of the sphere, only data in the region 7.5 - 25.0 cm are used in the present analysis. Although most of the detectors are embedded in the 90° plane, some are located at 0° and some at 135° to the direction of the incident beam. ^{238}U and Sc activation foils are placed at fore and aft positions in some capsules to verify that no significant flux distortion occurs near the samples.

Consistency of the Data Prior to Adjustment

Computations of the consistency of the neutronics data prior to adjustment may be logically separated from the determination of the consistency of the data after adjustment. In practice it is desirable to separate these constituent computational procedures since it is

possible that the consistency before adjustment will be sufficiently good that the adjustment will not be worth the additional calculational effort. The consistency of the data before adjustment is considered first. Here the procedures include 1) the calculation of the integral quantities from the evaluated cross sections, 2) the evaluation of the experimental integral quantities and the corresponding error matrix, and 3) the construction of the relative discrepancy vector and relative error matrix.

Calculation of Tritium Production

The geometrical properties of the Wyman experiment are sufficiently good that the experiment is essentially calculable by one-dimensional methods. Source anisotropy is accounted for by augmenting the uncertainties in the experimental integral values: that is, there is an uncertainty in what the tritium production would have been in an ideal, one-dimensional experiment. As indicated in a later section, this uncertainty may be estimated by theoretical analysis and by considerations of external consistency.

The tritium production for the Wyman experiment has been previously calculated[1] with the S_N code DTF. A similar calculation is used here. The calculational steps are: 1) the evaluation of energy-dependent cross sections, 2) the group averaging of these cross sections, and 3) the neutron flux calculation proper and the calculation of the response integral. These are explained in turn.

Evaluated Cross-Section Data. Target holder materials, moisture content, and aluminum fasteners are neglected. The principal nuclides of interest are deuterium, lithium-6, and lithium-7. Community evaluations exist for each of these three nuclides, but it is desirable to consider the comparative quality of the given evaluation and to identify shortcomings, if any.

The deuterium evaluation used in this work is the 1967 evaluation of A. Horsley and L. Stewart.[9] With the exception of the radiative capture cross section, which is negligible in the energy region of present interest, the total reaction cross section is composed of the elastic and (n,2n) partial reactions only. Two encodings exist for this evaluation. One was used for the neutron transport calculation. The other encoding, a more recent one, was used for the sensitivity calculations. That used for the transport calculations resides on the Los Alamos Master Data File and is known as Cross Section 2254. The sensitivity analysis encoding conformed to the ENDF/B-V format. For the purposes of the present work the evaluation is considered entirely satisfactory.

The lithium-6 evaluation used in these calculations is the 1964 E. Pendlebury evaluation,[10] as encoded in the ENDF/B format by M. Battat, D. Dudziak, and R. LaBauve.[11] While the concentration of ^{6}Li in ^{n}LiD is sufficiently small (3.75%) that the accuracy of the ^{6}Li total and scattering cross sections is not critical for the present calculations,

the $^{6}Li(n,t)$ reaction - which accounts for some 60% of the average tritium production in the sphere - must be rather accurately known and represented. Some modifications to the ENDF/B Version III cross section, used when these calculations were begun, have appeared in the current Version IV. However, the changes are sufficiently small in relation to the evaluated cross section errors that the Version III form was used throughout this work.

The lithium-7 evaluation is a reformatting, by the same authors, of the lithium-7 evaluation of Pendlebury et al.[12] Like deuterium, lithium-7 is a major transport nuclide in the system and the cross section detail should be known accurately. Moreover, the $^{7}Li(n,xt)$ tritium production reaction accounts for the remaining 40% of the average tritium production in the sphere. But the cross section is not known as accurately as those of the other important reactions, and a potentially significant amount of the transport information in the Pendlebury evaluation of the $^{7}Li(n,xt)$ reaction is lost or distorted in the ENDF/B representation because of early format and processing code limitations. The evaluated secondary neutron energy distribution, which is tabulated in detail by Pendlebury, is represented rather approximately by an evaporation spectrum in ENDF/B. In addition, the secondary neutron energy distribution is assumed to be the same at all secondary angles (at a given primary energy) in ENDF/B and represents a further loss of information relative to the correlated secondary

energy-angle distribution in the original British evaluation. From the viewpoint of the fission reactor community, these simplifications in the representation of a 2.8 MeV threshold reaction would not be considered serious. From the standpoint of fusion reactor neutronics, these simplifications are not desirable and the ^{7}Li ENDF/B Version III and IV representations used in the present work are considered less than satisfactory. For example, D. V. Markovskii et al have shown that the breeding ratio of a particular power reactor blanket design is overpredicted by 7% as a result of the evaporation spectrum device alone.[13]

Multigroup Cross-Sections. The group cross section set used in the calculation of the integral quantities is identical to that of Reference 1. This section summarizes: 1) the selection of energy group structure and the flux-weighting used, 2) the application of multigroup processing codes, and 3) the analysis of systematic error in the calculated integral quantities due to the multigrouping process.

The energy group structure and the within-group flux weighting follow those of Reference 1. Thus, the 100-group structure of the GAM-II library is used.[14] This structure divides the important ^{7}Li(n, xt) reaction into seventeen energy groups and gives an overall mesh which is much finer than that used in previous consistency analysis. Because of the matrix inversion simplification in DAFT3, where the order of matrix to be inverted is equal only to the number of integral data,

the use of this relatively fine mesh does not pose a serious computational obstacle. Apart from the general desirability of a fine mesh for purposes of systematic error reduction, the relative insensitivity to the flux weighting assumption in the finer mesh confers greater generality on the adjusted cross sections.

To choose the within-group flux weighting note that all cross sections of major significance are smoothly varying functions of energy, with the exception of certain broad resonances in the ^{6}Li and ^{7}Li partial cross sections near 250 keV. In the 100 energy group GAM-II structure used in this work, these resonances and the associated flux depression span an energy region some ten groups wide. Consequently, a weighting more sophisticated than a flat weighting should have only a small effect on calculated reaction rates in this energy region and should have a negligible effect on the energy integrated tritium production rate in any particular detector sample.

For the actual multigroup calculation of Reference 1, deuterium was processed with the code EVXS,[15] while lithium-6 and lithium-7 were processed with the code ETOG.[16] Transfer matrix Legendre coefficients were expanded in orders P_0 through P_3, except that the secondary neutrons contributed by inelastic collisions, such as $^{7}Li(n,xt)$, were represented in order P_0 only when ETOG was used. The multigroup cross sections prepared by ETOG, which were generated in the GAM library format, were subsequently converted to DTF format by a Los Alamos service code, GAMDTF4.

To investigate systematic error from multigrouping, the previously described cross section set was used in a discrete ordinates transport calculation to determine the leakage spectrum from a similar 14 MeV neutron-driven lithium deuteride sphere. The spectrum was compared with that from a continuous-energy Monte Carlo calculation. The differences were sufficiently small that the systematic error introduced by multigrouping is negligible. For a more specific test of the multigroup cross section set, the ETOG-processed ^{7}Li(n,xt) inelastic cross sections were replaced by NJOY-processed cross sections. NJOY[17] is a more advanced processing code which permitted the representation of the inelastic anisotropy to the required P_3 order. When the results of the two S_8P_3 calculations of the Wyman experiment were compared, it was found that omission of the ^{7}Li(n,xt) inelastic anisotropy increases the tritium production of the innermost regions of the sphere by less than 1% and decreases the tritium production in the outermost regions of the sphere by less than 2%. This effect is quite small in relation to the observed discrepancies between calculation and experiment. Similar small differences would be expected for the omission of the inelastic anisotropy of the ^{7}Li(n,n'γ) reaction. Since no other major partial reactions processed by ETOG are involved, the systematic error due to omission of inelastic anisotropy in the ETOG-processed cross sections is negligible. Figures 4-1 to 4-3 show NJOY-plotted multigroup data overlaid on ENDF/B-IV pointwise data.

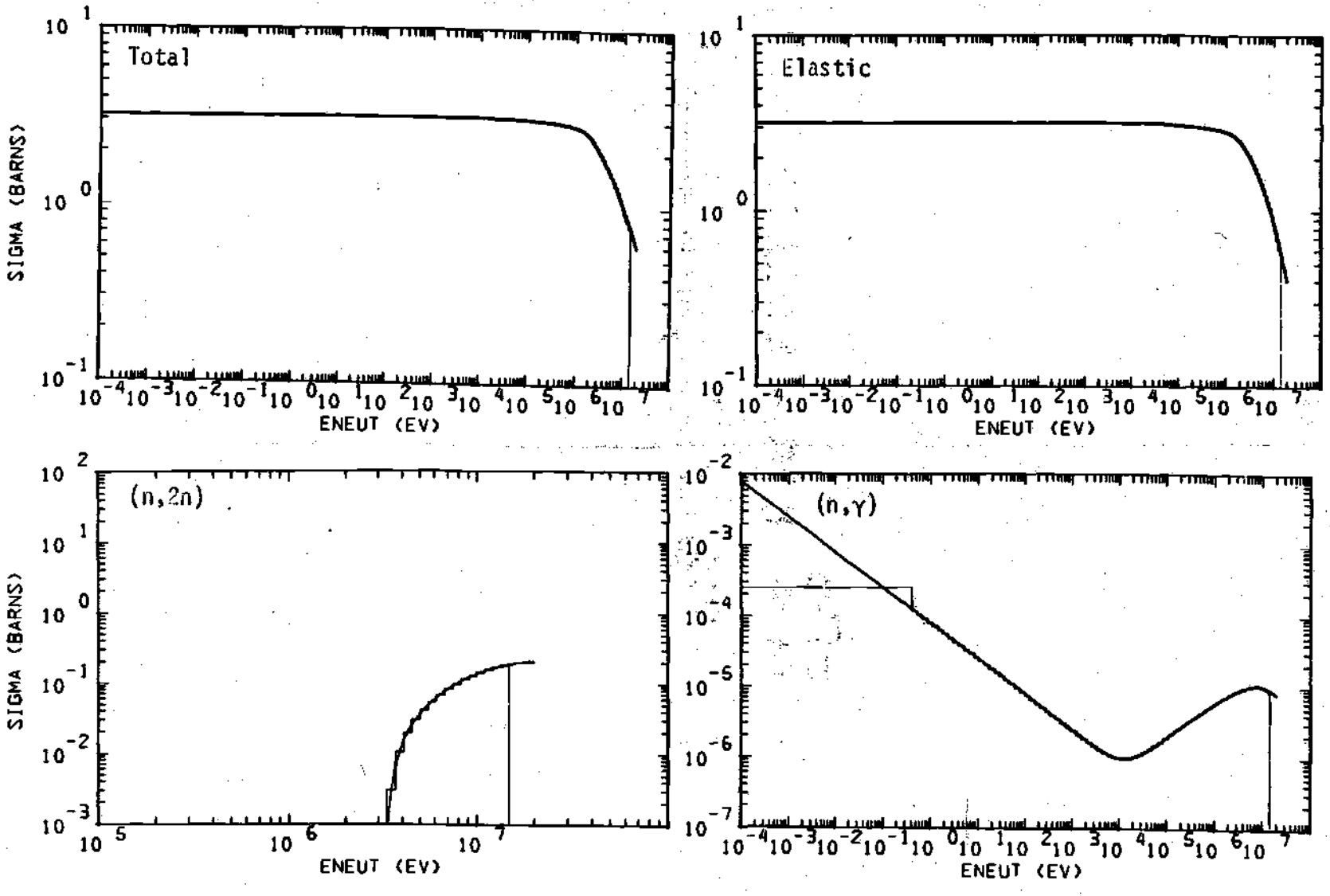

Figure 4-1. Deuterium Cross Sections.

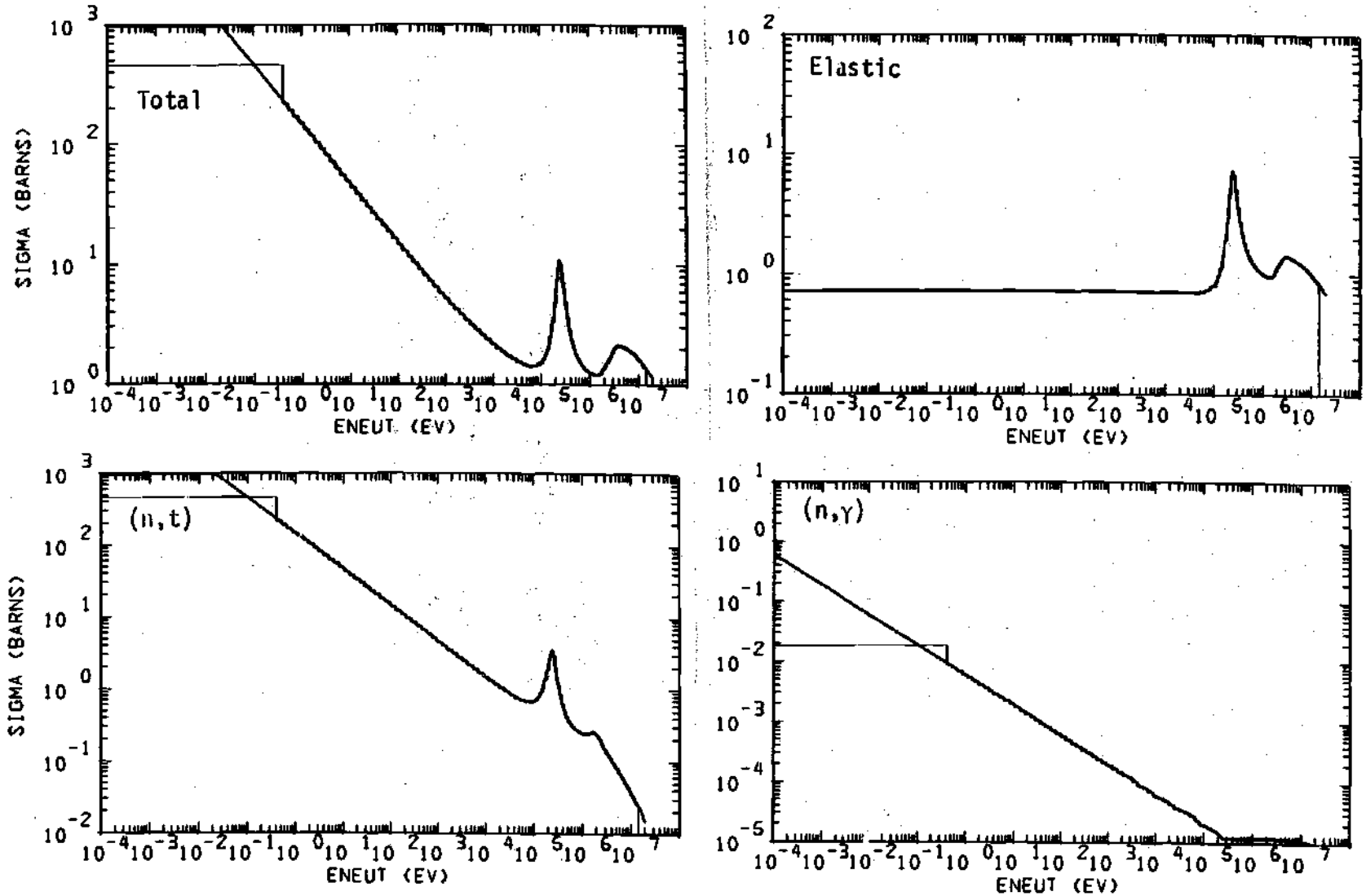

Figure 4-2. Lithium-6 Cross Sections.

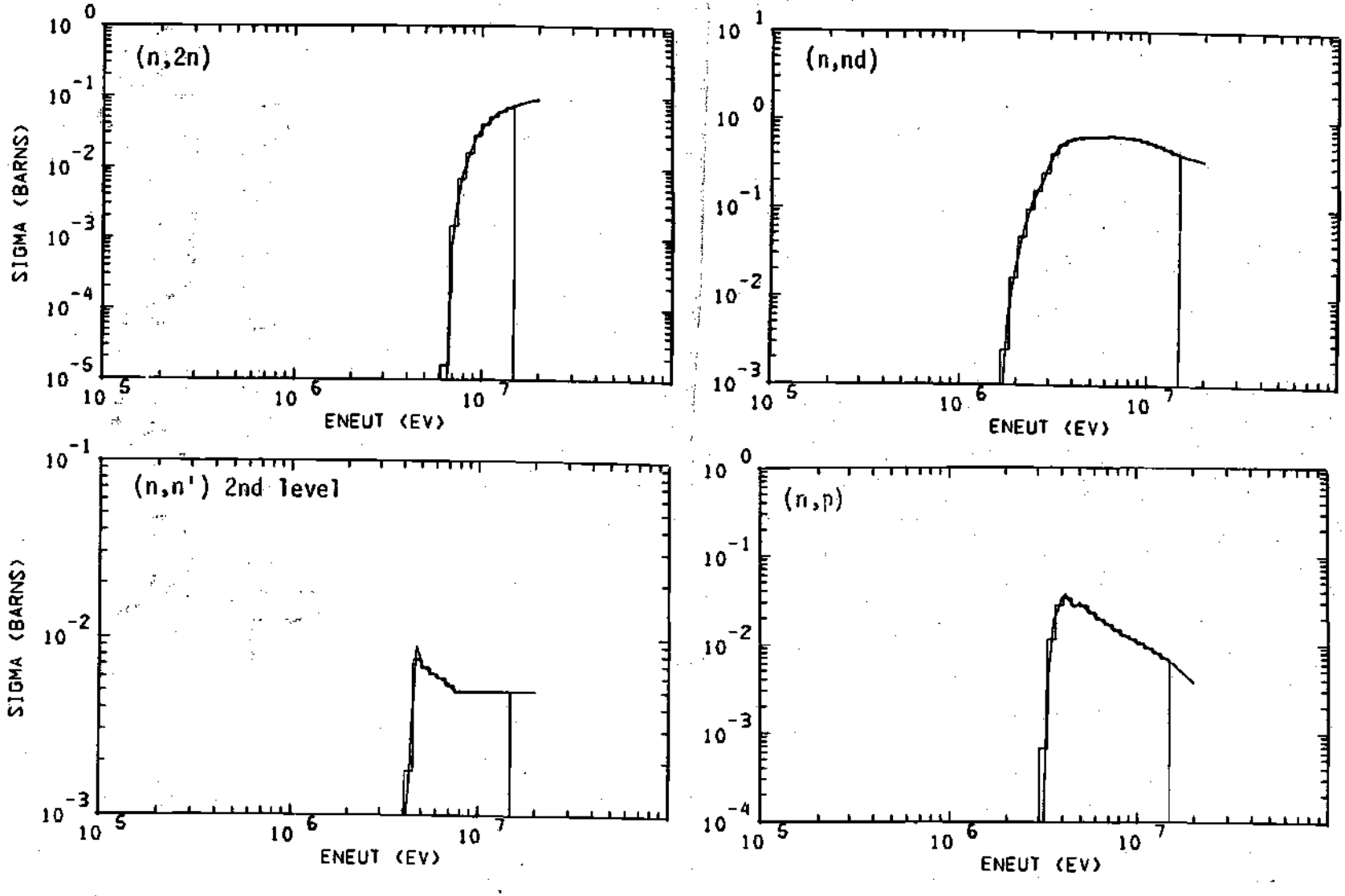

Figure 4-2 (continued). Lithium-6 Cross Sections.

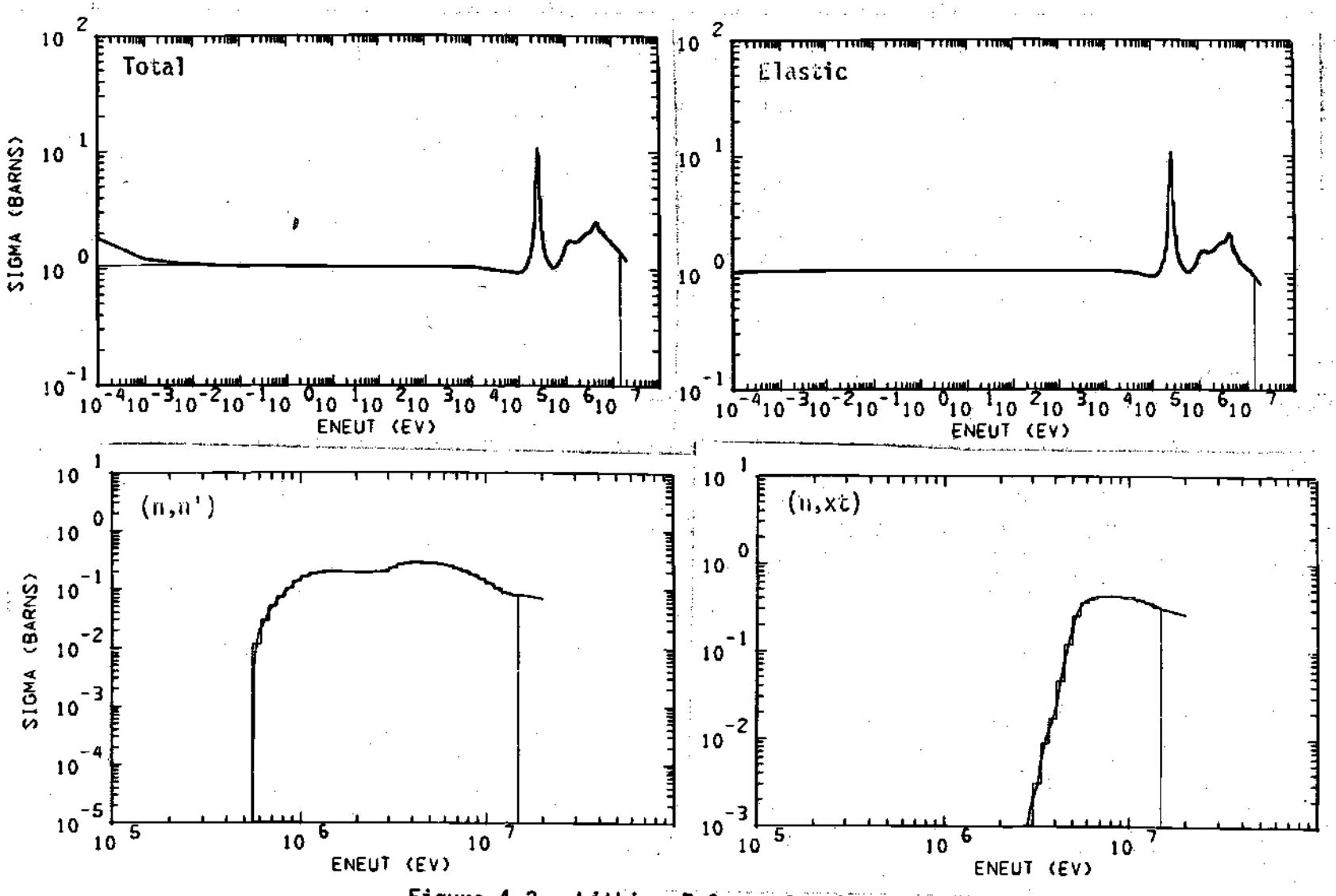

Figure 4-3. Lithium-7 Cross Sections.

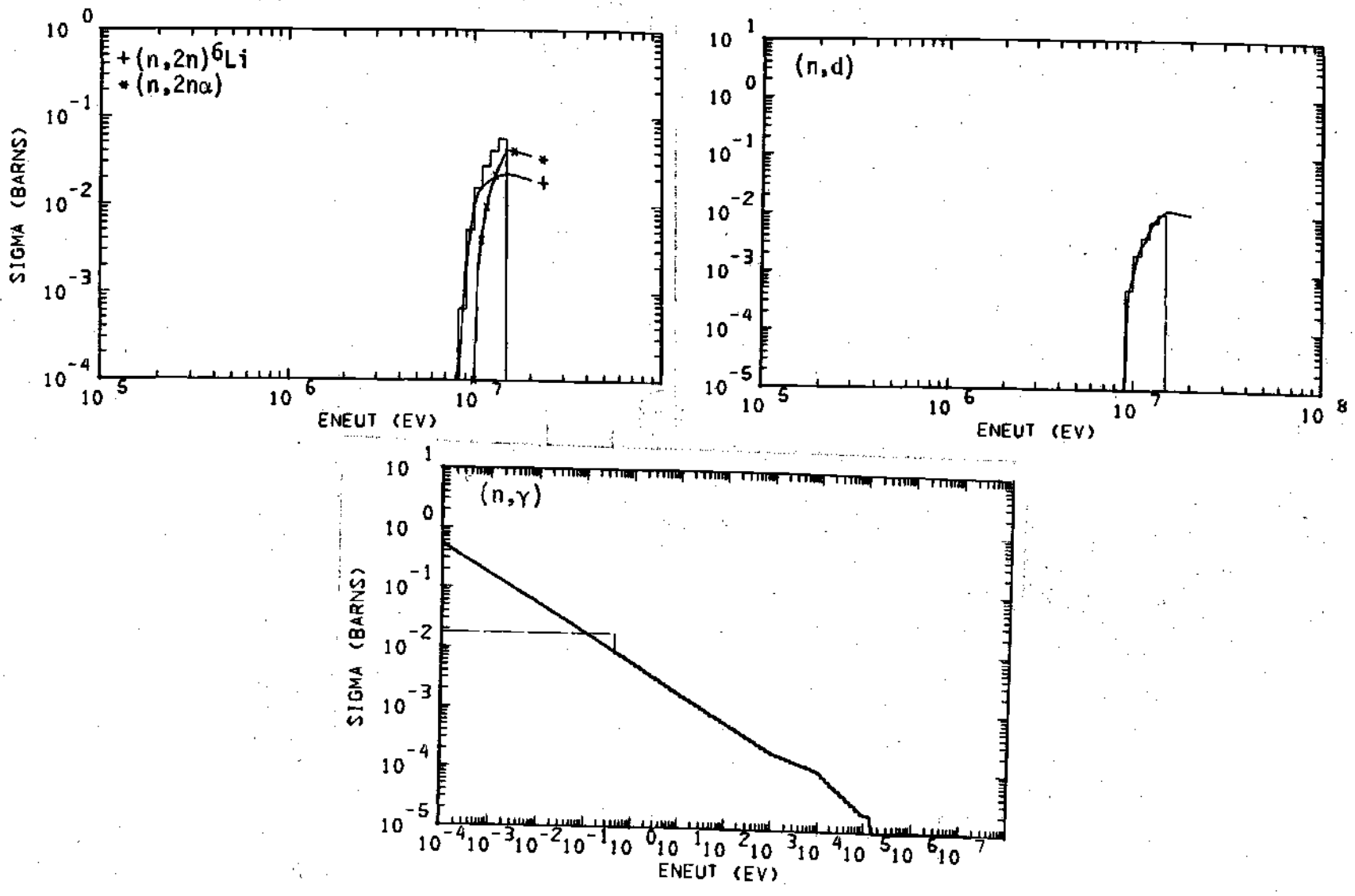

Figure 4-3 (continued). Lithium-7 Cross Sections.

Transport Calculation. Using the 100 group cross section set and the DTF-IV[18] discrete ordinates transport code, the radial distribution of tritium production was calculated. To accommodate computer storage limitations in combined sensitivity and data adjustment calculations the order of angular quadrature was reduced from sixteen to eight, and the number of spatial mesh intervals was reduced from 120 to 27. This change resulted in less than 2% change from the calculation described in Reference 1. In these calculations the effects of moisture traces in the LiD and the effects of surrounding reflecting structures were ignored. The detector response is obtained by homogenizing the ^{n}Li and ^{7}Li detector materials throughout annular regions. These regions are defined by the mesh intervals which straddle the given detector radii.

Figure 4-4 shows the calculated tritium production converted to the function f(R) of References 1 and 2. Here f(R) is defined as:

$$f(R) = \frac{4\pi R^2 T}{NQ} \quad , \qquad (4\text{-}1)$$

where R is the sample radius in cm, T is the sample triton count, N is the number of Li atoms in the sample, and Q is the total number of source neutrons. The overall tritium breeding ratio in ^{n}LiD, i.e., the number of tritons produced in the 30-cm radius sphere per source neutron, is calculated to be 0.928. Of this amount 0.547 is due to ^{6}Li(n,t) and 0.381 is due to ^{7}Li(n,xt).

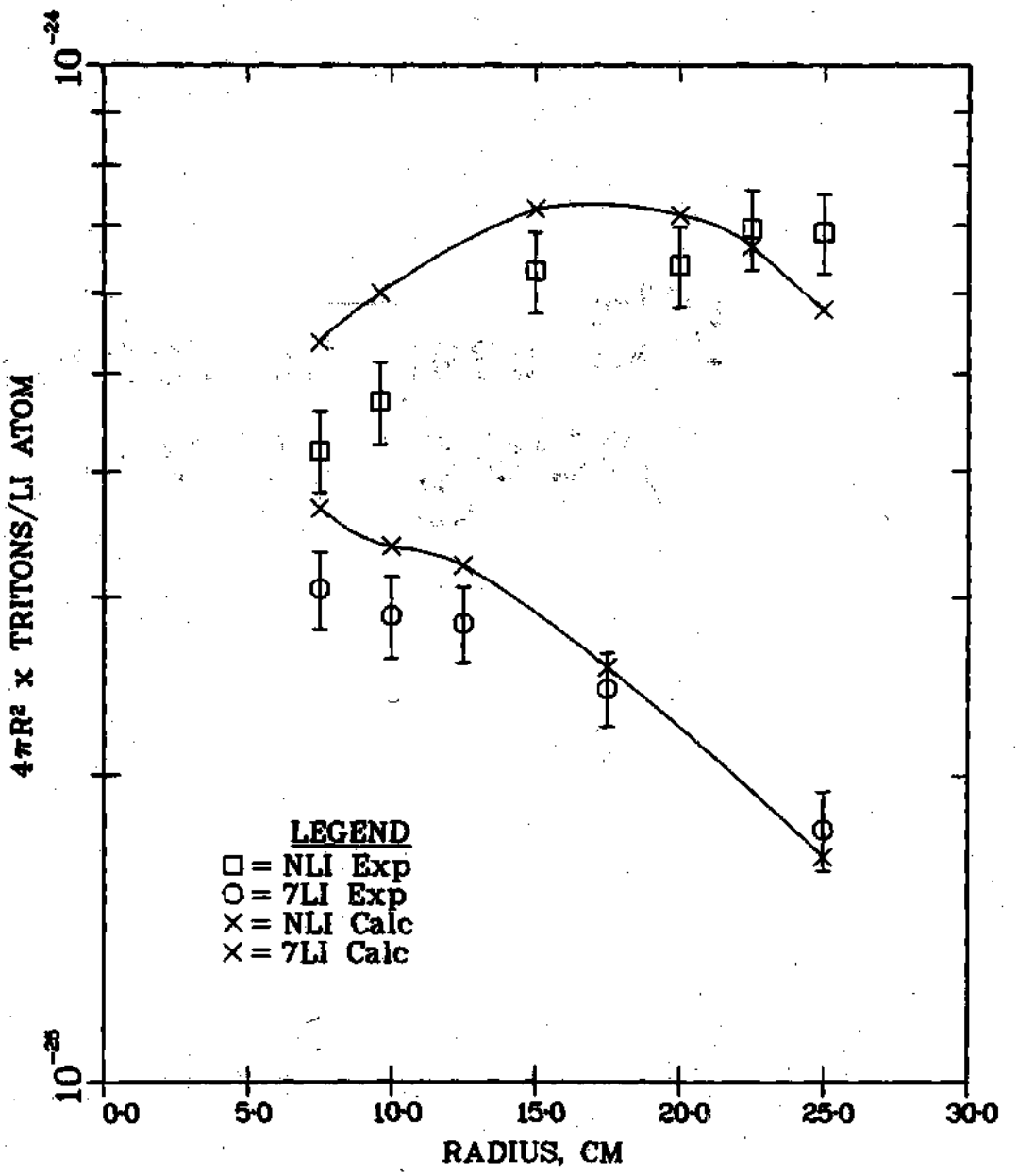

Figure 4-4. Radial Distribution of Tritium Production, Before Consistency Analysis.

A comparison of the neutron leakage spectrum from a 13-cm diameter lithium deuteride sphere, as calculated with the above discrete ordinates method and as calculated with the Monte Carlo transport code MCN,[19,4,20] yielded an estimate of the overall systematic error. In MCN, the cross sections are represented by a very finely divided pointwise-specified energy mesh (up to 2000 intervals in the present application), the anisotropy of the transfer cross section is represented by 32 equal-probability angle bins, and the neutrons are transported in a continuous energy, continuous direction phase space. For this calculation the neutron source was uniformly distributed in the 13.5-14.9 MeV interval of the uppermost GAM-II energy bin. Thus the comparison tests the combined effects of 1) within group flux weighting, 2) truncation of the Legendre expansion of the scattering anisotropy, 3) omission of inelastic anisotropy, 4) discretization of the spatial mesh, 5) discretization of the neutron transport direction, and 6) the finite convergence criterion for the iterated inner-loop solution. The comparison shows that the multigroup S_N method undercalculates the neutron leakage above the 2.8 MeV threshold of the $^{7}Li(n,xt)$ reaction by 2% and overcalculates the neutron leakage by 3% below this threshold. Moreover, the net neutron leakage is undercalculated by only 1%. It appears reasonable to conclude that similar differences would be found in the calculated tritium production. These differences are small compared to the calculation-experiment discrepancies and are well below the experimental errors.

Evaluation of Experimental Tritium Production and Error Matrix

This part of the description of calculational procedure reviews the evaluation of the experimental data proper. Then the details of the integral data error evaluation procedure are described. With the calculation of the relative discrepancy vector and relative error matrix the calculation of consistency prior to adjustment is possible.

Evaluation of Tritium Production Data. It is often the case that, as in the evaluation of differential data, the published integral data must be corrected or otherwise processed before analysis. D. W. Muir[1] previously screened out anomalous ^{7}Li data at 5.0 and 7.5 cm. In the present analysis two additional steps are taken.

First, the anomalously high ^{n}Li sample at 27.5 cm is excluded to eliminate possible data contamination by room return neutrons. Herzing et al postulate such a room return effect in the outer 8 cm of the metallic lithium medium of a similar experiment.[21]

Second, Wyman's notebooks record measurements from two samples at each of three radii, 7.5 cm, 12.5 cm, and 17.5 cm: one at 0° and one at 135° to the beam axis. Since the sample mass was nearly the same in each case and thus the statistical weight of each measurement was the same, the two measurements were statistically combined into an average effective measurement that could have been obtained if the measure-

ments had been performed in the 90° plane. The small difference that would result if the 0° and 135° measurements were more precisely weighted is treated as an uncertainty which is random in practice. Estimation of this error is discussed below.

After elimination of the one outermost measurement and reduction of the six paired measurements to three, there remain eleven 90°-effective tritium production data. In principle, these 90° data must be further corrected to account for variations in the tritium production due to the variation in source number yield and source energy with polar angle due to the previously noted neutron interaction effects in the target structure. Here the variations due to source anisotropy are regarded as a random in practice uncertainty in what the tritium production would have been in an ideal, isotropic experiment. Evaluation of the magnitude of these uncertainties is treated immediately below.

The eleven tritium production data are plotted with the calculated values in Figure 4-4.

Evaluation of Tritium Production Error Matrix. The integral data dispersion matrix is analyzed in terms of 1) strictly identified errors, and 2) unidentified errors. Sources of identified error include those which are identified by the experimenter in the published literature and sources which are identified during the evaluation process. Unidentified errors in the integral data are analyzed by considerations of 1) internal consistency, and 2) external consistency.

The experimenter-identified errors, as given in Reference 2, are listed in Table 4-2. All but the error in the total number of source neutrons are assumed to be uncorrelated. The latter is fully correlated for all samples irradiated in a single batch. The experimental notebooks provided the batch irradiation history. All of the samples retained for the present analysis were irradiated in the same batch except the ^{n}Li sample at 22.5 cm. The variance of the three ^{7}Li samples which are effective averages of two samples are reduced by one-half. Equation 4-1 and Equation 2-25d imply:

$$\frac{\text{var } f(R)}{f^2(R)} = 4\,\frac{\text{var } R}{R^2} + \frac{\text{var } T}{T^2} + \frac{\text{var } N}{N^2} \quad . \tag{4-2}$$

Equation 4-2 and Table 4-2 imply 4.7% uncorrelated error for the single samples and 3.3% for the averaged double samples. To the diagonal matrix must then be added the partially correlated component which represents the uncertainty in the total number of neutrons emitted. Every element of this second matrix has the value 3% with the exception of those off-diagonal elements which represent correlations with the 22.5 cm ^{n}Li sample and which are null.

The evaluator-identified error is an uncertainty in what the tritium production would have been in an ideal, isotropic experiment due to the anisotropy of the experimental neutron source. Appendix II gives a method of estimating the depth-dependent variance in the integral response due to the source yield and energy variances. This analysis

Table 4-2. Sources of Error in Tritium Production Data

Experimenter-identified Errors	
Total number of 14 MeV neutrons emitted by source	3%
Number of Li atoms in sample	3%
Radial position of sample	1%
Counting statistics	3%
Evaluator-identified Errors	
Anisotropy of Neutron Source — Near source	4%
Anisotropy of Neutron Source — Near periphery	2%
Unidentified Error by Internal Consistency	
Average value, all samples	7%

adds a component of uncorrelated variance to the tritium production error matrix. The component varies from approximately 4% near the source region to 2% near the periphery of the sphere. Appendix II lists the values used.

The unidentified error estimated by internal consistency is derived from an observed excess in the variance of the 0°-135° sample pairs when the sum of the identified variances is deducted. That is, after one allows for the experimenter-identified and the evaluator-identified errors, the spread in the two measurements (0°, 135°) at a given radius is more than can be accounted for by these identified errors. The average value of this excess for the three pairs gives an unidentified relative variance of .0044. This variance is added to the identified errors for all eleven data points. No evidence of correlation is apparent. Because the number of samples in this determination is small, the uncertainty in this estimate of unidentified variance is large. However, a rather uncertain estimate based on available data is better than a default value of zero. If ignored, the missing component of unidentified error would reappear in an estimate by external consistency, but the missing component would no longer be identified with the integral data.

In view of Equation 2-24, these separate components of variance may be summed to give the net relative variances needed to construct the tritium production error matrix. The result is shown in Figure 4-5,

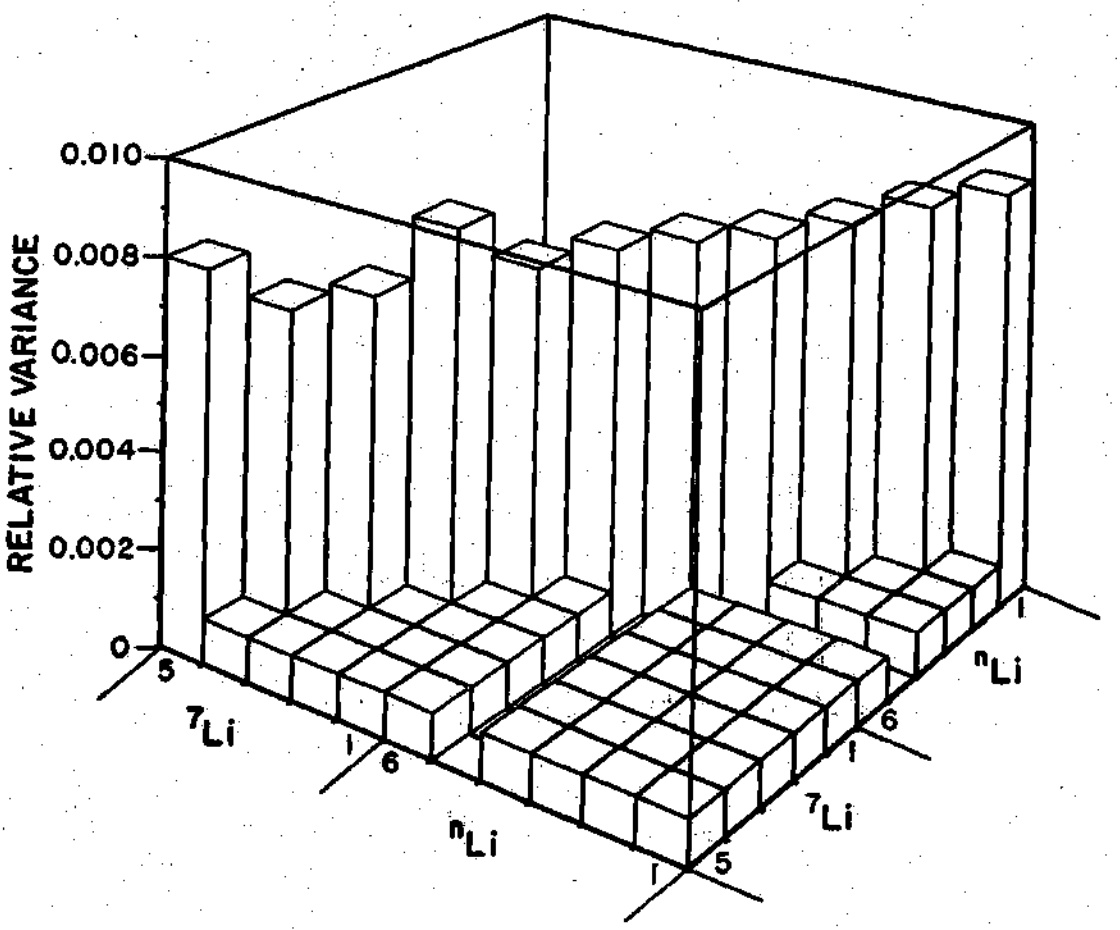

Figure 4-5. Tritium Production Dispersion Matrix, Before Consistency Analysis.

where the dominant uncorrelated components of error are apparent. Note the less dominant, correlated errors which are due to the uncertainty in the total number of neutrons emitted and note the notches which correspond to the separately irradiated ^{n}Li sample. The standard deviations shown in the tritium production data in Figure 4-4 are obtained from the diagonal elements of this matrix. Sample position numbers in Figure 4-5 are in order of increasing depth into the transport medium.

Tritium Breeding Ratio and Standard Error. Although the radial distributions are the experimental quantities used in the consistency analysis proper, it is of some interest to examine the volume integrated behavior or tritium breeding ratio. Define:

$$T = \int_{R_1}^{R_2} f^{n}(R) n_{LiD} dR, \qquad (4\text{-}3)$$

where T is the total tritium breeding ratio, $f^{n}(R)$ is the value of f(R) for a hypothetical, continuously distributed sample of ^{n}Li, e.g. $4\pi R^2$ times the tritium production per Li atom per source neutron, n_{LiD} is the atomic number density of Li in LiD, and R_1 and R_2 are the inner and outer radii of the sphere, respectively. Or exactly:

$$T = \sum_{i=1}^{N} \bar{f}^{n}(R_i) n_{LiD} \Delta R_i, \qquad (4\text{-}4)$$

where $\bar{f}^{n}(R_i)$ is the R^2-weighted average of the tritium production in a spherical annulus of thickness ΔR_i. The principle of the propagation

of errors then yields the relative variance:

$$\frac{\text{var } T}{T^2} = \left(\frac{{}^{n}\text{LiD}}{T}\right)^2 \sum_{i=1}^{N}\sum_{j=1}^{N} \bar{f}^{n}(R_i)\Delta R_i * \bar{f}^{n}(R_j)\Delta R_j * \frac{\text{cov}[\bar{f}^{n}(R_i), \bar{f}^{n}(R_j)]}{\bar{f}^{n}(R_i)\,\bar{f}^{n}(R_j)} \quad . \tag{4-5}$$

The above result is approximated as follows. Let "i" represent the six experimental ^{n}Li samples, choose the spherical boundaries to lie at the inner radius, the five mid-point radii, and the outer radius. Graphically estimate the weighted averages $\bar{f}^{n}(R_i)$ from the experimental profiles. Finally, replace $\text{cov}[\bar{f}^{n}(R_i), \bar{f}^{n}(R_j)]$ by the sample values.

Relative Discrepancy Vector and Relative Error Matrix. The calculated tritium production and the experimental tritium production must be combined into a discrepancy vector. In addition, the experimental tritium production uncertainties must be entered into the prescribed format of the input dispersion matrix. In ALVIN and ALVIN2, the dimensionless discrepancy vector of integral quantities is defined as the ratio of calculated-to-experimental quantities or C/E ratio. This ratio is formed by converting the calculated reaction rates in the detectors to f(R) values and dividing by the experimental f(R) values. The corresponding dimensionless dispersion matrix is just the already-evaluated relative dispersion matrix of tritium production data. Implementation of the ALVIN2 code, using the dimensionless discrepancy vector and the dimensionless dispersion matrix, completes that portion

of the calculation procedure used to determine the consistency of the data prior to adjustment.

Consistency of the Data Subsequent to Adjustment

Independent of the consistency prior to adjustment are 1) the sensitivity matrix and 2) the cross section dispersion matrix. It is often possible--and usually desirable--to first estimate the importance of the various partial reactions by considering only the rough magnitudes of the corresponding sensitivities and cross section errors. By such preliminary analysis, one may eliminate some partial reactions and simplify the analysis of others without significantly altering the calculational results. The reactions of principal interest are shown in Table 4-3.

Trial sensitivity calculations described below established that the transport contribution to the tritium production sensitivities of the $^{7}Li(n,xt)$ reaction was small in relation to the detector contribution. It is thus reasonable to expect that other partial reactions which affect only the neutron transport would have similar, small sensitivities. Most uncertain of these, and most likely to cause significant effect on the adjustment, are the D(n,2n) reaction and the $D(n,n_{el})$ reaction. The transport reactions in ^{6}Li and ^{7}Li were varied, but only in fixed proportion to each other, and such that the well-known total cross sections remained constant. In sum, the reactions allowed to vary independently were limited to D(n,2n), $^{6}Li(n,t)$ and $^{7}Li(n,xt)$

Table 4-3. Partial Reactions of Principal Interest

Tritium Breeding Reactions

$^{6}Li(n,t)$, $^{7}Li(n,xt)$

Other Reactions Affecting Neutron Transport

$D(n,n_e)$, $D(n,2n)$

$^{6}Li(n,n_e)$, $^{6}Li(n,n'd)$

$^{7}Li(n,n_e)$, $^{7}Li(n,n'\gamma)$, $^{7}Li(n,2n)$

reactions. The remaining reactions were allowed to vary only in an indirect manner.

Presented below is the calculation of sensitivities. This presentation is followed by the evaluation of the cross section dispersion matrices. The section concludes with a discussion of related quantities which may be calculated prior to the least-squares fit.

Calculation of Sensitivity Matrices

From Equations 3-29 and 3-35, it is apparent that the calculation of sensitivities requires: 1) the response integral (S^+,ψ), 2) the fluxes and adjoint functions, and 3) the densities and partial cross sections of the perturbed nuclides. Response integrals and fluxes and adjoint functions are calculated first. Preparation of the individual partial reaction multigroup data and the corresponding sensitivities follows.

Response Integral. The adjoint source S^+ is defined such that the inner product (S^+,ψ) yields the integral quantity of interest, namely the function F(R) defined by Equation 4-1. Eleven such response integrals and, hence, eleven adjoint sources are defined. The integrals are obtained by defining the adjoint source to be the tritium production macroscopic cross section in a ^{n}Li or ^{7}Li detector.

Fluxes and Adjoint Functions. Calculation of the neutron fluxes has been previously described. The adjoint function is similarly calcu-

lated by use of DTF-IV in the adjoint mode.† One such adjoint calculation is performed for each of the eleven adjoint sources. Thus, a total of twelve transport calculations is required.

The adjoint functions were validated by testing for the equivalence (Equation 3-7) of (S^+,ψ) and (ψ^+,S). Because of the numerical approximations inherent in the practical solution of the transport problem, the equation will be only approximately satisfied. For the Group One fluxes and adjoint functions, (S^+,ψ) and (ψ^+,S) agreed within 3%. This result confirms the normalization of the adjoint source and verifies the reasonableness of the approximations. Comparison of sensitivities calculated by the direct method and by the perturbation method further verifies the normalization.

In all of the sensitivity calculations SENSI used adjoint functions calculated by DTF in the same S_8P_3 approximation as the transport calculation and using the same mesh structure. PROFIL generated sensitivity profiles from transfer matrices which were truncated after the P_3 Legendre moment.

---

† It is important to note that the transport code automatically divides the input scalar source by 4π to obtain the angular source S^+ of the forward Boltzmann equation. Since the angular source S^+ of the adjoint Boltzmann equation is just the detector cross section, the adjoint input source must be pre-multiplied by 4π.

D(n,2n) Sensitivities. Total Cross Section Fixed. Since the total cross section is accurately known, it is appropriate to use the compound sensitivity profile. To calculate the compound profile, NJOY prepared 100-group P_0-P_3 cross section tables for the (n,2n) reaction and for the complementary (n,non-2n) reaction. As indicated previously, the (n,non-2n) reaction consists primarily of the elastic scattering reaction since the only other energetically possible reaction, namely the (n,γ) reaction, is less than one millibarn at all neutron energies of interest. The physics evaluation used was that of Horsley and Stewart (Reference 9) and is the same evaluation used in the transport calculation. However, the Los Alamos Master Data File formatted evaluation was replaced by a recent ENDF/B formatted evaluation.[22] The tables prepared by NJOY differed only slightly from the older (n,2n) tables, as expected.

To obtain the compound profile, the individual (n,2n) and (n,non-2n) multigroup profiles were calculated by independent ALVIN2 runs (KSENS=2, KADJST=1). The two simple profiles were then combined, according to Equation 3-42, in a separate operation. Since the (n,2n) reaction possesses a threshold of 3.3 MeV, only the applicable upper fifteen energy groups of the GAM-II structure were employed. The resulting sensitivity matrix is shown in Figure 4-6.

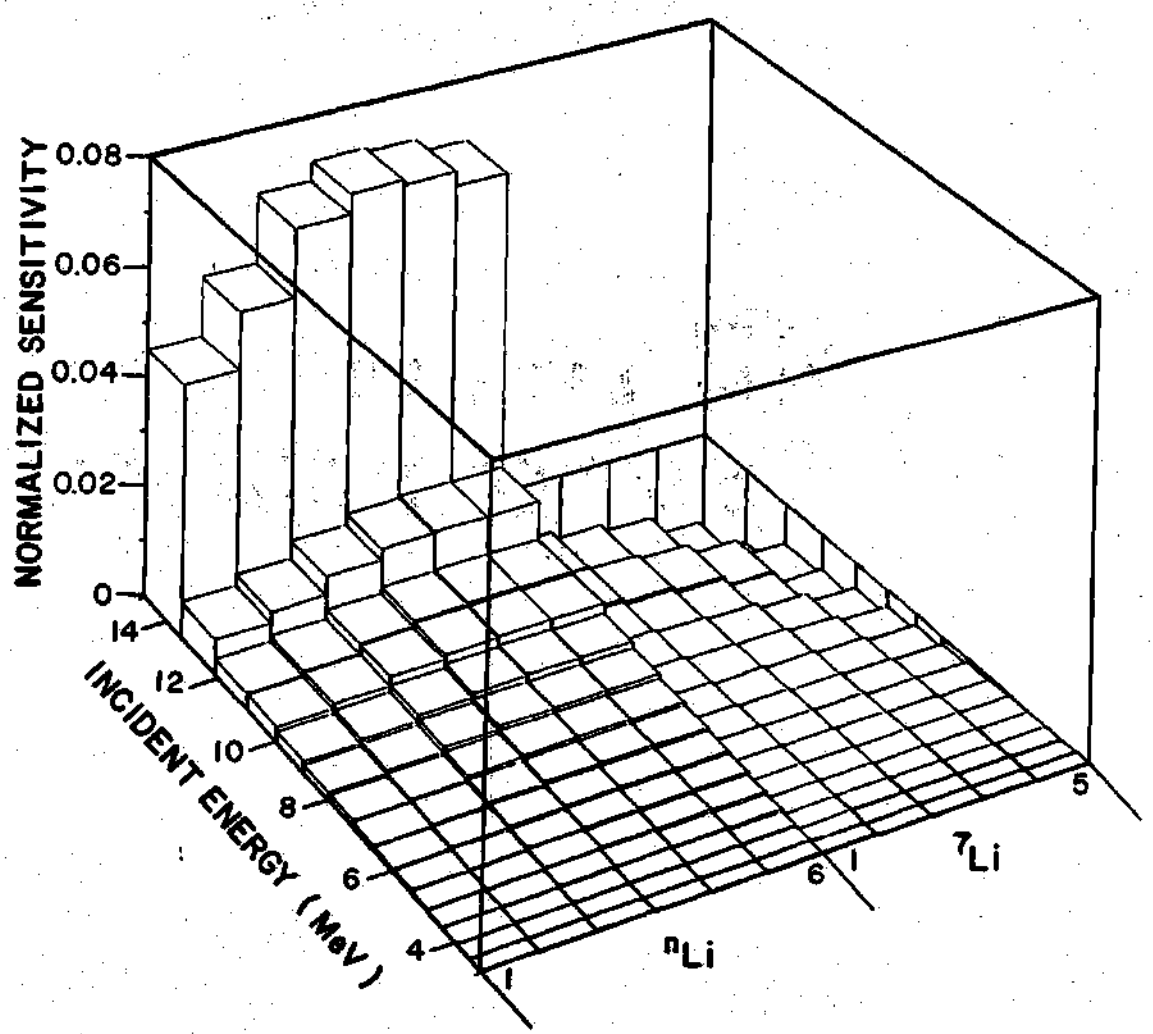

Figure 4-6. Multigroup Sensitivity Matrix, D(n,2n) Reaction, Total Cross Section Constant.

^{6}Li(n,t) Sensitivities. Total Cross Section Variable. In the simple ^{6}Li(n,t) profile only the transport loss and only the detector gain terms contribute. The requisite P_0-only table was prepared by a service code from the cross section set of Reference 1.

Since the uncertainty in the ^{6}Li(n,t) reaction is 1% or less below 10 keV and since earlier calculations for a similar 14 MeV lithium blanket showed a rapidly diminishing sensitivity per unit lethargy at these lower energies,[23] sensitivities were calculated only for the upper 60 energy groups of the GAM-II structure. The resulting 11 row x 60 column sensitivity matrix was in excellent agreement with direct calculations. (See Appendix III).

The ^{6}Li(n,non-t) profile needed to form the compound profile with fixed total cross section was not calculated in the present investigation for the following reasons. First, the effect of including the ^{6}Li(n,t) reaction in the consistency analysis, with the total cross section variable, is quite small. The just-calculated 60 group ^{6}Li(n,t) profile and preliminary ^{6}Li(n,t) error data were added to a previous trial adjustment involving only the ^{7}Li(n,xt) reaction. This test showed only a very small effect: the largest adjustment in the ^{6}Li(n,t) cross section was 1% (at 210 keV). Furthermore, the change in the consistency of the data after adjustment, as measured by the chi-square statistic, was apparent only in the fourth decimal place. The change in the ^{7}Li(n,xt) cross section adjustment pattern was also negligible. Thus, the impact of the ^{6}Li(n,t) reaction is very small, at least when the total cross section

is variable.

Second, separate calculations for the ^{7}Li(n,xt) reaction showed that the effect on the sensitivity matrix of fixing the ^{7}Li total cross section averaged less than 5%. This small effect is due to the general dominance of the sensitivity profile by the detector gain term. In the case of ^{6}Li, the (n,non-t) complement is an even smaller fraction of the total cross section (in the energy regions of interest) than in the case of ^{7}Li. Hence the additional effect of allowing for the (n,non-t) complement in the case of ^{6}Li should be even smaller than 5%.

Considering the two factors together - the small effect of the simple ^{6}Li(n,t) profile and the strong likelihood of a small additional effect when using the compound profile - the additional calculational expense involved in obtaining the compound profile is not justified. The sensitivity matrix is shown in Figure 4-7.

Li(n,xt) Sensitivity Matrix. Total Cross Section Variable and Total Cross Section Fixed. A 100 group ^{7}Li(n,xt) partial reaction P_0 table was prepared by converting the ENDF/B-III ETOG-processed ^{7}Li(n,xt) P_0 data of Reference 1 to the DTF table format. For this purpose a service code, GAMDTF4, formerly operational only on the LASL CDC6600 computer system, was converted to operate on the CDC7600 computer system with which the bulk of the consistency analysis calculation was performed. As indicated previously, ETOG does not process the

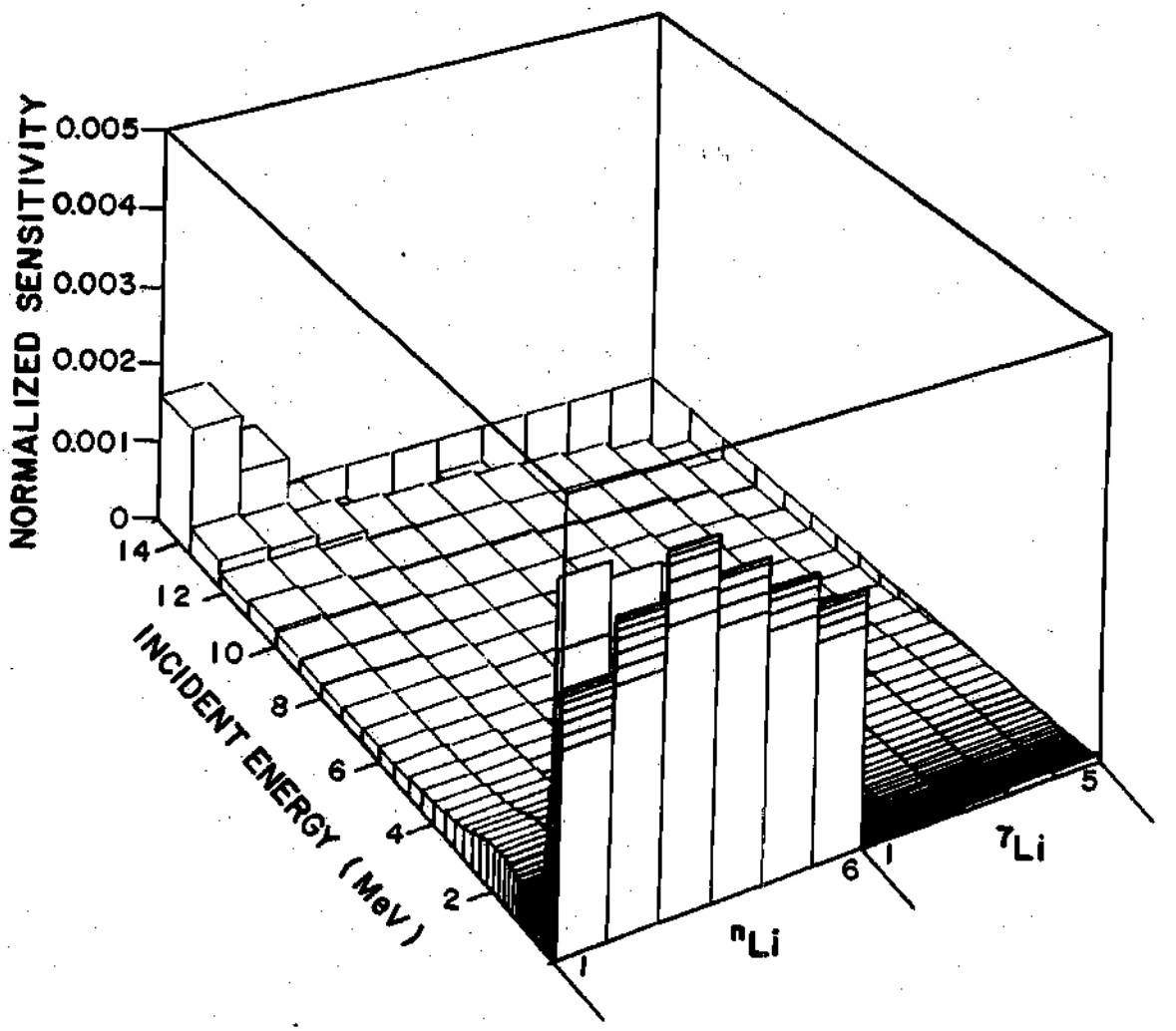

Figure 4-7. Multigroup Sensitivity Matrix, ^{6}Li(n,t) Reaction, Total Cross Section Variable.

inelastic anisotropy in the ENDF/B representation of the $^{7}Li(n,xt)$ reaction. However, replacement of the P_0-only tables by the P_0-P_3 tables prepared with the more advanced processing code NJOY resulted in less than 2% difference in the calculated tritium production. This effect is small compared to discrepancies between experiment and calculations. The complementary $^{7}Li(n,non\text{-}t)$ cross section tables were prepared by subtracting the above $^{7}Li(n,xt)$ table from the total reaction ^{7}Li tables used in the transport calculation.

Using the $^{7}Li(n,xt)$ P_0 table only, ALVIN2 calculated the simple profile with and without the detector gain term. Representative results are given in Table 4-4. It is apparent that the effect on tritium production in a given metal detector due to the perturbation of the $^{7}Li(n,xt)$ reaction in the ^{n}LiD transport medium is small compared to the effect of the same perturbation in the detector metal. Thus, to a rough approximation, the group sensitivity is proportional to the flux-weighted macroscopic group cross section. The $^{7}Li(n,xt)$ sensitivity matrix was validated by spot comparisons with the results of direct sensitivity calculations. Further details are given in Appendix III.

The compound sensitivity profile was calculated by ALVIN2 from the $^{7}Li(n,xt)$ and $^{7}Li(n,non\text{-}t)$ profiles as for deuterium. Here, however, several complementary reactions are involved. It is assumed that all vary in their ENDF/B-represented proportion. Since the transport effect is small relative to the detector effect, the exact proportion

Table 4-4. Sensitivity of Tritium Production in 15 cm ^{n}Li Metal Sample to ^{7}Li(n,xt) Group Cross Section. Total Cross Section Variable.

Energy, MeV	Without Detector Term	With Detector Term	Without Dectector Term/ With Detector Term
14.2-12.9	1.6 E-2	1.4 E-1	.12
11.1-10.0	1.2 E-3	3.1 E-2	.04
7.4- 6.7	1.6 E-4	1.8 E-2	.008
5.0- 4.5	5.7 E-4	4.7 E-3	.12
3.3- 3.0	1.8 E-5	1.2 E-4	.14

is not critical. The complete matrix is illustrated in Figure 4-8.

Evaluation of Cross Section Dispersion Matrices

Multigroup cross section dispersion matrices are prepared by the processes of cross section error evaluation, formatting, and multigrouping. Cross section evaluation leads naturally to error evaluation when performed by the quantitative statistical analysis of experimental data and of experimental data error estimates. In the present case, the reference D, ^{6}Li, and ^{7}Li cross section data were not evaluated in this way and error data must be supplied ex post facto.

In a manner analogous to the formatting and multigroup processing of cross section libraries proper, the formatting of error data and the multigroup processing of error data is a process which functions best when economies of scale are at stake. However, for the error analyses used in this work, the formatting and multigrouping stages are not formally distinguished from the evaluation process and all three stages are performed more or less simultaneously.

D(n,2n) Dispersion Matrix. No prior estimates of the uncertainties in the deuterium evaluated data are known. For purposes of the present investigation, estimates were prepared by drawing a smooth envelope around the plotted ensemble of experimental data,[24] by determining graphically the width of the envelope at each of the GAMII group midpoint energies, and dividing by the previously computed group cross section value to obtain a relative error. ALVIN2 then used the corres-

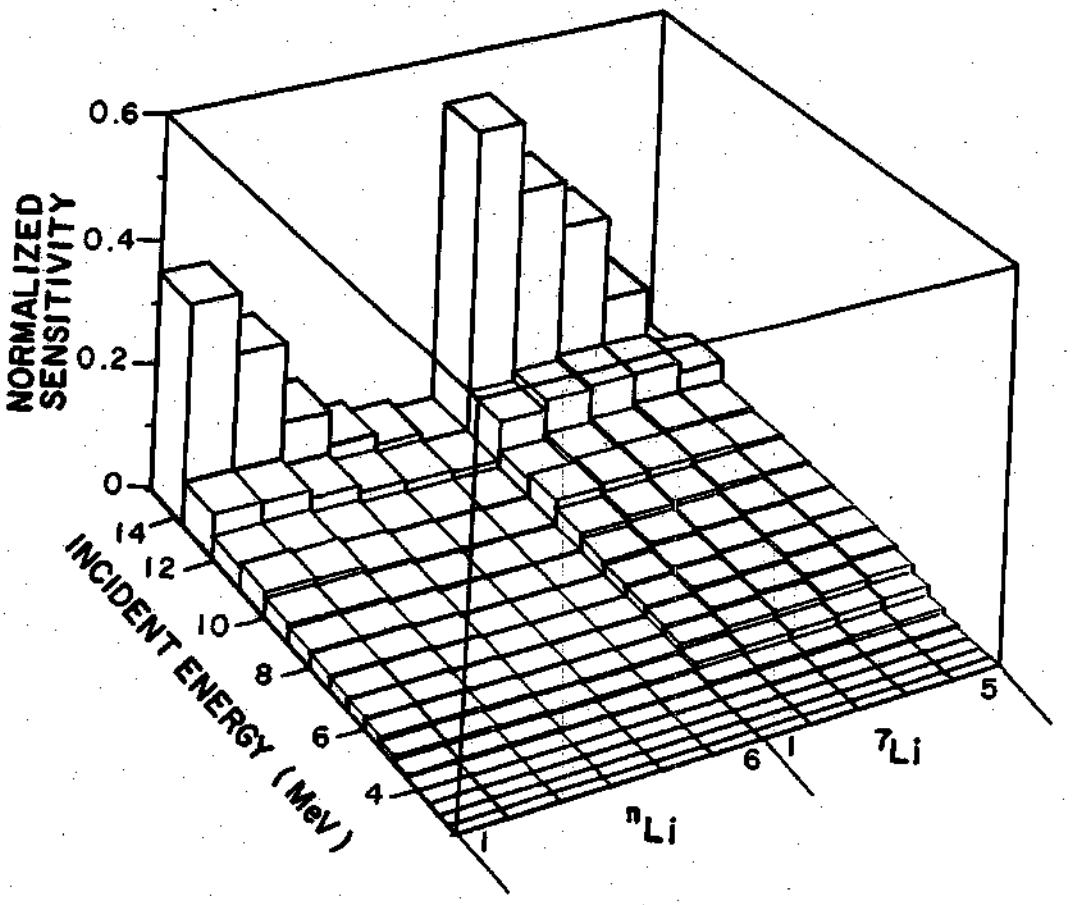

Figure 4-8. Multigroup Sensitivity Matrix, $^{7}Li(n,xt)$ Reaction, Total Cross Section Constant.

ponding diagonal matrix of variances in a trial tritium production consistency calculation to determine the significance of the D(n,2n) reaction relative to the other partial reactions of interest. The incremental effect of including the D(n,2n) reaction, with the total cross section held constant, was found to be quite small. Only the 14 MeV energy group contributed significantly to this small effect. For purposes of the present investigation, a more sophisticated evaluation of the dispersion matrix was unnecessary. The relative errors used are shown in Table 4-5.

^{6}Li(n,t) Dispersion Matrix. Energy-dependent relative errors in the ^{6}Li reactions have been previously evaluated[25] by methods similar to that used for the D(n,2n) reaction. The variances used in the present investigation were obtained by linearly interpolating the variances shown in Table 4-6 to the group energy mid-points of the 100 group GAMII structure. With this preliminary dispersion matrix and the 60 group sensitivity matrix described above, a trial adjustment was performed to determine the general significance of the ^{6}Li(n,t) partial reaction adjustment. No correlations were postulated in the 60 group dispersion matrix. As indicated previously, the effect of including the 60 group reaction was negligible. Note that the "1/v" region of the ^{6}Li(n,t) cross section begins at about 10 keV and hence lies just below the 60 group region used in this test.

To assess the uncertainty in the test resulting from the exclusion

Table 4-5. Evaluated Multigroup Errors of the D(n,2n) Reaction

GAMII Energy Group	Group Energy Midpoint,MeV	Relative Error
1	14.21	.08
2	12.87	.09
3	11.63	.09
4	10.53	.10
5	9.52	.11
6	8.67	.12
7	7.80	.13
8	7.06	.14
9	6.38	.16
10	5.78	.18
11	5.23	.20
12	4.73	.26
13	4.49	.34
14	3.87	.50
15	3.50	.75
16	3.17	--

Table 4-6. Evaluated Errors of the $^{6}Li(n,t)$ Reaction. (From Reference 25)

Energy	Relative Error
.025 eV	.005
.01 MeV	.01
.3 MeV	.20
1.0 MeV	.10
3.0 MeV	.08
5.0 MeV	.10
14.0 MeV	.10

of the fully correlated 1/v region it is noted from Reference 1 that some 75%-85% of the $^{6}Li(n,t)$ reactions occur below 10 keV. However, the uncertainty of the cross section in this region and the normalized sensitivity are both less than 1%. (See Figure 4-7 and discussion in text.) Thus, variation of the 1/v portion of the cross section within its uncertainty limits should have an effect of order 0.01% or less upon the overall $^{6}Li(n,t)$ reaction rate. This effect is of the same low order as the effect of varying the top 60 energy groups alone. Consequently, the exclusion of the fully correlated 1/v part of the reaction from the test does not alter the conclusion that the $^{6}Li(n,t)$ reaction adjustment provides negligible incremental effect compared to the $^{7}Li(n,xt)$ reaction adjustment. For the purposes of the present investigation, no further refinement of either the sensitivity matrix or the dispersion matrix was considered profitable.

$^{7}Li(n,xt)$ Dispersion Matrix. The construction of the dispersion matrix for the $^{7}Li(n,xt)$ reaction proceeded in two stages. In the first stage, a preliminary matrix was constructed using previously estimated relative errors: 0.15 at all energies from threshold to 14 MeV. A trial adjustment was performed using this diagonal matrix with the $^{7}Li(n,xt)$ reaction alone. The adjustment was found to improve the chi-square by some 20%. This effect is large compared to the incremental effect of the D(n,2n) and $^{6}Li(n,t)$ trial adjustments. (Trial adjustments were performed in order of decreasing *a priori* likelihood of effect.

Thus the $^{7}Li(n,xt)$ trial adjustment was performed first, the $^{6}Li(n,t)$ second, etc.) Because of the significant effect, a more sophisticated evaluation of the $^{7}Li(n,xt)$ cross section dispersion matrix was indicated.

To aid in the determination of the scope of this evaluation, an additional test was performed to estimate the influence of correlations in the multigroup dispersion matrix.[26] In the trial calculation, by far the largest cross section sensitivities, as well as the largest cross section adjustments, corresponded to the 14 MeV source-energy group. Consequently, the effect of correlations, e.g. between the uncertainties in the source energy group and the next lowest group, might be relatively small. To test this hypothesis, the structure of the $^{7}Li(n,xt)$ dispersion matrix was varied smoothly from the zero correlation of the initial trial calculation to full correlation, according to the empirical prescription:

$$\frac{\mathrm{cov}(x_i,x_j)}{x_i x_j} = \exp\left\{-\frac{|i-j|}{(R_i R_j)^{\frac{1}{2}}}\right\}, \qquad (4\text{-}6)$$

where R_i and R_j represent arbitrary energy group correlation ranges.[27,28] Separate consistency analyses were performed for each structure so created. The principal result of this analysis is that the chi-square of the data after adjustment is raised only by some 10% when the cross section dispersion matrix correlation strength is increased from zero correlation ($R_i=R_j=0$) to full positive correlation ($R_i=R_j=\infty$). This value is of the same order as the statistical uncertainty in the final chi-

square itself. For intermediate correlation ranges the increase in the final chi-square assumes intermediate values. Since a precisely evaluated ^{7}Li(n.xt) dispersion matrix is unlikely to be fully correlated, the effect of neglecting the correlations should be well within the statistical uncertainty of the final chi-square.

A method of dispersion matrix evaluation one step beyond the simple eye-guide banding method is based on a direct interpretation of the fundamental definition of covariance. As implemented by F. Perey and F. Difilippo,[29,30] Equation 2-11 takes the form:

$$\mathrm{cov}(x_i,x_j) = \frac{1}{M}\sum_{k=1}^{M}(x_{ik}-\bar{x}_i)(x_{jk}-\bar{x}_j). \qquad (4\text{-}7)$$

It is assumed that there exist M independent, equally likely sets of observations on both x_i and x_j. Here $\bar{x}_i$ and $\bar{x}_j$ are the means of the parent distribution or true means. When $\bar{x}_i$ and $\bar{x}_j$ are estimated directly from the sample means, i.e. the arithmetic averages, then the means are no longer independent and the denominator M is replaced by M-1. However, as used by Perey et al the true means are estimated from a reference evaluation, e.g. ENDF/B. It is of interest that while such evaluated means are usually not independent of the observations, the method is implemented as if the means were independent.

Since cross sections are not always measured by various investigators at the same energies, it is customary to connect the experimental points of a given investigator and to interpolate the cross section

observations to a common energy grid. Alternatively, the connected data of a given investigator may be averaged within the energy groups used in the neutron transport calculations.

An analogous method could be used to estimate the dispersion matrix of integral data. Here the estimated means would be the integral quantities as calculated from the reference evaluation, such as ENDF/B. Indeed, such a procedure could have been used instead of the method of evaluation implemented in a previous section of this chapter in connection with the radial tritium production dispersion matrix. The principal difference is that the method based on Equation 4-7 is based entirely on external consistency while the method discussed in a previous section is based essentially on internal consistency.

In the interest of methodological consistency it is desirable to evaluate the input cross section dispersion matrix in a manner analogous to the evaluation of the input dispersion matrix of integral data. The principal difference in the implementation of this procedure, in the case of cross section data, is that usually many investigators report in any given energy region. This feature is readily accommodated by application of the least-squares method itself to fit the observations. The procedure, which uses both considerations of internal and external consistency, goes a step beyond Equation 4-7.

The least-squares analysis adopts the unknown group cross sections themselves as formal parameters and uses the available experimental data

as observations on these parameters. As discussed above, the equivalent group cross section observations are constructed by connecting the experimental points of a given investigator and estimating graphically the average value of the cross section in a given energy group. The construction of the design matrix is trivial since each group cross section observation is related to the corresponding formal parameter by the identity operator. Hence every row of the design matrix is empty except for one identity element. When the standard least-squares algorithm is implemented on these equivalent observations there results an output parameter dispersion matrix which is interpreted directly as the desired group cross section dispersion matrix. This formal parameterization is tantamount to a re-evaluation of the cross section. It also distinguishes the method from the method of Equation 4-7, which requires an external evaluation.

The equivalent group cross section observations were constructed from the data compiled by Pendlebury[12] and from the original experimental reports. Resulting multigroup data are shown in Table 4-7. A few values near threshold were constructed by extrapolating the nearest available observation in direct proportion to the group cross section processed previously from ENDF/B. These values are shown in parentheses.

For purposes of the present investigation all group cross section observations were assigned equal weight. Similarly, correlations arising from experimental method were ignored. Thus, the analysis is by

Table 4-7. Equivalent Group Cross Section Observations (in millibarns) for $^{7}Li(n,xt)$ Reaction. GAM-II Energy Group Structure

Gp	ENDF	(a)	(b)	(c)	(d)	(e)
1	328	325	350	302		
2	358			360		
3	387			405		
4	407			400		
5	415			507		
6	420			510	350	
7	423			452	360	350
8	423			440	370	425
9	399			375	350	500
10	358			365	337	365
11	256			262	150	220
12	121				115	205
13	45				62	190
14	17				15	165
15	9				[8]	[87]
16	3				[3]	[29]
17	1				[1]	[10]

(a) = Thomas

(b) = Osborn and Wilson

(c) = Rosen and Stewart

(d) = Brown et al

(e) = Batchelor and Towle

[ ] = See text

external consistency only, although the method is more general. For a diagonal input matrix, the output dispersion matrix of formal group cross section parameters, given by Equation 2-40, assumes the simple form:

$$\hat{D}(X) = \hat{s^2}(A^TA)^{-1}, \tag{4-8}$$

where A^TA may be shown to be diagonal, and where:

$$\hat{s^2} = \frac{1}{L-N}\,[O(AX)-\hat{O}(AX)]^T[O(AX)-\hat{O}(AX)]\,. \tag{4-9}$$

Here L-N is the number of available equivalent cross section observations minus the number of equivalent cross section parameters.

The standard least-squares algorithms may be implemented with a general purpose least-squares program or with the ALVIN codes. To perform a standard least-squares calculation with ALVIN or ALVIN2 the codes must be modified or special input data must be supplied. In the first case, the DAFT2 module, which internally augments the input sensitivity submatrix S with a suitable identity submatrix I to give the complete design matrix A, must be modified to accept an arbitrary input design matrix.

In the second case, the standard least-squares algorithm is simulated by formally treating the equivalent group cross section observations as indirect observations O(SX). As before, the direct observations O(X) are the reference group cross sections derived from ENDF/B, but they must be regarded here merely as dummy observations or observations of vanishing weight.

In the present calculations the special input method of implementing the standard least-squares algorithm was used. The input dispersion matrix of dummy observations D[O(X)] was weighted at 10^{-5} of the dispersion matrix of equivalent cross section observations D[O(SX)]. The resulting matrix is shown in Figure 4-9. Note the diagonal character of the matrix as required by Equation 4-9. For cases in which the correlation structure of the cross section dispersion matrix is known to be significant in the combined adjustment, observation correlations should be assessed. Under such circumstances the presence of off-diagonal elements in the evaluated matrix would be expected.

Error in Calculated Transport Results

By using the cross section dispersion matrix and the sensitivity matrix to calculate $SD[O(X)]S^T$ one may propagate the cross section uncertainties to the integral transport results. While these quantities are not part of the input data, their calculation is mentioned here because they are useful in interpreting the uncertainties which result after adjustment.

Error in the Calculated Radial Distribution of Tritium Production. The cross section dispersion matrix was combined with the complete sensitivity matrix by adding the appropriate coding to ALVIN2. The resulting relative variances in the radial distribution of tritium production are printed and are also written to a graphics interface file for display as standard errors on the radial tritium production plot.

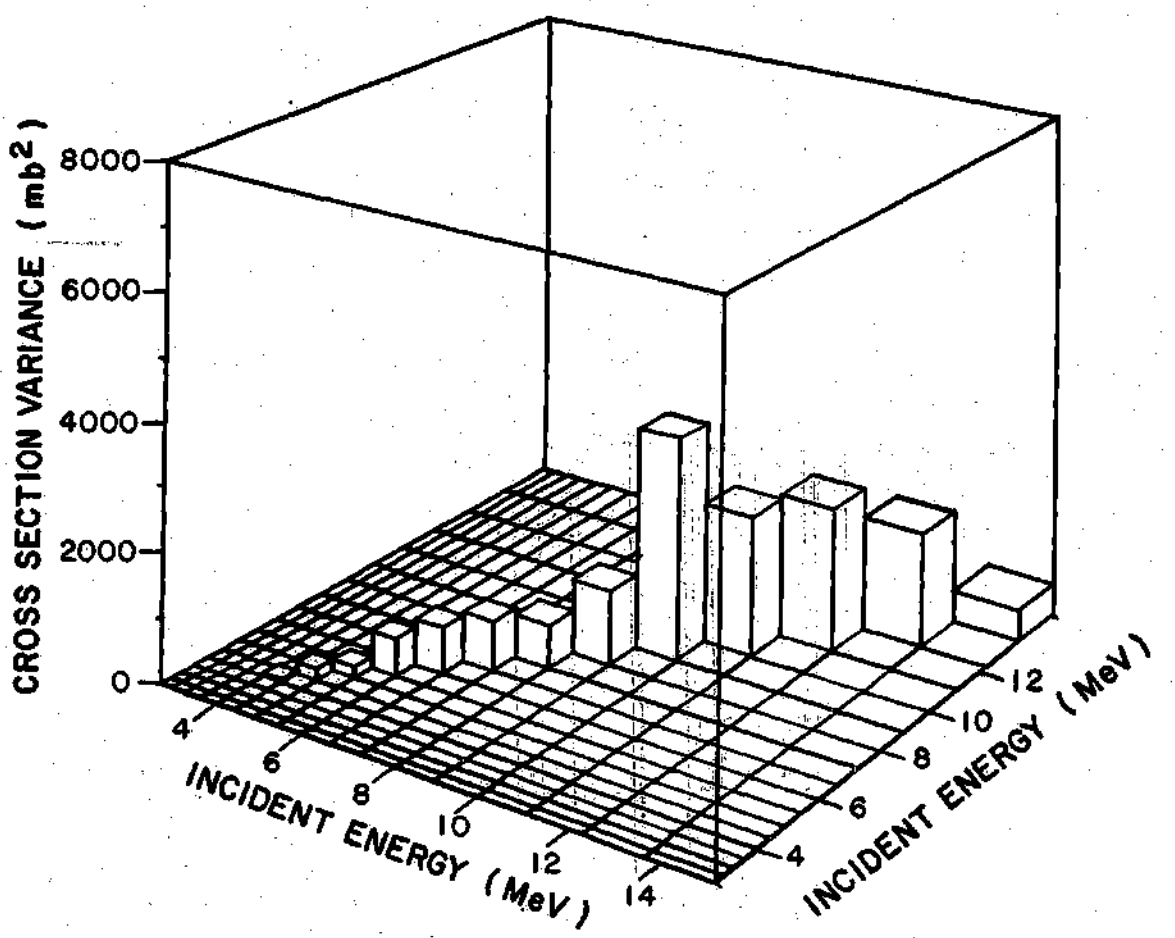

Figure 4-9. ^{7}Li(n,xt) Reaction Multigroup Dispersion Matrix, Before Consistency Analysis.

Numerical results are given in the next chapter.

Error in the Calculated Breeding Ratio. The tritium production per source neutron integrated over the sphere, namely the tritium breeding ratio, has been previously calculated. To determine accurately the uncertainty in the calculated tritium breeding ratio due to the cross section uncertainties, one may calculate the group cross section sensitivities of the tritium breeding ratio and combine the resulting vector with the cross section dispersion matrix as above.

A second method estimates the calculated tritium breeding ratio from the calculated radial distribution for production in ^{n}Li. Another application of the law of propagation of errors is used to express the variance in the breeding ratio in terms of the already-calculated covariances in the calculated sample production. The method is the same as that used to determine the uncertainty in the experimental tritium production, Equations 4-3 to 4-5. Thus, the cost of a new sensitivity calculation is saved.

To provide a check on the various calculations used in this work, the uncertainty in the calculated tritium breeding ratio was evaluated using both of these methods. The agreement was excellent.

Cross-type Correlations

As indicated in Chapter II, a simplification of the least-squares algorithms results when correlations between differential data are absent. The existence of cross correlations thus determines, as indicated in

Chapter III, whether or not the less time-consuming DAFT3 module may be used in place of the more general DAFT2. Insofar as it is possible, the nature of such cross-type correlations, like the correlations amongst the integral data, is determined by internal considerations. It must be established, therefore, whether common techniques involved in the determination of the cross sections and in the determination of the integral data lead to covariant or contravariant sources of error. No significant correlated sources of error are determinable by scrutiny of the published reports of the cross section measurements used to evaluate the ENDF/B data. However, it should be noted that one measurement series, that of Brown et al, which uses a tritium extraction technique similar to that of Wyman, may contain a correlated source of error. Unfortunately, the magnitude of such error cannot be assessed by internal considerations. For purposes of the present investigation, cross-type correlations in the input data were not considered further and the DAFT3 algorithm was used.

Response Functions After Consistency Analysis

The response functions after consistency analysis may be calculated by preparing a new multigroup cross section library from the output of ALVIN2. This library is prepared with the aid of a separate code, PERTLIB. A second forward transport calculation may then be performed with this new library to obtain the response functions after consistency analysis. In the present work this procedure is illustrated by calculation

of the overall tritium breeding ratio after consistency analysis. The uncertainty of the breeding ratio after consistency analysis is obtained by the method of Equations 4-3 to 4-5. Here the radial tritium production dispersion matrix after consistency analysis is used.

Summary of Computational Procedure

A general calculational procedure for combined differential and integral neutronic data consistency analysis is shown in Figure 4-10. The procedure used here differs only in that cross section dispersion matrix evaluation and multi-grouping were performed in a single operation.

In the preceding discussion of the calculational procedure the role of several preliminary or trial calculations was discussed. Each trial calculation represents a new pass through the procedure of Figure 4-10 with systematic refinement of particular calculational steps. This use of the method of successive approximations is summarized in Table 4-8. Iterative use of least-squares algorithms thus serves to guide the general analysis of data as well as to provide a consistency analysis.

The detailed pattern of consistency findings for the final iteration is presented in the next chapter. Additional details of the computer implementation are treated in Appendix I.

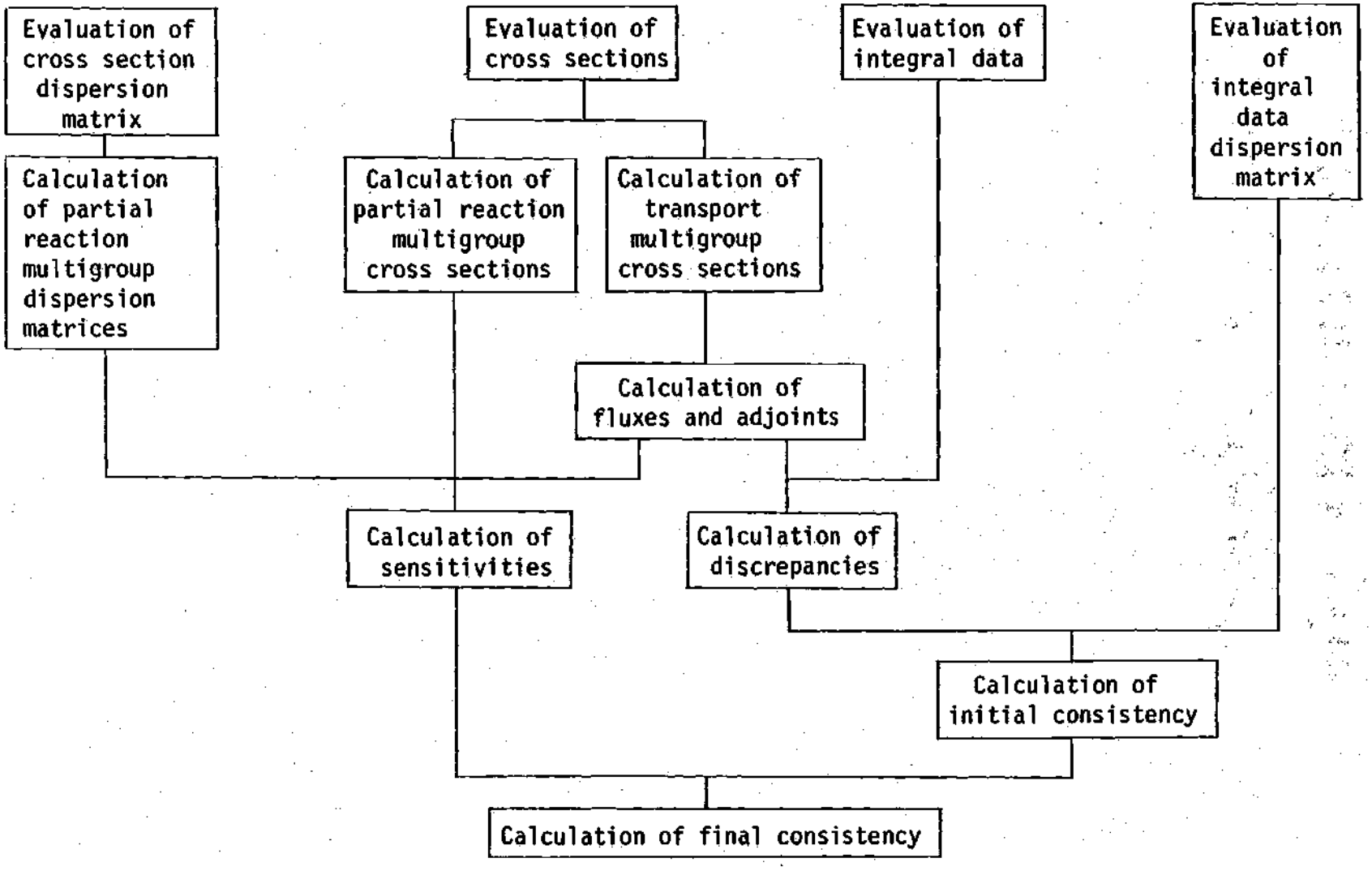

Figure 4-10. Flow Diagram of Consistency Analysis

Table 4-8. Development of Successive Approximations.

	Integral Data	Differential Data	Sensitivity Matrix	χ^2/DF Initial	χ^2/DF Final
Initial calculation with ALVIN2.	15% uncorrelated	^{7}Li(n,xt) only, 15% uncorrelated	σ^{tot} variable	1.2	0.9
Begin iteration on integral data input error matrix.	Experimenter-identified errors only.	"	"	6.5	4.3[a]-5.2[b]
Begin iteration on differential data input error matrix. Add ^{6}Li(n,t) reaction.	"	^{6}Li(n,t) added, USNDC-1 errors, uncorrelated.	"	6.5	4.3[a]
Final iteration on integral data input error matrix.	All identified errors.	^{7}Li(n,xt) only, 15% uncorrelated.	"	3.0	1.6[a]-1.8[b]
Final iteration on ^{7}Li(n,xt) input error matrix.	"	Least-squares evaluation.[c]	"	3.0	2.3
Final iteration on ^{7}Li(n,xt) sensitivity matrix.	"	"	σ^{tot} constant	3.0	2.3

Table 4-8 (continued)

	Integral Data	Differential Data	Sensitivity Matrix	χ^2/DF Initial	χ^2/DF Final
Add D(n,2n) reaction Final iteration.	All identified errors.	D(n,2n) errors eye-guide banded.	σ^{tot} constant.	3.0	2.3

χ^2/DF = Chi-square per degree of freedom (reduced chi-square).

a = Cross section errors uncorrelated.

b = Cross section errors fully correlated.

c = External consistency only.

σ^{tot} = Total cross section.

REFERENCES

1. D.W. Muir and M.E. Wyman, Technology of Controlled Thermonuclear Fusion Experiments and the Engineering Aspects of Fusion Reactors, p. 910, CONF-72111, U. S. Atomic Energy Commission (1974).

2. M.E. Wyman, An Integral Experiment to Measure the Tritium Production from ^{7}Li by 14-MeV Neutrons in a Lithium Deuteride Sphere, LA-2234 (Rev.), Los Alamos Scientific Laboratory (1972).

3. C. Wong, J.D. Anderson, P. Brown, L.F. Hansen, J.L. Kammerdiener, C. Logan, and B. Pohl. Livermore Pulsed Sphere Program: Program Summary Through July 1971, UCRL-51144, Rev. 1, Lawrence Livermore Laboratory (1972).

4. M.E. Wyman, LANB-6452, Los Alamos Scientific Laboratory (Nov. 9, 1953, Unpublished).

5. E. Meyer, R. Maltrud, and M.E. Wyman, LANB-5164, Los Alamos Scientific Laboratory (June 23, 1954, Unpublished).

6. L.D.P. King, C.W. Zabel, and M.E. Wyman, LANB-5644, Los Alamos Scientific Laboratory (Feb. 17, 1956, Unpublished).

7. J.D. Seagrave, E.R. Graves, S.J. Hipwood, and C.J. McDole. $D(d,n)He^{3}$ and $T(d,n)He^{4}$ Neutron Source Handbook, LAMS-2162, Los Alamos Scientific Laboratory (1958).

8. A. Hemmindinger, Los Alamos Scientific Laboratory, Private Communication (1976).

9. A. Horsley and L. Stewart. Evaluated Neutron Cross Sections for Deuterium, LA-3271, Los Alamos Scientific Laboratory (1968).

10. E.D. Pendlebury, Neutron Cross-Sections of Li^{6} in the Energy Range 0.001 eV to 15 MeV, AWRE-O-60/64, United Kingdom Atomic Energy Authority (1964).

11. M.E. Battat, D.J. Dudziak, and R.J. LaBauve. Li-6 and Li-7 Data in the ENDF/B Format, LA-3695, Los Alamos Scientific Laboratory (1967).

12. E.D. Pendlebury, Neutron Cross-Sections of Li^7 in the Energy Range 0.001 eV to 15 MeV, AWRE-O-61/64, United Kingdom Atomic Energy Authority (1964).

13. D.V. Markovskii, G.V. Yankov, and G.E. Shatalov, Influence of Neutronic Constants on the Neutron Physics Blanket Calculations in Thermonuclear Reactors, IAE-2579, I.V. Kurchatov Institute of Atomic Energy (1975).

14. G.D. Joanou and J.S. Dudek, GAM-II: A B_3 Code for the Calculation of Slowing Down Spectrum and Associated Multigroup Constants, GA-4265, Gulf General Atomic (1963).

15. M. Asprey, R. Lazarus, and R. Seamon. EVXS: A Code to Generate Multigroup Cross Sections from the Los Alamos Master Data File. LA-4855, Los Alamos Scientific Laboratory (1974).

16. D.E. Kusner, S. Kellman, and R.A. Dannels. ETOG-1, A Fortran IV Program to Process Data from the ENDF/B File to the MUFT, GAM, and ANISN Formats. WCAP-3845-1 (ENDF 114), Westinghouse Nuclear Energy Systems (1969).

17. R.E. MacFarlane and R.M. Boicourt, Trans. Am. Nucl. Soc. 22, 720 (1975).

18. K.D. Lathrop, DTF-IV, A Fortran-IV Program for Solving the Multigroup Transport Equation with Anisotropic Scattering, LA-3373, Los Alamos Scientific Laboratory (1965).

19. E.D. Cashwell, J.R. Neergaard, W.M. Taylor, and G.D. Turner, MCN: A Neutron Monte Carlo Code, LA-4751, Los Alamos Scientific Laboratory (1972).

20. J.M. Wallace, D.W. Muir, and W.A. Reupke, in P.G. Young, Applied Nuclear Data Research and Development, January 1-March 31, 1975, LA-6018-PR, Los Alamos Scientific Laboratory (1975).

21. R. Herzing, L. Kuypers, P. Cloth, D. Filges, R. Hecker, and N. Kirch, Nucl. Sci. Eng. 10, 169 (1976).

22. L. Stewart and P.G. Young, Personal Communication, Los Alamos Scientific Laboratory, 28 October 1977.

23. D.E. Bartine, R.G. Alsmiller, Jr., E.M. Oblow, and F.R. Mynatt, Cross Section Sensitivity of Breeding Ratio in a Fusion Reactor Blanket, ORNL-TM-4208, Oak Ridge National Laboratory (1973).

24. D.I. Garber and R.R. Kinsey, Neutron Cross Sections, Volume II, Curves. BNL-325, 3rd ed., Vol. 2, Brookhaven National Laboratory (1976).

25. L. Stewart, in D. Steiner, The Status of Neutron-Induced Nuclear Data for Controlled Thermonuclear Research Applications, USNDC-CTR-1, Oak Ridge National Laboratory (1974).

26. W.A. Reupke and D.W. Muir, in C.I. Baxman, G.M. Hale, and P.G. Young, Applied Nuclear Data Research and Development, Jan. 1-Mar. 31, 1976, LA-6472-PR, p. 52, Los Alamos Scientific Laboratory (1976).

27. D.R. Harris, P.G. Young, and G.M. Hale. Trans. Am. Nucl. Soc. 16, 323 (1973).

28. S.A.W. Gerstl, D.J. Dudziak, and D.W. Muir. Nucl.Sci. Eng. 62, 137 Appendix A (1977).

29. F.G. Perey, G. de Saussure, and R.B. Perez, in J.M. Kallfelz and R.A. Karam, eds., Advanced Reactors: Physics, Design, and Economics, p. 578, Pergamon Press, Oxford (1975).

30. F.C. Difilippo, SUR, A Program to Generate Error Covariance Files. ORNL-TM-5223, Oak Ridge National Laboratory Report (1976).

CHAPTER V

RESULTS AND DISCUSSION OF RESULTS

This chapter presents and elucidates the many results of the consistency analysis. The significance of the initial and final chi-square is analyzed, multigroup cross section adjustment patterns are explained, and the structures of the corresponding dispersion matrices are compared and contrasted. The adjusted radial distribution of the tritium production is interpreted in the light of the input calculated and experimental distributions, and the shapes of the dispersion matrices of the optimized distributions are analyzed. In addition, the adjusted tritium breeding ratio is evaluated. Finally, the chapter assesses the significance of the cross-type correlations which appear between the optimized cross section data and the optimized tritium production data.

Chi-Square of System

Here the statistical significance of the initial and final chi-square values is discussed, the final chi-square is compared with other typical fitting results, and the contributions of significantly large terms in the chi-square quadratic sum are analyzed. The chi-square per degree of freedom, χ^2/DF, or reduced chi-square, of the system before least-squares optimization is found to be 3.0; and after least-squares optimi-

zation 2.3. The variance in the optimized χ^2/DF is calculated to be 0.1. If the statistical errors are assumed to be sampled from a multivariate Gaussian distribution with eleven degrees of freedom, then the probability of equaling or exceeding the initial reduced chi-square of 3.0 is 5.3×10^{-4}, and the probability of equaling or exceeding the final reduced chi-square of 2.3 is 8.2×10^{-3}. These results refer to the initial, or input, dispersion matrix. If the scale of this input matrix were arbitrarily increased by a factor of 2.3, i.e., by scaling the input standard errors by the rather nominal factor of 1.5, then the final reduced chi-square would become unity. For eleven degrees of freedom the probability of equaling or exceeding this value is 0.44. The above probabilities were obtained from a program of Bevington[1] to integrate under the chi-square distribution.

Note that the method of consistency analysis does not establish that the cause of the poor consistency is an underestimation of the input errors. The method merely suggests underestimation of the input errors as one among several possibilities.

These low consistency probabilities must be placed in context. A more realistic interpretation of the consistency results is obtained by comparison with other fitting results in physical science. In Table 5-1, it is seen that an error scale factor of 1.5 is typical of the goodness-of-fit in many physical science situations. When it is recalled that the probability of equaling or exceeding a given value of the reduced

Table 5-1. Present Results in Context of Typical Fitting Results

	DF	Error Scale Factor, $\hat{s}$
Mass of ρ° particle	13	1.3
Mass of Λ particle	4	1.3
^{10}B data for ENDF/B-V, R-matrix fit	100's	1.3
Present work	11	1.5
Decay rate of K°_S particle	12	2.5
1952 atomic constants adjustment	8	2.6
1961 nuclidic masses adjustment	100's	2.7

Particle data from Reference 8 of Chapter II.

R-Matrix results from G. Hale, Private Communication (1977).

Atomic constants data from Reference 13 of Chapter II.

Nuclidic masses data from Reference 9 of Chapter II.

DF = Degrees of freedom.

$\hat{s} = (\chi^2/DF)^{\frac{1}{2}}$

chi-square decreases with the number of degrees of freedom, the consistency measures reported in the present work are even more favorable than would appear from Table 5-1 at first glance.

Contributions to Chi-Square

One may plot an entire matrix of quadratic contributions to chi-square and discern the principal anomalies before and after adjustment. At present, the ALVIN programs give only a summary diagnostic package which lists the initial and final diagonal contribution to chi-square of the differential data as a whole and the integral data as a whole. In addition, the individual diagonal contributions for the final or adjusted data are given. These summary diagnostics, shown in Table 5-2, are useful in interpreting the system chi-square behavior. Values in the table are expressed directly in terms of the chi-square and are not reduced.

As expected, the differential data initially provide no contribution to chi-square since these data are equated with their reference values on input. Thus, the initial chi-square is contributed entirely by an 11 x 11 submatrix of quadratic forms which represents only the tritium production. The diagonal alone of this matrix contributes somewhat in excess of the initial chi-square. In sum, the off-diagonal elements provide a small negative contribution.

Unlike the initial chi-square, the final chi-square generally contains contributions from the differential data since the latter have

Table 5-2. Contributions to Chi-Square

	Initial		Final	
	χ^2_D	χ^2	χ^2_D	χ^2
^{7}Li(n,xt)				
Group 1	0.		3.7	
Group 2	0.		0.3	
Groups 3-17	0.		0.3	
Subtotal	0.		4.3	
Tritium				
^{n}Li 1	8.9		5.0	
2	9.1		6.0	
3	2.7		1.8	
4	1.8		1.3	
5	0.2		0.3	
6	3.2		3.6	
^{7}Li 1	5.2		1.4	
2	3.4		1.0	
3	2.7		.8	
4	0.4		.01	
5	0.4		.8	
Subtotal	37.9		22.1	
Total	37.9	32.5	26.4	25.7

been adjusted away from their reference values to obtain a minimum in the system chi-square. In the present case, the diagonal contributions of the differential data to the final chi-square are quite nominal, namely 4.3 out of 25.7. The bulk of this contribution is provided by the ^{7}Li(n,xt) uppermost energy group. This group is found to suffer the largest adjustment. Similarly, the off-diagonal quadratic terms in the differential data submatrix must provide a small fraction of the already nominal contribution of the differential data. On the other hand, the diagonal contributions of the integral data form a substantial part of the final chi-square. Half of this contribution originates from the 7.5 cm and 9.6 cm ^{n}Li samples, and a smaller but still significant contribution arises from the 25.0 cm ^{n}Li sample. Note that the sum of the diagonal contributions from both the differential data and the integral data also are in excess of the chi-square. Again, a net-negative off-diagonal contribution is indicated, although it is relatively smaller than for the initial chi-square.

In summary, by least-squares analysis a 15.8 unit decrease in the diagonal tritium production chi-square is won at the small expense of a 4.3 unit increase in the diagonal ^{7}Li(n,xt) reaction chi-square.

Multigroup Cross Sections: Results

As indicated in the preceding chapter, the relative changes in the cross sections are dominated by the changes in the ^{7}Li(n,xt) reaction.

Selected results for the D(n,2n) and ^{6}Li(n,t) reactions are presented here as well as complete results for the ^{7}Li(n,xt) reaction.

D(n,2n) Cross Section. The largest D(n,2n) adjustment occurs in the uppermost energy group. Here the adjusted cross section is 98% of the input value. The decrement is a small fraction of the input error of 8%. As the group energy decreases the adjusted cross sections change monotonically from 99% of the input value in the second group to essentially no adjustment in the fifteenth group, at threshold.

^{6}Li(n,t) Cross Section. A trial adjustment listed in Chapter IV used a preliminary version of the integral data dispersion matrix and a ^{6}Li(n,t) 88 group sensitivity matrix. The maximum ^{6}Li(n,t) adjustment occurred in the region of 210 keV, where the adjusted cross section was 99% of the input cross section. This decrement again is a very small fraction of the input error of 15%. Outside of this region the adjustments are nil.

^{7}Li(n,xt) Cross Section. Figure 5-1 shows the multigroup ^{7}Li(n,xt) reaction before and after analysis. The maximum adjustment occurs in the uppermost energy group where the adjusted cross section is 87% of the input or reference cross section. This result is discussed below.

Multigroup Dispersion Matrices: Results

As discussed in Chapter II, all elements of the output dispersion matrix are multiplied by the same scale factor, $\hat{s}^2$ or 2.3 in the present case. While the relative changes in the D(n,2n) and ^{6}Li(n,t) cross

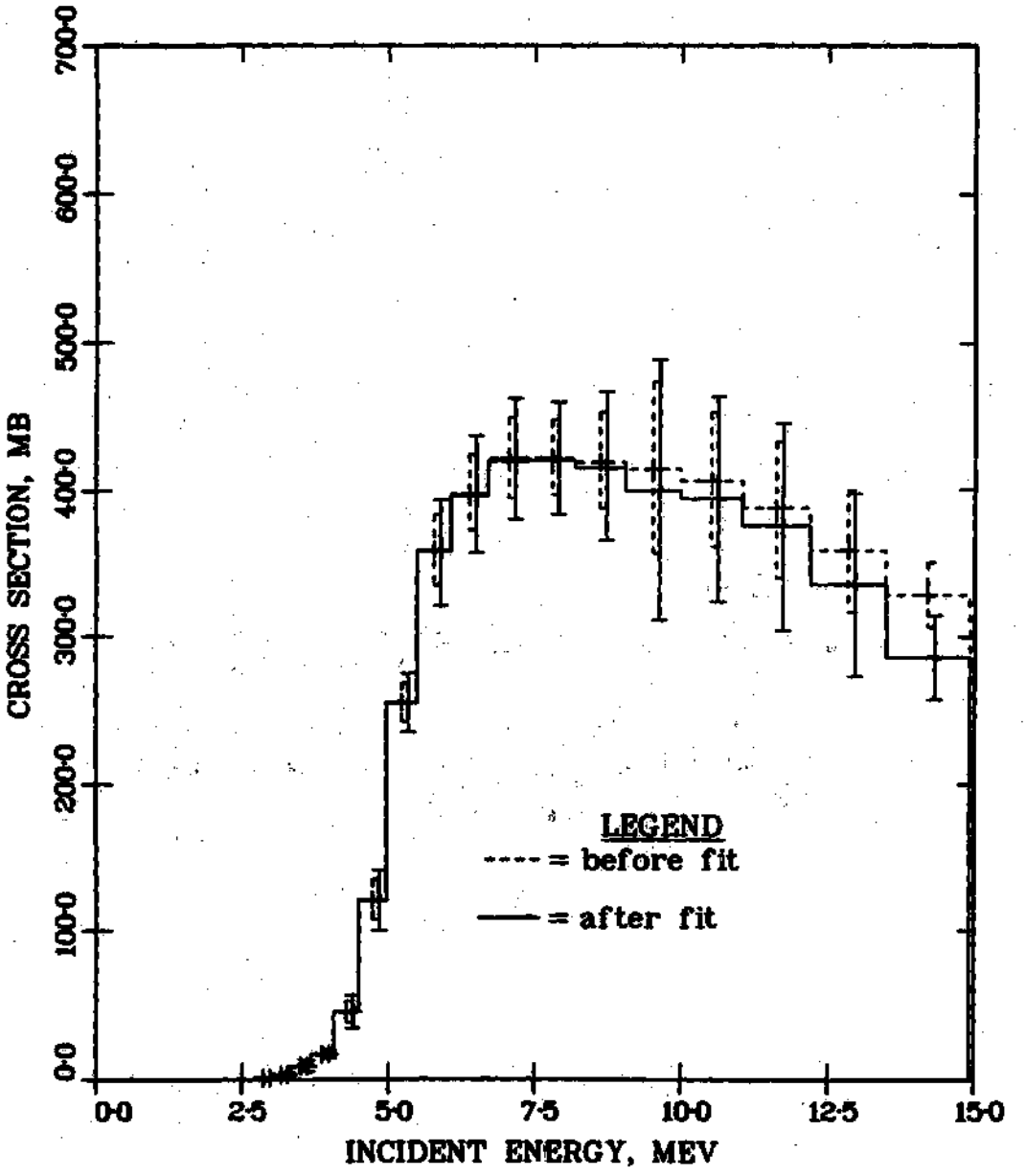

Figure 5-1. $^{7}Li(n,xt)$ Reaction Group Cross Section Before and After Consistency Analysis.

sections are small in relation to the changes in the ^{7}Li(n,xt) cross section, the relative changes in the dispersion matrix elements for all three cross sections are thus of similar scale. Since the rescaled dispersion matrix elements of the D(n,2n) and ^{6}Li(n,t) cross sections are of limited interest, only characteristic results are given here. The ^{7}Li(n,xt) output dispersion matrix is given in full.

D(n,2n) and ^{6}Li(n,t) Dispersion Matrices. Output D(n,2n) standard errors are generally $ times the input standard errors, except in the uppermost energy group. Here the standard error is increased by a factor of only 0.87 $. In the trial calculation which included the ^{6}Li(n,t) reaction, all ^{6}Li(n,t) standard errors are increased by the factor $.

^{7}Li(n,xt) Dispersion Matrix. Figure 5-2 shows the full ^{7}Li(n,xt) dispersion matrix. The standard error in the uppermost energy group is increased by the factor 0.85 $, in the second group by 0.97 $, and in lower groups by $.

Multigroup Cross Sections and Dispersion Matrices: Discussion

This section discusses both individual cross section adjustments and the corresponding adjustments in the dispersion matrices. It has already been noted that the principal contribution to the differential data components of the final chi-square is the change in the ^{7}Li(n,xt) source-energy cross section. This adjustment is discussed in more detail. In general, it is noted that the maximum adjustment for a given partial reaction occurs in the energy group which displays the largest sensitivi-

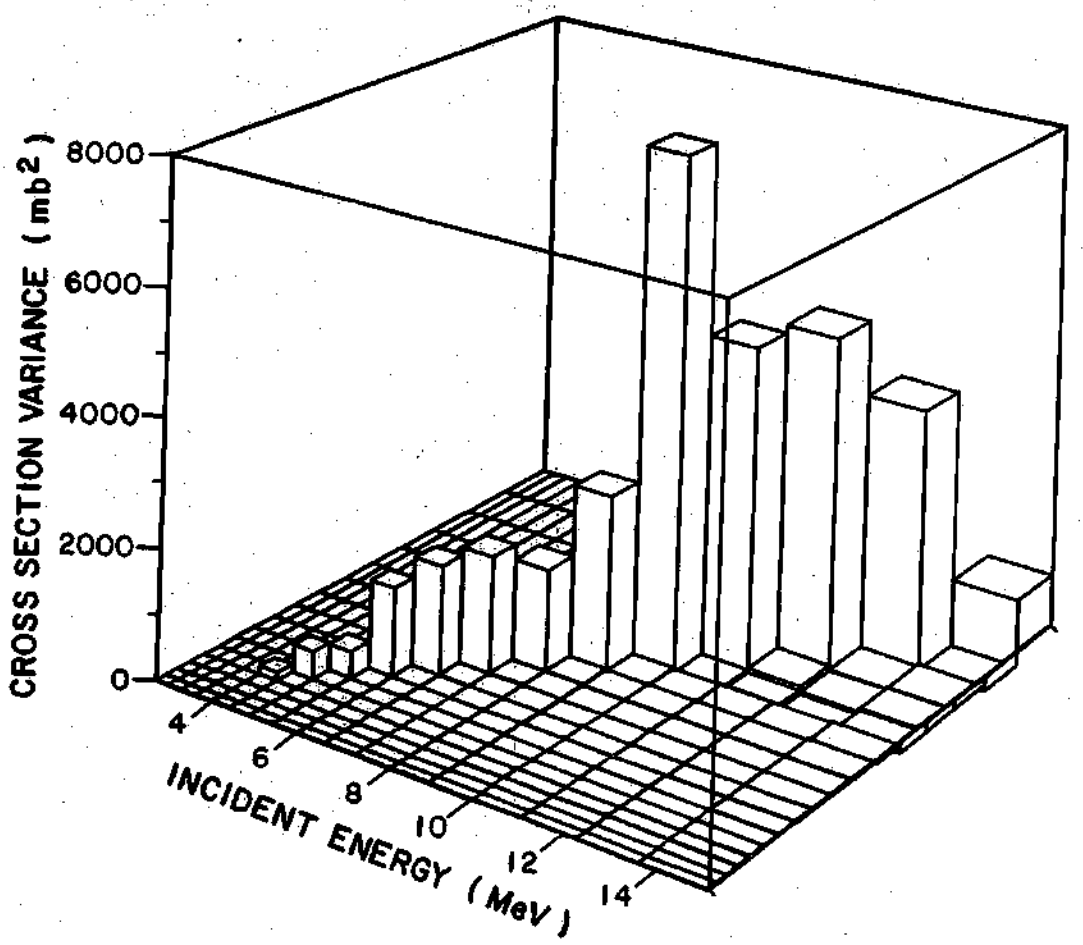

Figure 5-2. $^{7}Li(n,xt)$ Reaction Multigroup Dispersion Matrix, After Consistency Analysis.

ties. The dispersion matrix is found to be increased uniformly by the ratio of external-to-internal consistency, with exceptions as noted. Finally, brief comment is made on the effect of these adjusted cross sections on other neutronic problems.

D(n,2n) Cross Section Adjustment. As stated in the presentation of numerical results, the D(n,2n) group cross section adjustments are dominated by the uppermost or source-energy group, where the adjustment is by a factor 0.98. The latter is small compared to the input cross section error of 8%. Adjustments in lower energy groups are even smaller.

Insight into this pattern is obtained by study of the D(n,2n) sensitivity matrix, Figure 4-6, and the D(n,2n) error vector, Table 4-5. Maximum sensitivity lies in the source-energy group - positive for ^{n}Li and negative for ^{7}Li. An increase in ^{6}Li(n,t) breeding and a decrease in ^{7}Li(n,xt) breeding accompanies a positive increment in the D(n,2n) reaction rate. This effect explains the reversal in sign of the sensitivities. The increase in lower-energy (n,2n) neutrons at the expense of higher-energy elastically scattered neutrons enhances tritium production by the lower-energy ^{6}Li(n,t) breeding reaction in ^{n}Li, but it decreases tritium production from the ^{7}Li(n,xt) reaction. Since the principal discrepancy is the overpredicted tritium production at the 7.5 cm and 10.0 cm ^{n}Li samples, and since the positive ^{n}Li sensitivities clearly outweigh in magnitude the negative ^{7}Li sensitivities, consistency is improved by a decrease in the D(n,2n) reaction, as observed. It is

also evident from the D(n,2n) sensitivity matrix that the source-energy group has more leverage than any other group. Consequently the adjustment is concentrated in this group.

In addition to sensitivity arguments, consider the role of the D(n,2n) error vector. In general, the smaller the relative error of a cross section the lesser the adjustment, and vice versa. Table 4-5 does indicate progressively larger relative errors at lower energies. This effect, taken by itself, would argue against the observed adjustment. However, comparison of the scales of the energy variation of the sensitivities and the energy variation of the relative errors confirms that the sensitivity effect outweighs the relative variance effect, in accordance with the observed results.

^{6}Li(n,t) Cross Section Adjustment. It is recalled that the preliminary calculation with the total cross section variable showed a maximum adjustment by a factor of only 0.989, at about 210 keV. This is indeed a small fraction of the input error of 15% in this energy group. Adjustments in other groups were found to be even smaller and, consequently, the ^{6}Li(n,t) adjustment was not pursued further. Some interest, however, is attached to this trial adjustment, since it is the only case in which the maximum adjustment for the given partial reaction occurred outside the source energy group. Again, the explanation is found by consideration of the ^{6}Li(n,t) sensitivity matrix, Figure 4-7, and the error vector, Table 4-6. Examination of the sensitivity matrix, particularly the ^{n}Li submatrix,

indicates a maximum sensitivity precisely in the region of maximum adjustment. Both features correspond closely to the location of a pronounced resonance in the $^{6}Li(n,t)$ cross section, Figure 4-2. Further study of the cross section input variances, which reach a maximum at 300 keV, supports the observation of maximum adjustment in this region.

$^{7}Li(n,xt)$ Cross Section Adjustment. As indicated previously, the $^{7}Li(n,xt)$ reaction completely dominates the adjustment pattern. As in both other reactions, maximum adjustment occurs in the group of maximum sensitivity. As in the case of the other smoothly varying reaction, the D(n,2n) reaction, maximum sensitivity occurs in the source-energy group. See Figure 4-8. The adjustment is by a factor of 0.87 and represents a decrement of about twice the input relative error. This result differs from an earlier adjustment (Chapter IV, Reference 1) of a factor of 0.65. The relative changes in lower energy groups decrease monotonically and are generally smaller than the input relative error.

As before, the adjustment pattern is explained in terms of the sensitivity matrix and input variances. The $^{7}Li(n,xt)$ sensitivity matrix confirms not only the sensitivity maxima in the source-energy group but reveals also the very large magnitude of the source-energy sensitivities of the $^{7}Li(n,xt)$ reaction compared to the D(n,2n) and $^{6}Li(n,t)$ maximum sensitivities. Although the input relative variances increase somewhat in the lower energy groups, the increase hardly offsets the rapid decrease in the sensitivities. Because of the dominant source-energy

^{7}Li(n,xt) sensitivity, the bulk of the adjustment is concentrated here to obtain maximum leverage on the discrepant tritium production data with minimum overall impact on the cross sections. It has already been observed that, despite the two standard deviation decrease in the source-energy group cross section, the effect of this adjustment on the final chi-square is quite nominal relative to the benefit.

Figure 5-3 compares the adjusted source-energy ^{7}Li(n,xt) cross section with the various 14.1 MeV differential measurements. Error bars shown on individual measurements are the errors quoted by the experimenter and do not reflect external consistency. The error shown on the adjustment datum includes the external consistency scale factor. While the adjusted cross section value, 288 mb, is somewhat lower than other results, the value is not grossly inconsistent with the ensemble of data. In view of the weight of the reference cross section data in the consistency analysis this result is not surprising. However, sufficiently discrepant integral data which are also of sufficient weight could yield virtually any result. Thus, the agreement shown is of interest. The Wyman and Thorpe datum, though not explicitly used in the Pendlebury/ENDF evaluation or in the consistency analysis, is included in Figure 5-3 as a matter of additional interest.

Cross Section Dispersion Matrix Adjustment. Except in cases of the D(n,2n) and ^{7}Li(n,xt) uppermost energy groups, the output matrix of D(n,2n), ^{6}Li(n,t), and ^{7}Li(n,xt) cross sections is generally the input

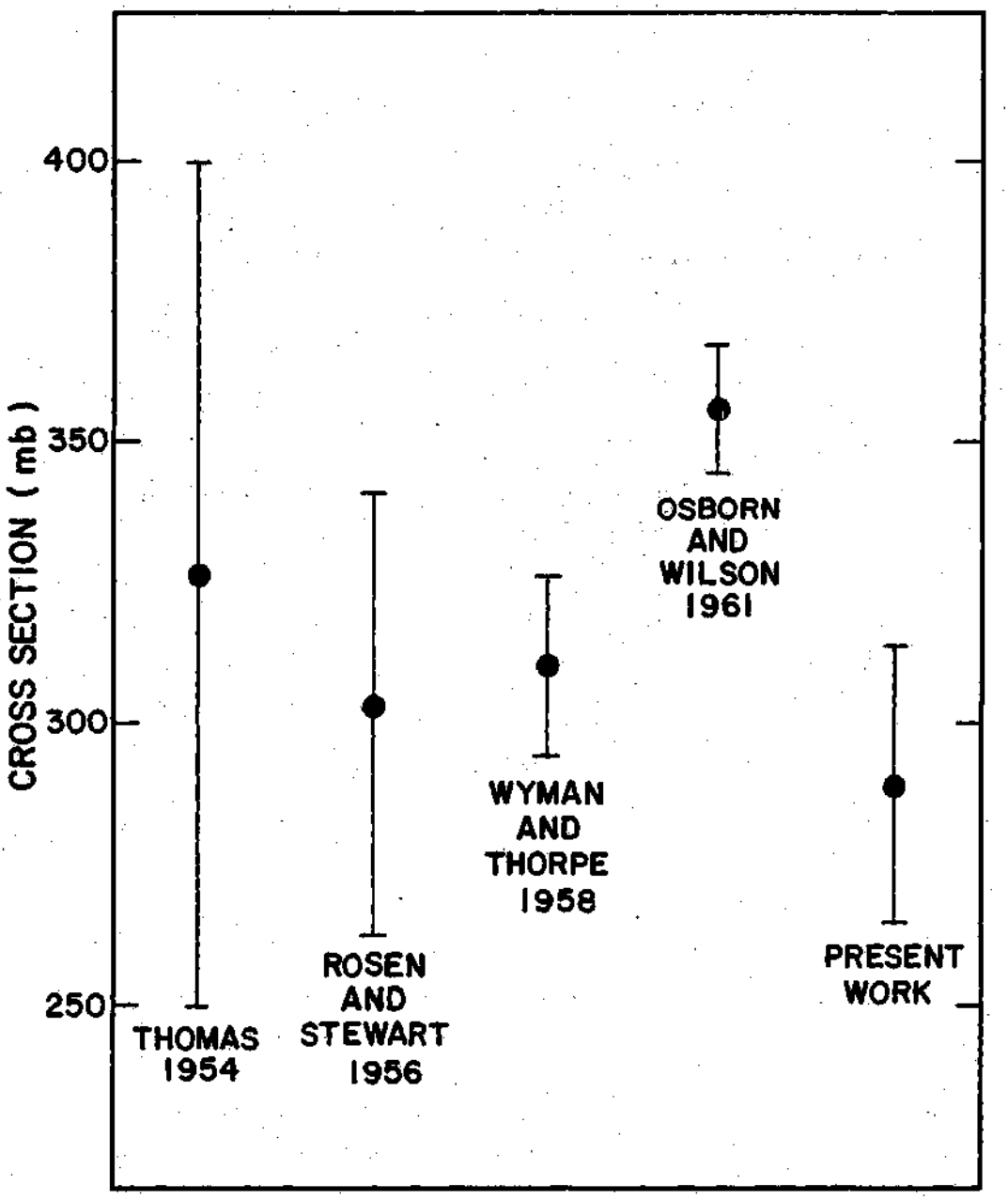

Figure 5-3. Comparison of 14 MeV $^{7}Li(n,xt)$ Reaction Cross Section Data (see text).

value scaled by the ratio of external-to-internal consistency. In these uppermost energy groups the variances and covariances are less than the scale factor alone would predict. Thus, the ^{7}Li(n,xt) group one error is not increased by $\hat{s}$ but by only $0.85\hat{s}$. The explanation for this phenomenon again lies in the sensitivities. For the more sensitive, uppermost energy groups the integral data are closely enough coupled to serve as indirect cross section measurements. Apart from the ratio of external-to-internal consistency scale factor, they serve to reduce the variance of the reference cross section as would any other cross section measurements. For the less sensitive energy groups and partial reactions, this effect is smaller or negligible.

This behavior is more exactly analyzed in terms of Equation 2-48:

$$\hat{D}\hat{(X)} = \hat{s}^2\left\{D^{-1}[O(X)]+ S^{T}D^{-1}[O(SX)]S\right\}^{-1}.$$

As shown below, the weight of the second summand - which corresponds to the uncertainty of the experimental tritium production - is relatively small. Thus the output matrix is approximately $\hat{s}^2$ D[O(X)] or a scalar multiple of the input matrix. Note, however, the small, negative off-diagonal components in groups two through five (Figure 5-2).

An undesirable feature of the scale factor, discussed in Chapter II, is the indiscriminate enhancement of errors for cross section data which participate only weakly in the analysis. Thus, the errors in some of the rather insensitive D(n,2n) and ^{6}Li(n,t) energy groups are scaled

in the same proportion as are the errors in the much more sensitive ^{7}Li(n,xt) groups three to seventeen. To take an extreme case, if the trace moisture content in the LiD were included in the analysis, the input errors for H and O would also be scaled by $. In view of this peculiarity of the scale factor, the augmentation of errors in the less sensitive partial reactions and energy groups is not given further consideration here.

Application of Adjusted Cross Sections to Other Problems

Since the adjustment is carried out with the constraint that the total ^{7}Li cross section remains constant the decrease in the ^{7}Li(n,xt) reaction is accompanied by an increase in the complementary elastic, (n,n'), (n,2n), and (n,d) reactions. In the present adjustment, the complementary partials are all increased in proportion to their ENDF/B values. Figure 4-3 shows that the principal, absolute increase occurs in the elastic channel. For 14 MeV incident neutrons the average energy of elastically scattered neutrons is 11 MeV, while the average energy of (n,xt) secondary neutrons is only 5 to 6 MeV. In 14 MeV neutron-driven systems using the adjusted cross sections, this effect alone should harden the spectrum relative to the spectrum calculated from the reference cross sections. Similarly, the effects of the increases in the other complementary reactions may be estimated. The effect on a given response function in a given neutronic system will vary with the nature of the response function and no general prediction can be made. An accurate

analysis for a given system can always be obtained by performing suitable sensitivity calculations. In general, however, the uncritical application of cross sections adjusted for one response function to quite different response functions is not to be recommended.

The adjusted cross sections may be applied with a greater logical basis to similar, tritium production integral experiments. Two such experiments are considered here. In a recently performed Los Alamos experiment[2] the radial distribution of the tritium production in a 14 MeV neutron-driven lithium deuteride sphere was measured using ^{6}LiD and ^{7}LiD detector samples. The dissolved tritium β^- activity was counted by a radiochemical method. On the basis of preliminary findings, the experimental distribution of f(R) in ^{7}LiD is overcalculated in the inner region. This discrepancy pattern is qualitatively similar to that observed in the metal-detector experiment analyzed in the present work. Consequently, it is expected that the adjusted cross sections would more reliably predict the tritium production for this recent experiment than would unadjusted cross sections. In a Jülich experiment,[3] 14 MeV neutrons drove a ^{n}Li metal cylinder containing ^{n}Li metal, $^{n}Li_2CO_3$, and $^{7}LiCO_3$ detectors. The tritons from the metal were counted after thermal extraction, and those from the carbonete were counted by liquid scintillation. Comparison of the ^{n}Li metal thermal extraction results with the experimenter's most recent[4] multigroup Monte Carlo calculations using ENDF/B-III shows an overcalculation of the triton production per cubic centimeter

of order 20% near the inner regions and an overcalculation of some 10% in the outer regions. The shape discrepancy is qualitatively similar to that observed in the Wyman experiment and it is possible that use of the adjusted cross sections would improve agreement. Nearly perfect agreement exists between the liquid scintillation results[4] and calculation for $^{n}Li_2CO_3$; but for $^{7}Li_2CO_3$ 15-20% overcalculation is observed near the inner regions and 10% overcalculation is observed near the outer regions. The shape discrepancy for the $^{7}Li_2CO_3$ liquid scintillation measurement is again qualitatively similar to the general pattern in the three experiments and the adjusted cross sections might again yield improvement.

Tritium Production Distribution and Dispersion Matrix

This section examines in greater detail both the optimized radial distribution of tritium production and the corresponding dispersion matrix. The volume integrated tritium production is treated in a later section.

Radial Distribution of Tritium Production

The interpretation of the changes in the radial distribution of tritium production requires an understanding of the uncertainties in the calculated distribution due to cross section uncertainties. As discussed previously, the errors in calculated transport results - the radial distribution of tritium production and the tritium breeding ratio - are obtained by combining the evaluated cross section dispersion matrix and

the calculated sensitivity matrices. The results of this calculation are shown in Figure 5-4. Standard errors in the calculated tritium production are presented in the form of dashed lines for both ^{n}Li and ^{7}Li-enriched metal samples. The dashed lines represent plus and minus one standard deviation about the mean value and are obtained by connecting the discrete sample results with a cubic spline.

Figure 5-4 also depicts the radial distribution of tritium production after least-squares optimization. The standard deviation of the optimized tritium distribution is shown in the form of solid lines representing plus and minus one standard deviation. As before, the curved lines are constructed by connecting discrete sample points with a cubic spline.

Among the features of interest is the occurrence of the largest adjustments near the inner regions of the sphere. There are three reasons for this phenomenon. First, the discrepancies - which act as driving terms in the adjustment - are largest near the interior. Second, it is apparent from the ^{7}Li(n,xt) sensitivity matrix that by far the largest sensitivities occur in the innermost regions of the sphere, as expected. For a given set of decreases in the ^{7}Li(n,xt) cross section the decrease in the distribution will be the largest in the inner regions. Third, the variances in the calculated radial distributions are much larger near the interior of the sphere. In regard to the calculated distribution, a greater absolute change is possible in the inner regions with less

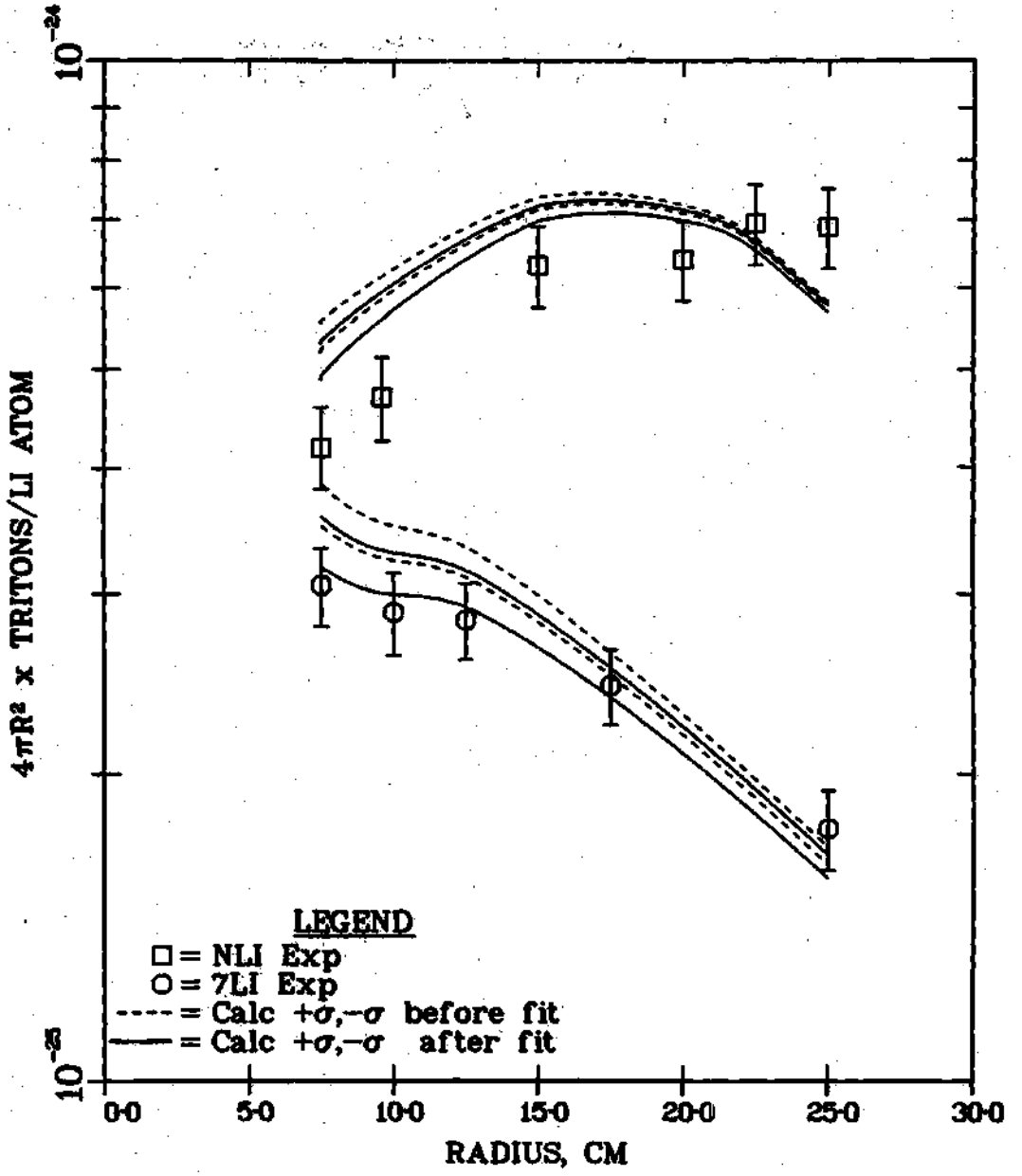

Figure 5-4. Radial Distribution of Tritium Production Before and After Consistency Analysis.

penalty in final chi-square than is possible in the outer regions (see Equation 2-50). Of course, the larger variance in the calculated distribution in the inner region is itself due to the larger sensitivity.

As noted previously, even after adjustment the 7.5 cm and 9.6 cm ^{n}Li points continue to contribute significantly to the chi-square. The relatively small change from calculated values in these ^{n}Li samples, when compared to the innermost ^{7}Li samples, is due to the relatively smaller sensitivity and to the related, smaller variance in the calculated distribution.

At the outer regions the errant 25 cm ^{n}Li sample is responsible for the third largest contribution to the integral data chi-square. Because of the very small variance in the calculated production, the adjusted value cannot vary much from this calculated value. Although the 27.5 cm ^{n}Li datum has been excluded from the analysis because of the likelihood of room return thermal neutron contamination, the possibility cannot be excluded that this effect contaminates, to some degree, the 22.5 cm and 25.0 cm ^{n}Li samples. Such a systematic effect lies outside the scope of statistical adjustment.

Note that the 25.0 cm ^{n}Li and, especially, the 25.0 cm ^{7}Li points are adjusted away from <u>both</u> calculated and experimental values. The explanation of this phenomenon is that the present cross section adjustments cannot both decrease the tritium production at the inside and increase the production at the outside of the sphere. A tradeoff is

required, and the $^{7}Li(n,xt)$ group cross section slightly penalizes the undercalculated, outer few samples to win larger gains for the half dozen overcalculated inner samples.

Tritium Production Dispersion Matrix

Examination of the diagonal of the tritium production radial distribution dispersion matrix after adjustment, Figure 5-5, confirms the pattern shown on Figure 5-4. Larger variances are observed in the inner regions than in the outer regions. The pattern is similar to that of the dispersion matrix of the calculated radial distribution. Thus, the adjusted dispersion matrix - a weighted sum of the experimental and calculated dispersion matrices - is strongly biased towards the calculated matrix. This observation is confirmed by a comparison of the general magnitudes of the two matrices. The magnitude of the relative experimental dispersion matrix, Figure 4-5, is of order 10^{-2}, while the magnitude of the relative calculated dispersion matrix is of order 10^{-3}, at the inner regions, to 10^{-6} at the outer regions. Since the weights of the matrices are inversely proportional to the variances, it is evident that little of the experimental matrix will be manifest in the output matrix. The precise shape of the output matrix is given by Equations 2-48 and 2-49 as:

$$S\left\{D^{-1}[O(X)] + S^{T}D^{-1}[O(SX)]S\right\}^{-1}S^{T}.$$

If the relative contribution of $D[O(SX)]$ is vanishing, then the result, $SD[O(X)]S^{T}$, is identical to the dispersion matrix as calculated from the

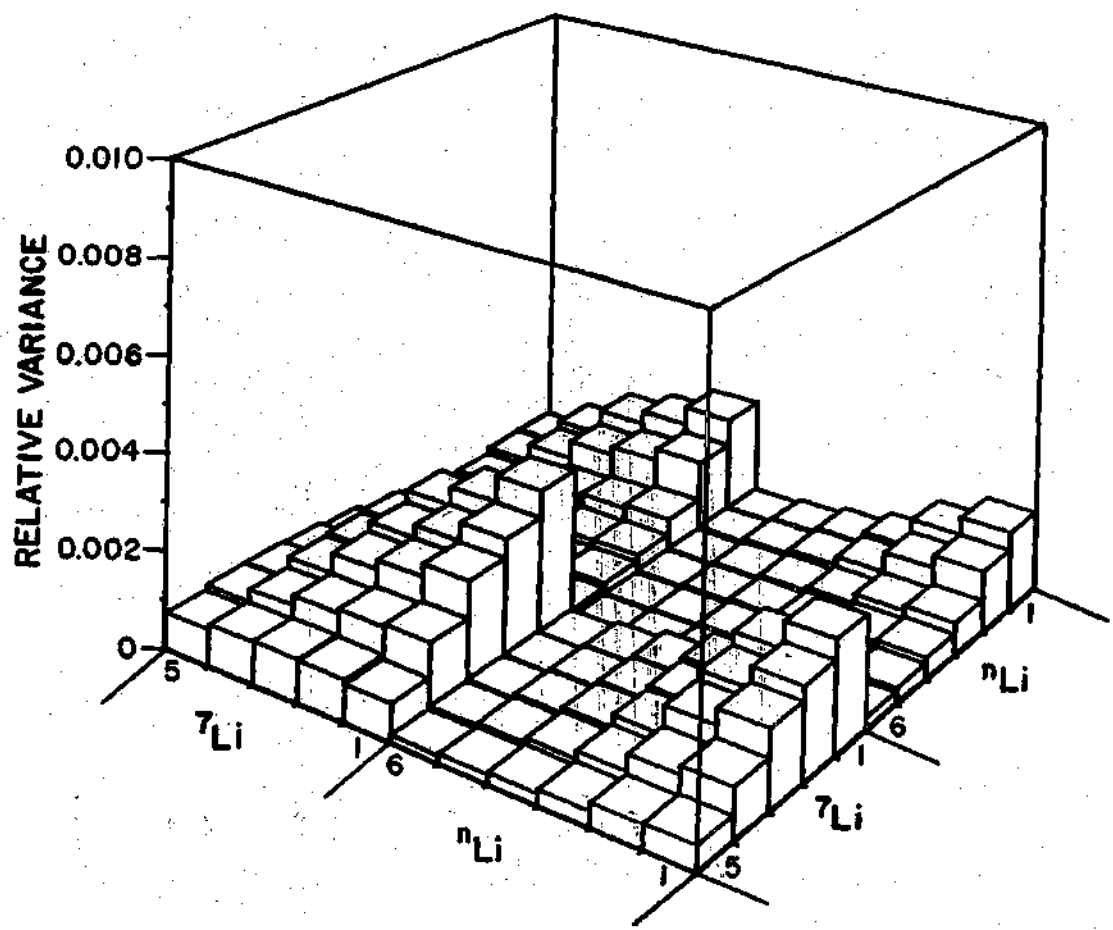

Figure 5-5. Tritium Production Dispersion Matrix, After Consistency Analysis.

cross section uncertainties, Equation 2-25d. Considering the shapes of S, Figure 4-8, and of D[O(X)], Figure 4-9, the shape of the output tritium production dispersion matrix is not surprising.

Note that the scale of the output tritium production matrix, even after multiplication by the scale factor, $\hat{s}$, is reduced when compared to experimental values. This result is in contrast to the behavior of the cross section dispersion matrix. The net reduction in scale is explained in terms of the small variance of the dispersion matrix of calculated tritium production, expecially in the outer regions.

Tritium Breeding Ratio

As estimated from the ^{n}Li sample distribution, the previously described graphical method yields an experimental tritium breeding ratio of 0.86 with a standard deviation of 4.5%. The standard error in the calculated tritium breeding ratio of 0.93, due to cross section uncertainty, and prior to least-squares analysis, is found to be 1.7%. This result includes the effect of the off-diagonal elements of the dispersion matrix of calculated radial production. The pattern of adjustment, Table 5-3, follows the general trend of the adjusted radial distribution and the fitted breeding ratio, 0.90, lies closer to the initially calculated value, 0.93, than to the experimental value, 0.86. In general terms the phenomenon is attributed to the fact that the initial uncertainty of the former, 1.7%, is much smaller than the initial uncertainty of the latter, 4.5%. However, if the calculated and experimental breeding ratios are

Table 5-3. Tritium Breeding Ratio Before and After Consistency Analysis.

Tritium Breeding Ratio	Before Consistency Analysis		After Consistency Analysis
	Calculated	Experimental	
T_6	0.547		0.546
T_7	0.381		0.358
T	0.928	0.86[a]	0.904
Standard Error in T	1.7%	4.5%	2.1%

[a] Determined graphically from ^{n}Li sample data.

combined in a simple weighted average, according to their input uncertainties, the resulting breeding ratio, 0.92, is even closer to the calculated value. That the actual output value is lower is partially attributed to the fact that only the ^{n}Li metal data were used to estimate the experimental value of the breeding ratio, whereas the consistency algorithms include also the low-lying ^{7}Li metal data.

In regard to the output uncertainty, were it not for the operation of the ratio of external-to-internal consistency or scale factor, the output error would be somewhat smaller than the calculated input error of 1.7%. The actual value of 2.1% reflects the operation of the scale factor. Thus, the net effect of considering the experimental results is to increase the uncertainty in the tritium breeding ratio over the value calculated from the initial cross section uncertainties, much as in the case of the radial distributions.

Assessment of the significance to weapon technology of the decrease in the tritium production is beyond the scope of the work at hand. In the broader context of controlled fusion reactor blanket design, it would appear at first inspection that such a decrease would lie well within acceptable margins since, at least in early blanket conceptual designs, the calculated breeding ratio is well above unity. Recently, however, breeding ratios near unity appear more frequently[5] and the effects of a further decrease in tritium breeding may be significant. Consistency analysis using measurements on prototype blankets may place these calcu-

lations in better perspective.

Correlation Coefficient Matrix

The correlation of uncertainties in the fitted ^{7}Li(n,xt) group cross section data and the fitted tritium distribution data, as shown in Figure 5-6, clearly differs from the input values of zero. As indicated in Chapter II, the appearance of cross-type correlations on output is a natural consequence of the functional relationship between the output differential and integral data. Thus, the +0.86 covariance between the normalized ^{7}Li(n,xt) group one and ^{n}Li 7.5 cm tritium data indicates that if the optimized ^{7}Li(n,xt) group one cross section were in error by 10% on the high side, then the optimized ^{n}Li 7.5 cm tritium production should be some 9.2% on the high side. These cross-type correlations characterize only the adjusted values of the particular input data used in this analysis. Correlations arising from the choice of an entirely different integral experiment might have an entirely different character.

The shape of the matrix $S\hat{D}$ is not obvious from the shapes of S and of $\hat{D}$. However, in the present case an element of $S\hat{D}$:

$$\rho_{ij} = \sum_{k} p_{ik} \, \mathrm{cov}(\hat{x}_k, \hat{x}_j), \tag{5-1}$$

where p_{ik} is an element of S and $\mathrm{cov}(\hat{x}_k, \hat{x}_j)$ is an element of $\hat{D}$, is simplified, since $\hat{D}$ is nearly diagonal. Thus, very nearly:

$$\rho_{ij} = p_{ij} \, \mathrm{var}(\hat{x}_j, \hat{x}_j). \tag{5-2}$$

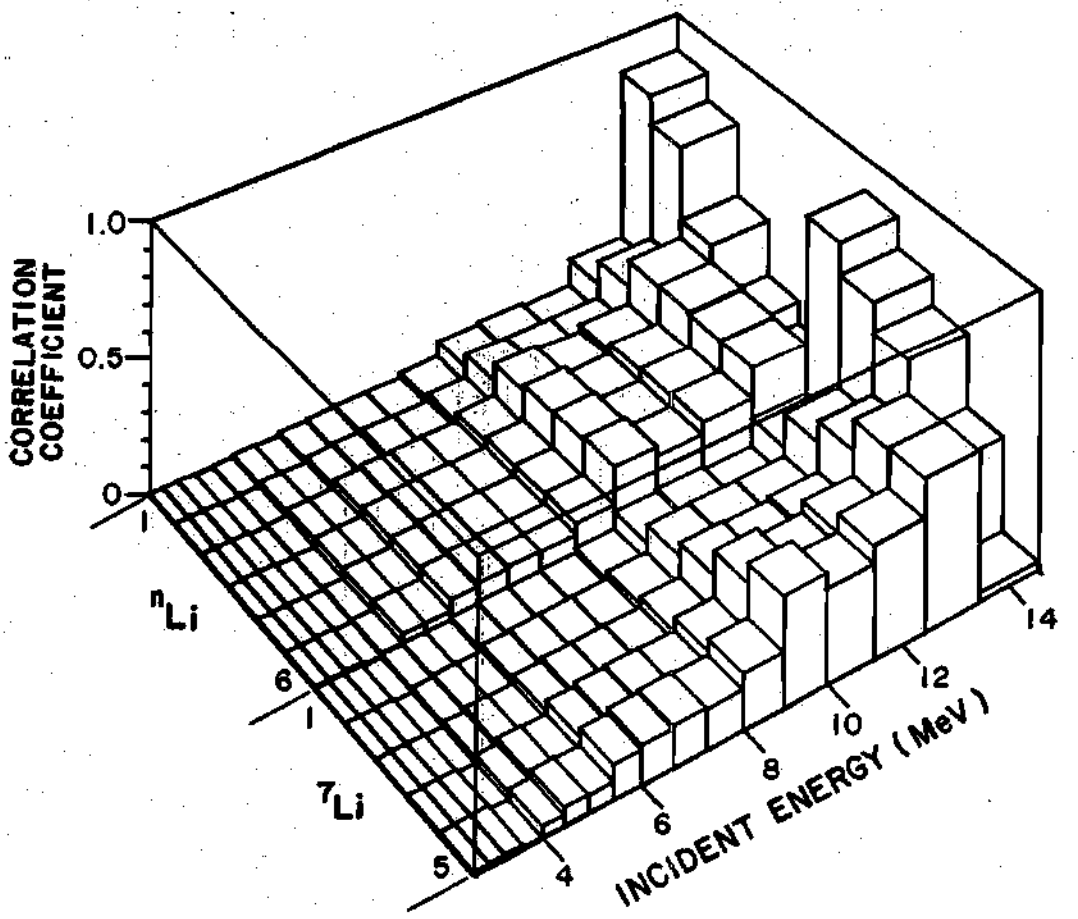

Figure 5-6. Cross-Type Correlation Coefficient Matrix, After Consistency Analysis.

When the row index i is held constant, for example i = 1(^{n}Li 7.5 cm), the columnar variation j, groups one to seventeen, should track the product of the corresponding sensitivity vector p_{ij}, $1 \leq j \leq 17$, and the changing diagonal element of $\hat{D}$. The generally decreasing correlations with decreasing energy reflect a similar pattern in the sensitivity matrix, Figure 4-8, but the correlations are equally modulated by the shape of $\hat{D}$, Figure 5-2. Thus, a local maximum at group five is observed in all rows. This maximum is not observed in the sensitivity matrix but reflects the absolute maximum in $\hat{D}$.

Summary

The significance of the initial and final system chi-square has been evaluated. Multigroup cross section adjustment patterns have been analyzed and the structures of the cross section dispersion matrices have been explained. The adjustment of the tritium production radial distribution was assessed in terms of the initial calculated and experimental distributions and the patterns of the dispersion matrices of the optimized distributions were elucidated. Further, the significance of the cross-type correlations has been delineated. In the following, final chapter, conclusions derived from the present discussion are set forth.

REFERENCES

1. P.R. Bevington, Data Reduction and Error Analysis for the Physical Sciences, McGraw-Hill, New York (1969).

2. J. Wallace, A. Hemmendinger, and C. Ragan III, Los Alamos Scientific Laboratory, Private Communication (1977).

3. P. Cloth, D. Filges, H. Geiser, R. Herzing, G.L. Stöcklin, and R. Wölfe, Proc. 8th Symp. Fusion Technology, 17-21 June 1974, Noordwijkerhout, Netherlands.

4. R. Herzing, L. Kuypers, P. Cloth, D. Filges, R. Hecker, and N. Kirch, Nucl. Sci. Eng., 60, 169 (1976).

5. J.R. Powell, J.A. Fillo, B.G. Twining, and J.J. Dorning, Proc. Magnetic Fusion Energy Blanket and Shield Workshop, ERDA-76/117/2, U.S. Energy Research and Development Administration (1975).

CHAPTER VI

CONCLUSIONS AND RECOMMENDATIONS

Conclusions

1. With a newly developed computer program it is feasible to perform a statistical consistency analysis of combined differential and integral neutronic data in which the multigroup cross-section energy mesh is at least as fine as 100 energy groups, thus relaxing the similarity-of-spectrum restriction inherent in few-group procedures.

2. The statistical consistency analysis may be performed with significant saving in computer execution time provided that initially there are no statistical correlations between the differential data and the integral data.

3. It is feasible to perform a statistical consistency analysis of combined differential and integral data in which the integral data consists of many, space-dependent data obtained from one, or a few, assemblies, as well as in the more common case in which one, or a few, space-independent data are obtained from each of many assemblies.

4. By suggesting sources of previously unidentified systematic and statistical errors, statistical consistency analysis may be used in an iterative mode to refine the input error matrix and thus to improve the ultimate accuracy of the consistency analysis.

5. In the statistical consistency analysis of selected thermonuclear neutronics data, namely the consistency of evaluated neutron cross section data and radially-dependent tritium production measurements for a 14 MeV neutron-driven 30 cm diameter ^{n}LiD sphere, it is found that:

a) The large sensitivities of the ^{7}Li(n,xt) reaction, relative to the D(n,2n) and ^{6}Li(n,t) reactions, result in the dominance of the consistency results by the ^{7}Li(n,xt) reaction.

b) The sensitivity matrix for the ^{7}Li(n,xt) reaction is dominated by the source-energy group at small radii, with corresponding dominance of the consistency findings by changes in the source-energy group cross section and by changes in the tritium production at small radii.

c) As a result of the dominance of the sensitivity matrix by the source-energy group cross section, the detailed magnitude of the statistical correlations among the cross sections is found to have little effect on the consistency analysis.

d) The tritium production sensitivities to the dominant ^{7}Li(n,xt) tritium production reaction, as well as to the ^{6}Li(n,t) reaction, may be resolved into a relatively large detector response contribution and a relatively small transport effect contribution, except near the periphery of the sphere, where the transport effect is of the same order of magnitude as the detector response effect.

e) As a result of the dominance of the tritium production sensitivities by the detector response contri-

bution, which is independent of the shape of the secondary neutron energy and angle distributions, the results of the consistency analysis do not depend greatly on these distributions.

f) The combined adjustment of the group cross section data and the tritium production data, without multiplication of input errors by the ratio of external-to-internal consistency, improves the chi-square per degree of freedom of the system from 3.0 to 2.3, a fifteen-fold improvement in the statistical likelihood of the combined data.

g) The improvement in the statistical consistency is accompanied by a reduction in the source-energy $^{7}Li(n,xt)$ group cross section from its nominal value of 328 mb to 284 mb.

h) And, finally, the improvement in the statistical consistency is accompanied by an adjustment of the tritium production considerably closer to the initially calculated values than to the experimental values.

Recommendations

Due to the limitations of finite resources, potentially fertile areas of investigation were passed over in pursuing the most direct path to the results of present interest. Given here are recommendations to future investigators for additional exploration.

1. An investigation should be undertaken to determine if the consistency algorithm should be revised so that the augmentation of output errors by the ratio of external-to-internal consistency is responsive to the magnitude of the corresponding sensitivity coefficients, in order that the output errors of insensitive variables are not arbitrarily augmented.

2. The execution time of the consistency analysis code implemented in this work should be improved significantly by modifying the matrix inversion subroutine to take advantage of the symmetry properties of the matrix forms.

3. The sensitivity analysis and least-squares parts of the consistency analysis code should be incorporated as separate overlays to increase the available core storage and to permit the solution of larger problems.

4. The individual graphics programs developed for the consistency analysis code should be incorporated as integral parts of the code to reduce the amount of software manipulation.

5. The scope of the consistency analysis program should be increased by the addition of a two-dimensional discrete ordinates sensitivity module.

6. The flexibility of the consistency analysis code may be increased by the development of a cross section adjustment module which incorporates theoretical parameterizations of the cross sections.

7. The scope of the consistency analysis code should be increased by coupling the output modules to the input modules to facilitate an iterative approach to the solution of non-linear adjustment problems.

8. Initiatives should be made to require more complete discussion of experimental errors in the report literature, particularly with regard to the identification of correlated components of error.

9. Sensitivity analysis and consistency analysis should be incorporated in the design of new integral experiments to maximize the utility of the experiment in reducing the uncertainty of predicted neutronics design parameters.

APPENDIX I

DATA PROCESSING CONSIDERATIONS

Details of the calculation procedure are treated here. Included is a brief description of the data processing facility, system flowcharts, and a glossary of computer programs.

Data Processing Facility

The Central Computing Facility (CCF) of the Los Alamos Scientific Laboratory, Los Alamos, New Mexico, implemented the calculations described herein. The principal system used was the LASL Hydra network. This network consists of a central Control Data Corporation Model 6600 digital computer linked to four CDC Model 7600 digital computers. Each 7600 operates with a characteristic add time of 30 to 110 nanoseconds and contains two types of core storage: small-core memory, with a capacity of 4×10^6 bits and a storage cycle time of 0.3 microsecond; and large-core memory, with a capacity of 3×10^7 bits and a storage cycle time of 1.8 microsecond. The central 6600 machine is linked to a CDC Model 821 disc memory with 7.2×10^9 bits storage capacity and to an IBM Model 1360 photodigital memory (symbolized by an ellipse in the flowcharts) with a capacity of 10^{12} bits. The foregoing hardware was used for the bulk of the calculations.

Two dimensional graphics were prepared with a second 6600 computer and CDC Model 844 disc memory used in conjunction with a Texas Instruments 4015 CRT terminal.

System Flowcharts

Flowcharts of the consistency analysis computation are given in the figures. The general scheme follows Figure 4-10.

Glossary of Computer Programs

Table 1 summarizes the computer programs used in the present work. Unless indicated otherwise, all programs listed were written expressly for the present work. Some offer wider application.

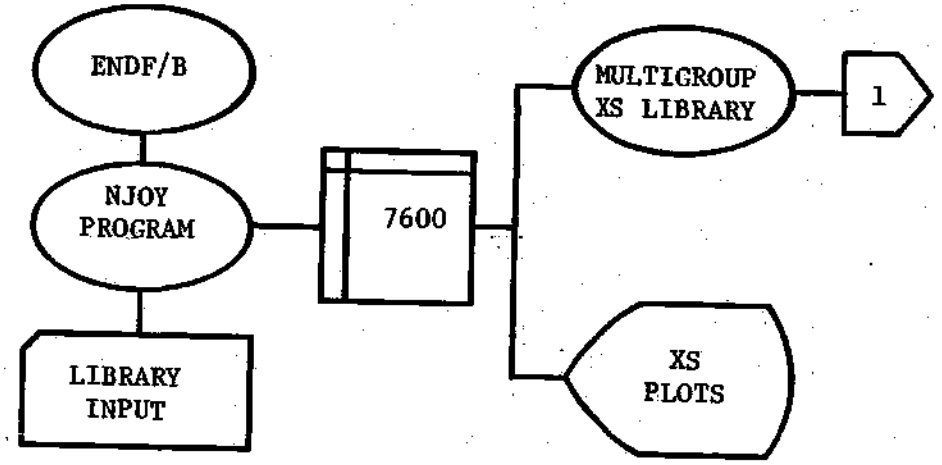

Figure 1. Multigroup Cross Sections.

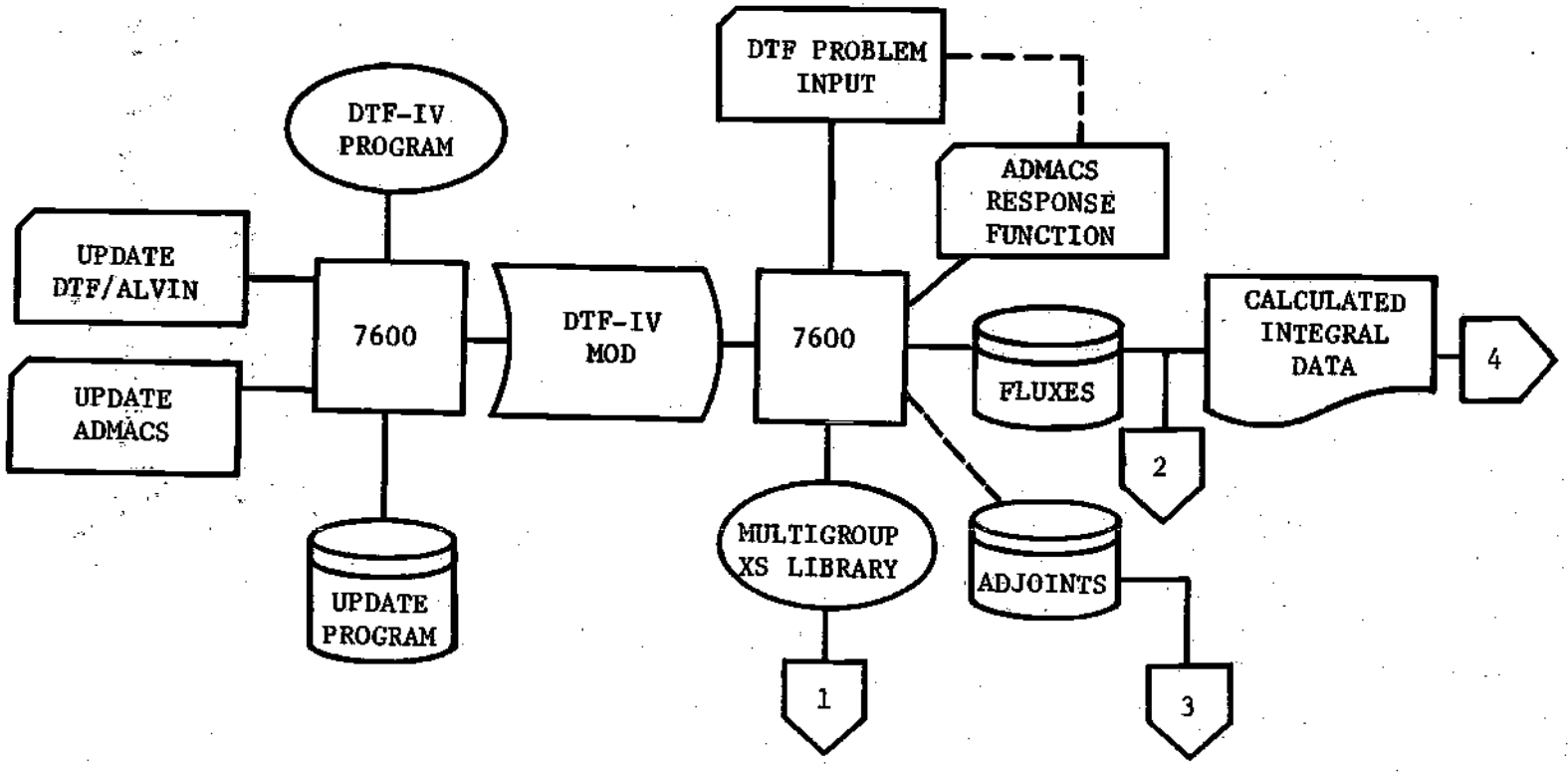

Figure 2. Fluxes and Adjoints.

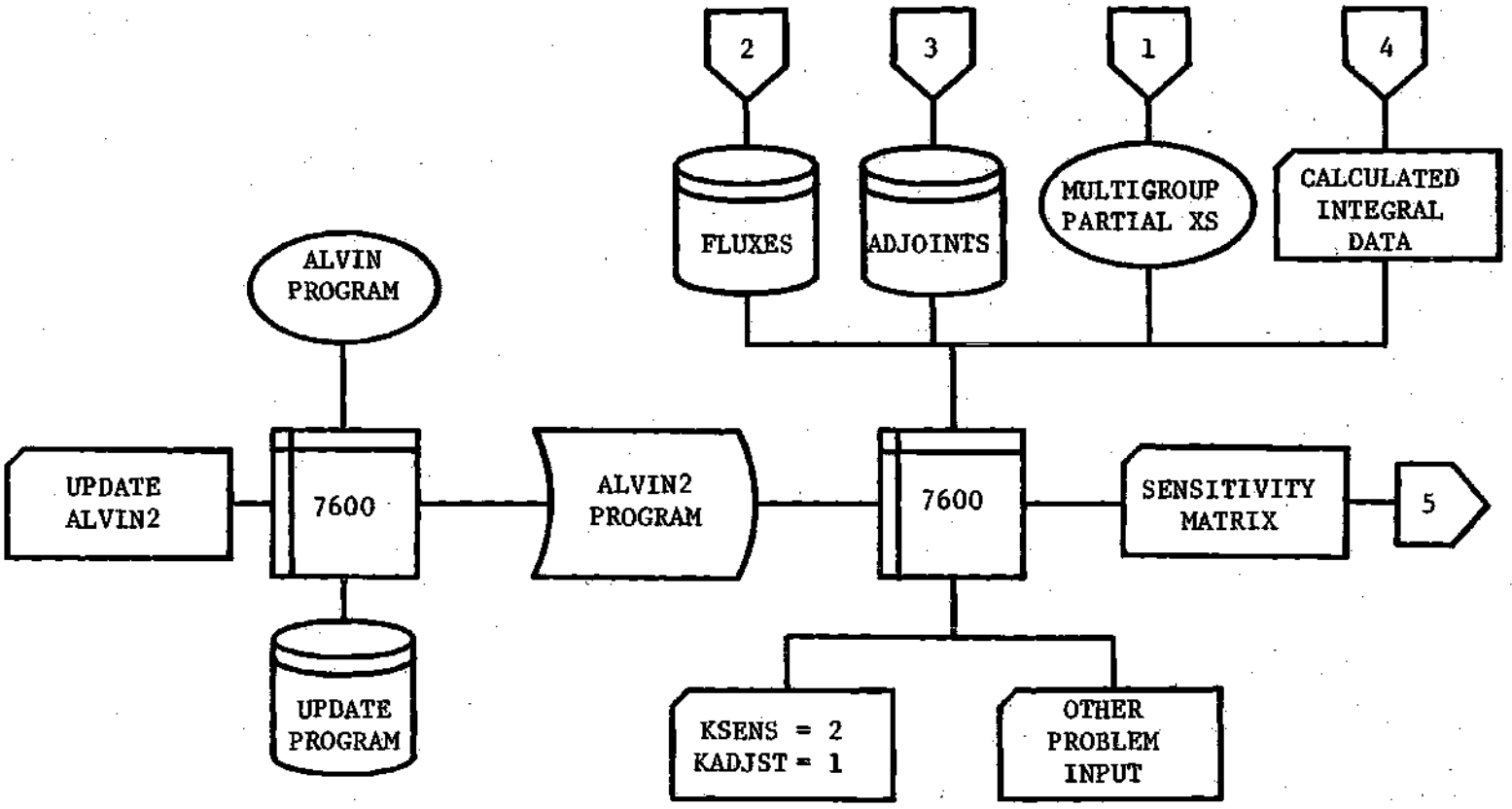

Figure 3. Calculation of Sensitivities.

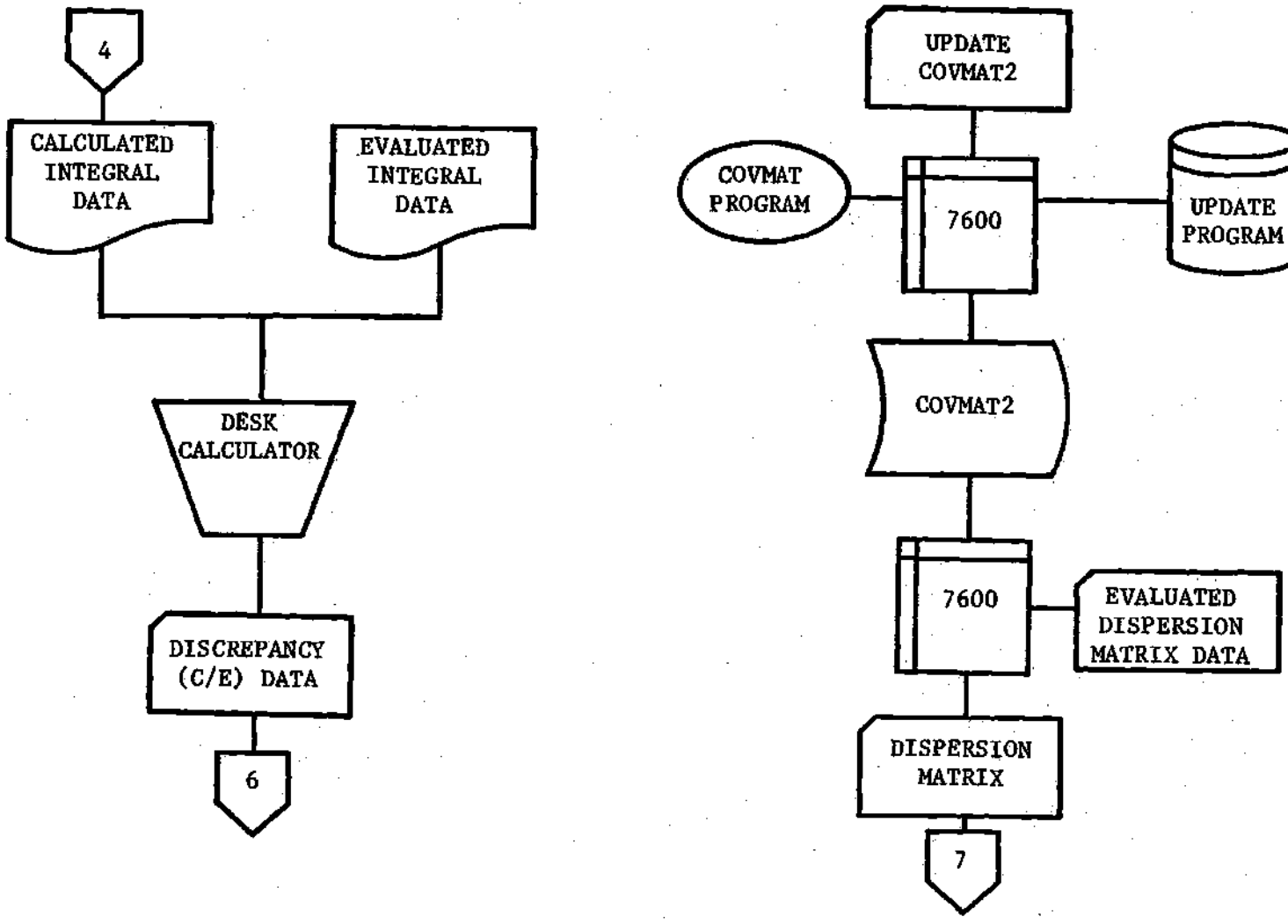

Figure 4. Discrepancy Vector and Dispersion Matrix.

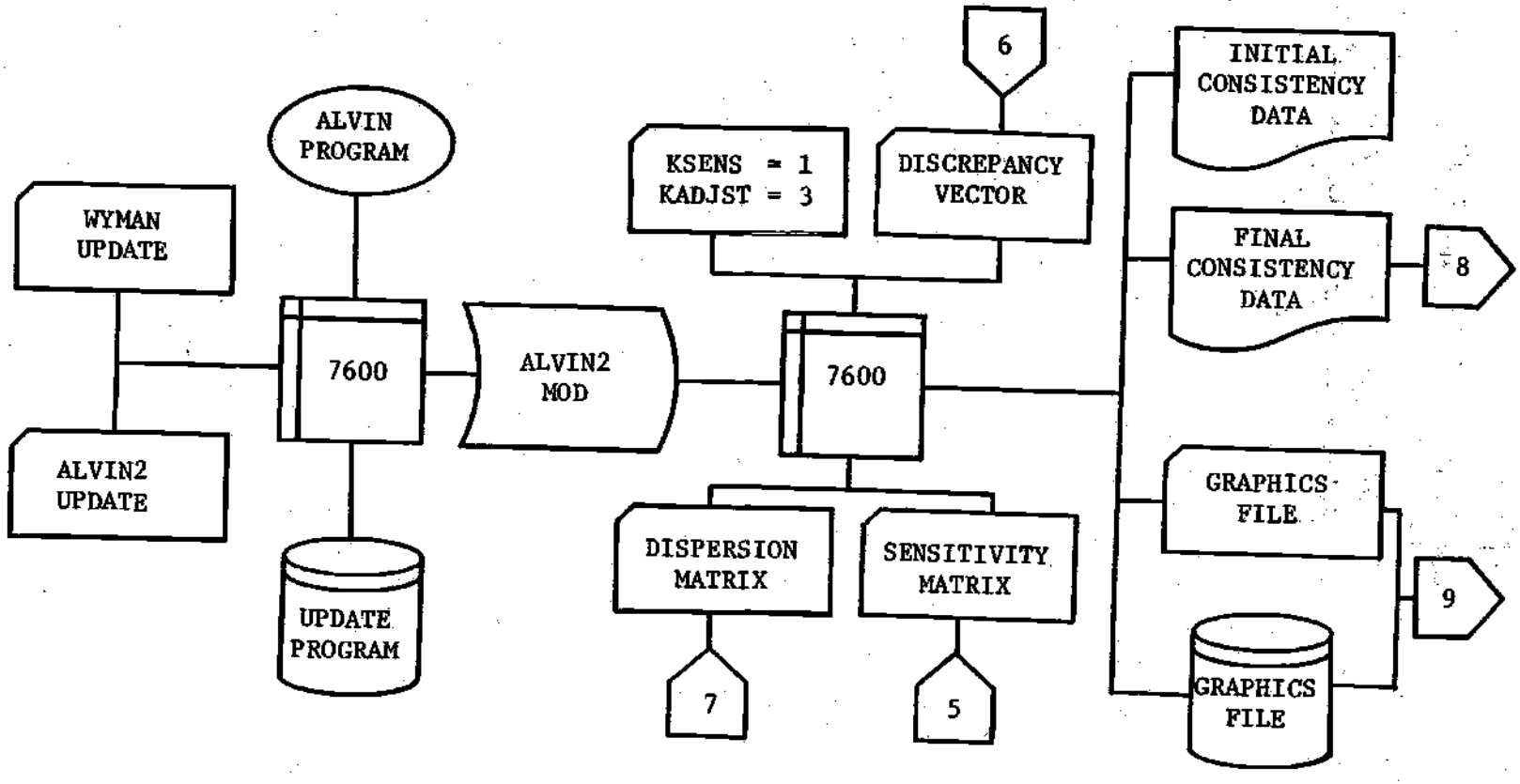

Figure 5. Consistency Calculation.

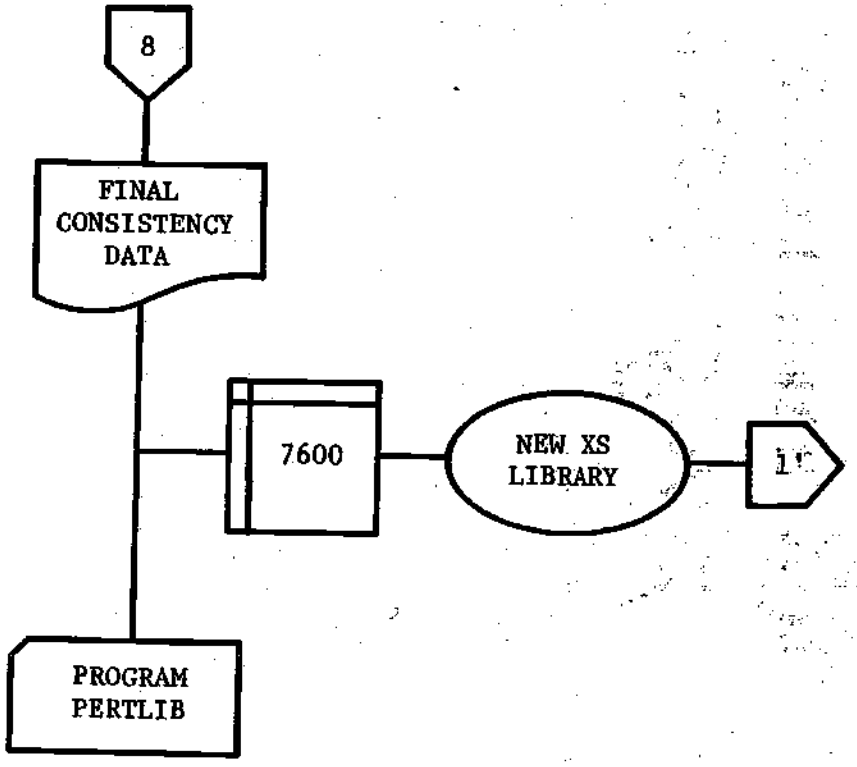

Figure 6. Generation of New Multigroup Cross Section Library.

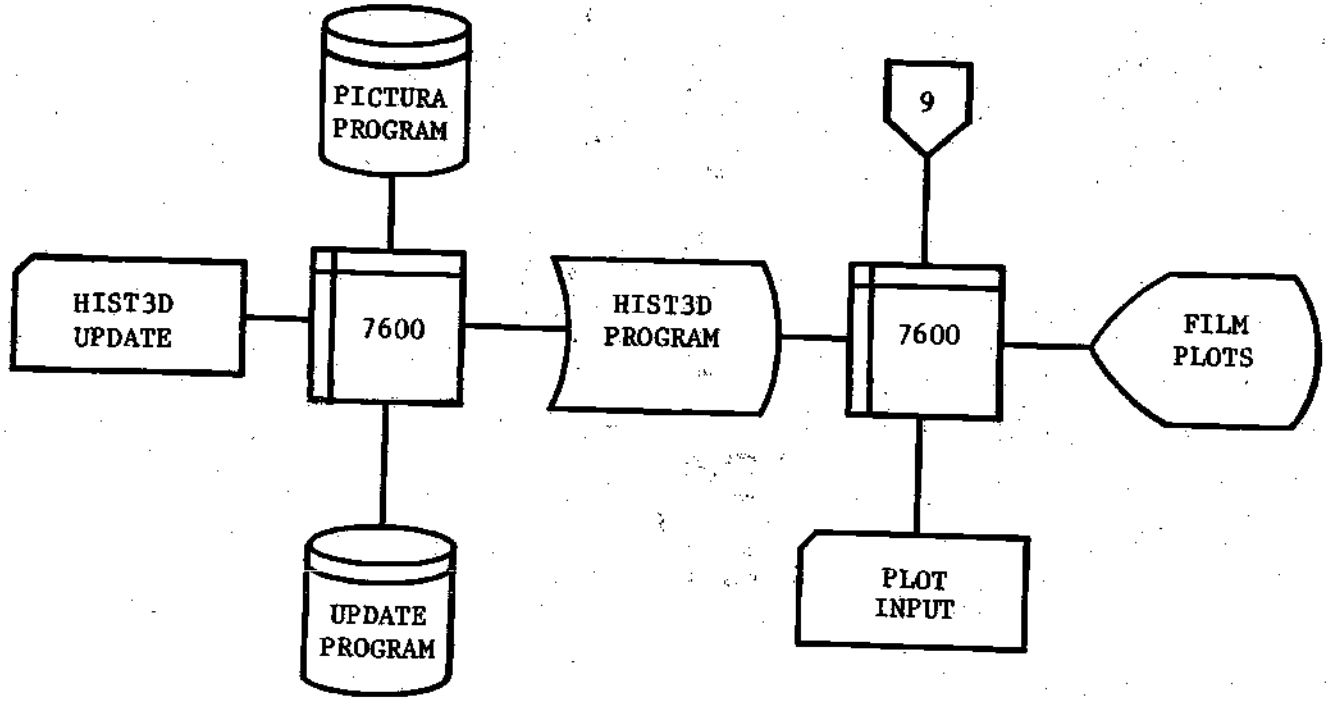

Figure 7. Three Dimensional Graphics System.

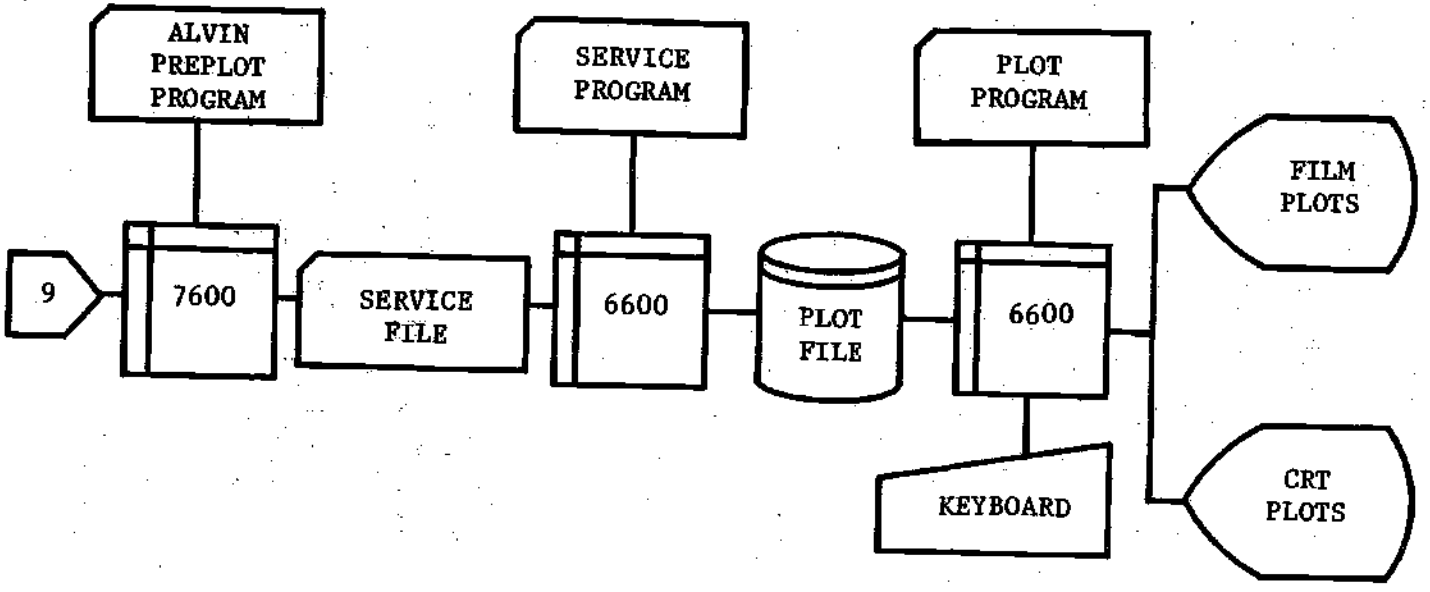

Figure 8. Two Dimensional Graphics System.

Table 1. Glossary of Computer Programs Used in Present Work.

Program or Program Modification	Modification of Program	Description
ALVIN		See Reference 13, Chapter III.
ALVIN2	ALVIN	Certain improvements incorporated (see Chapter III).
ADMACS	DTF-IV	Adjoint source written as interface file from forward transport calculation mixture table.
CBYE		Calculates χ^2/DF with effect of statistical uncertainty in Monte Carlo transport considered. (Written in collaboration with D.W. Muir, 1976.)
COVMAT		See Reference 28, Chapter IV.
COVMAT2	COVMAT	Adds capability to build up dispersion matrix from several component matrices.
DTF-IV		See Reference 18, Chapter IV.
DTF/ALVIN	DTF-IV	Writes flux data from DTF to interface file for use with ALVIN. (W.B. Wilson, Private Communication, 1975.)
DYDXAD		Service code to build sensitivity matrix from component matrices of individual partial reactions.
DYDXCOM		Service code to compound sensitivity matrix (total cross section constant) from complementary sensitivity matrices (total cross section variable).
EVALCOV		Test code to evaluate cross section dispersion matrices by method of Perey et al. Similar to SUR (Reference 29, Chapter IV).
GAMDTF4/7600	GAMDTF4	Revision of GAMDTF4 to permit operation on CDC7600 CROS operating system. (Written in collaboration with D.W. Muir, 1975)

Program or Program Modification	Modification of Program	Description
HIST3D	PICTURA	Adds simplified input to plot three-dimensional histograms.
MCNG		See Reference 19, Chapter IV.
MIXCX		Service code to mix cross sections when all cross sections cannot be stored by DTF.
NJOY		See Reference 17, Chapter IV.
PERTLIB		Perturbs given cross sections in a reference cross section library.
PICTURA	PICTURE	Performs three-dimensional plots (M. Prueitt, LASL, Private Communication, 1977). For PICTURE, see M. Prueitt, Computer Graphics, Dover Publications, Incorporated, New York (1975).
PLOT	DISSPLA	Interactive version of proprietary graphics program (J. George, Private Communication, 1976).
POSTMCN		Processes MCN output (TALFILE) into Livermore pulsed sphere spectra and creates graphics interface file.
PREPLOT		Processes ALVIN graphics interface file for input to PLOT.
QDTFEE		Processes DTF output into Livermore pulsed sphere spectrum and creates graphics interface file.
SOURCE		MCN subroutine simulating Livermore D-T source distribution. (LASL Group TD-6, Private Communication, 1976.)
TALFILE	MCN	Creates interface file from MCN to POSTMCN.
TOFFEE		Processes Livermore pulsed sphere experimental time-of-flight data for fine-mesh and coarse-mesh energy spectra with corresponding dispersion matrices.
UPDATE		Proprietary program (CDC) for on-line program editing.

Program or Program Modification	Modification of Program	Description
WYMAN	ALVIN2	Adds certain features to ALVIN2 unique to Wyman experiment analysis.
XEDIT		LASL program for interactive file editing.

APPENDIX II

Method of Estimating Response Function Variance Due to Source Anisotropy

This appendix develops approximate expressions for the variance in the response function as a function of depth in the neutron transport medium due to the combined effects of the angle-variation in the source number yield and in the source energy.

Recall that for elastic scattering the maximum energy loss of the incident particle may be computed from the energy of the backward-reflected particle as follows:

$$\frac{E_{180°}}{E_{0°}} = \left(\frac{A-1}{A+1}\right)^2 \quad , \tag{1}$$

where all energies are measured in the laboratory system. Let the incident particle, at the mid-point energy of energy group one, suffer maximum energy loss and fall into energy group G.

It is assumed for the rough purposes of the present calculation that the fraction F_1 of tritium production due to uncollided flux (essentially all of the group one flux) at the sample location reflects the yield variation 100%, the fraction F_{2-G} of tritium production due to collided flux from group two to group G reflects the yield variation by 50%, and the remaining fraction does not reflect the yield factor at all. The factors F_1 and F_{2-G} may be determined by combination of the previously

calculated group scalar fluxes and the known tritium production group cross sections. When this is done, one obtains an estimate of the variation T_{aniso}/T_{iso} in tritium production for a given sample location in terms of the variation in neutron number yield at the source Y_{aniso}/Y_{iso}:

$$\frac{T_{aniso}}{T_{iso}} = 1 + F_y \left(\frac{Y_{aniso}}{Y_{iso}} - 1 \right), \tag{2}$$

where

$$F_y \equiv F_1 + 0.5\, F_{2\text{-}G}. \tag{3}$$

The variation in tritium production due to the variation in source energy is estimated by a similar argument, with the result:

$$\frac{T_{aniso}}{T_{iso}} = 1 + F_E \left(\frac{E_{aniso}}{E_{iso}} - 1 \right), \tag{4}$$

where

$$F_E = F_1 D_1 + 0.5 \sum_{g=2}^{G} F_g D_g, \tag{5}$$

and where D_g is the dimensionless derivative of the sample tritium production cross section at group mid-point energy E_g:

$$D_g = \frac{d\Sigma}{\Sigma_g} \Big/ \frac{dE}{E_g}. \tag{6}$$

The combined effects of yield variance and energy variance are then obtained by using the law of propagation of errors on Equations 2 and 4, to give:

$$\mathrm{var}\left(\frac{T_{aniso}}{T_{iso}}\right) = F_y^2 \,\mathrm{var}\,\frac{Y_{aniso}}{Y_{iso}} +$$

$$2F_y F_E \,\mathrm{cov}\left(\frac{Y_{aniso}}{Y_{iso}}, \frac{E_{aniso}}{E_{iso}}\right) \cdot \qquad (7)$$

$$+ F_E^2 \;\mathrm{var}\;\frac{E_{aniso}}{E_{iso}} \cdot$$

It remains to evaluate the variances and covariances of Y_{aniso}/Y_{iso} and E_{aniso}/E_{iso}, based on the previously mentioned published and unpublished data. These quantities are estimated for both the 0°-135° pairs and the 90° samples and with regard to both D-T kinematic effects (including target slowing down) and neutron target interaction effects. For the 0°-135° pairs, the azimuthal energy and yield variances are roughly 5% each due to D-T kinematics. These variances are fully correlated: a higher yield implies a higher energy and conversely. In regard to neutron target interaction effects, the spread in yield is some 5%. The energy spread is believed to be small and is here ignored. For the 90° samples, the uncertainty in yield and energy due to D-T kinematic effects is estimated to be only 1% due to approximate cancellation of the azimuthal asymmetries. The uncertainty due to neutron target interaction effects is similar to that for the 0°-135° samples. Finally, the effects of kinematics and the effects of neutron interaction effects in the target are assumed to combine as if they were uncorrelated.

The tritium production variances due to source anisotropy, as finally estimated from Equation 7 from the previously calculated group fluxes and cross sections, and from the available source anisotropy data are as follows:

^{n}Li		^{7}Li	
cm	relative variance	cm	relative variance
7.5	.0013	7.5	.0013
9.6	.0011	10.0	.0011
15.0	.0008	12.5	.0009
20.0	.0006	17.5	.0007
22.5	.0006	25.0	.0005
25.0	.0005		

The above values are not correlated between samples.

APPENDIX III

VALIDATION OF SENSITIVITY CALCULATIONS

To validate the SENSI and PROFIL subroutine coding and to determine the correctness of the sensitivity calculation input data (general problem specification, forward fluxes and adjoints, and cross section tables) the program PERTLIB was developed to perturb a given partial group cross section vector for a given nuclide. PERTLIB operates on the DTF format tables of the 100 group cross section library used in the transport calculation. The transport results obtained with the perturbed library and the results obtained from the unperturbed, or reference, library yield a direct sensitivity which may be compared with the results of the first-order perturbation theory sensitivity. PERTLIB assumes a fixed secondary neutron spectrum shape. The user may alter the cross sections in such a manner as to maintain the total cross section constant, and he may resolve the transport and detector contribution. Finally, all energy groups may be simultaneously altered, each by a different amount, in accordance with the results of a data consistency analysis or data adjustment, in order to determine the effect of the cross section adjustments on an arbitrary response function or even to determine the effect of the adjustment on a different neutronic assembly. But here interest is centered on the validation

of sensitivity calculations.

Table 1 shows a selected comparison of sensitivities for variable total cross section in the uppermost energy group of the $^{7}Li(n,xt)$ reaction. All calculations used S_8 quadrature and P_3 cross section anisotropy. ALVIN2 used Legendre components of flux expanded to order P_3. PERTLIB used a 10% change in the group cross sections. For smaller changes differencing anomalies appear, and for much larger changes non-linear effects appear. From Table 1 it is apparent that excellent agreement exists near the center of the sphere. Good agreement is found at the periphery. The sensitivities at the periphery are more accurately calculated by ALVIN2 since the direct calculations are increasingly distorted by the differencing of increasingly small quantities which are subject to the effects of numerical approximation error.

Similar results were obtained in a validation of the $^{6}Li(n,t)$ sensitivity matrix.

Table 1. Validation of Sensitivity Calculations. $^{7}Li(n,xt)$ Reaction, Total Cross Section Variable.

Sample	Perturbation	Direct
^{n}Li 7.5 cm	3.7 E-1	3.6 E-1
^{n}Li 15.0 cm	1.4 E-1	1.3 E-1
^{n}Li 25.0 cm	4.4 E-2	3.8 E-2
^{7}Li 7.5 cm	5.4 E-1	5.3 E-1
^{7}Li 12.5 cm	3.4 E-1	3.2 E-1
^{7}Li 25.0 cm	4.1 E-2	3.0 E-2

APPENDIX IV

LEAKAGE SPECTRA FROM PULSED SPHERES

Comparisons of calculated and measured leakage spectra[1] from 14 MeV neutron-driven spheres of C, O, Al, Fe, and ^{238}U recently have been interpreted by Wong et al within the context of fusion reactor blanket design requirements.[2,3] However, these calculation-experiment comparisons have not as yet been treated from the point of view of quantitative consistency analysis. Since the experimental technique and quantitative results of these pulsed sphere experiments continue to be of interest, it was deemed to be both timely and useful to extend the methods of consistency analysis developed in the main text to the pulsed sphere experiments. The pulsed sphere computational procedure, numerical results, discussion of results, and conclusion and recommendations are given here.

Computational Procedure

The ^{7}Li (0.5 mfp, 1.0 mfp, 1.6 mfp radius) neutron leakage energy spectra data were integrated over several broad energy bands, namely 15-10, 10-5, and 5-2 MeV. The view angle of the leakage neutron detector in each case was 30°. Because the steel corrosion encapsulation was not present in the sphere-out, or blank, runs the published

problem specification[4] modified to include the encapsulation. Preliminary calculations demonstrated that omission of the encapsulation leads to +2%, -3%, and -8% change in leakage fluence, integrated over the energy bands 15-10, 10-5, and 5-2 MeV, respectively, compared to the case with encapsulation included.

Consistency of the Data Before Adjustment

The present section treats the calculation of energy spectra and the evaluation of experimental energy spectra. The construction of the respective dispersion matrices is outlined and the combination of data to form the dimensionless input quantities is reviewed.

Calculation of Spectra. Examined here are the evaluated differential data, the processing of cross section data, and the neutron transport calculation. In these calculations the target structure, surrounding air, and collimator/detector are not modelled.

The evaluated differential data for the principal transport nuclide, ^{7}Li with trace amounts of ^{6}Li, as well as the data for the stainless steel, Fe, Cr, Ni, Mn, and Si, were taken from ENDF/B-IV. As discussed in the main text, the ^{7}Li secondary neutron energy and angle spectra in ENDF/B-III and -IV are not fully satisfactory for 14 MeV transport calculations of high accuracy.

For the multigroup discrete ordinates calculations performed herein, NJOY processed the ENDF/B-IV data into a 100 group library with the GAM-II energy grid, with flat flux weighting, with infinite dilution

at 0°C, and to six Legendre orders. To accommodate these cross sections within the nominal DTF-IV cross section storage block, the constituents of the stainless steel were pre-mixed by a specially developed auxiliary code. The Monte Carlo calculations used continuous-energy cross sections prepared by R.J. LaBauve and D. George in a pointwise representation.[6]

Both discrete ordinates and Monte Carlo methods were used to calculate leakage spectra. For the discrete ordinates calculations a one-dimensional problem specification was obtained by transforming the experimental quasi-sphere into a system of concentric spherical shells in which the volumes and densities were adjusted to preserve the masses and the average radial positions of the original components. The spatial mesh interval was 0.5 cm, well below characteristic interaction lengths, and the order of angular quadrature was sixteen. Execution time on the LASL CDC 7600 was approximately two minutes. DTF output fluences, generated in the GAM-II 100-group structure, were renormalized to the convention of Reference 1, i.e., to neutrons (sphere in) per MeV/total neutrons (sphere out). Here the "sphere in" condition refers to the standard run with D-T target and surrounding sphere, and the "sphere out" condition refers to a normalization run with only the D-T target. The fluences were subsequently rebinned into the selected coarse-mesh energy band structure with a code, DTFEE, written specifically for this purpose.

Monte Carlo calculations were performed with the continuous-

energy code MCNG cited previously. The geometry specification included the accelerator tube hole as well as the 30° off-axis detector. A time-dependent, energy-angle- and intensity-angle-correlated neutron source subroutine and a relativistic energy correction, as developed by the LASL Monte Carlo group, were used in the calculations. The neutron spectrum at a point detector 765 cm from the sphere center was binned into 0.2 MeV energy intervals. Approximately 80 000 neutrons were started in each run to give a typical standard deviation of 7-8% in a fluence energy bin. Execution time on the LASL CDC 7600 was fifteen minutes. The fine mesh (0.2 MeV) neutron tally from MCNG was written to a transfer file (TALFILE) and subsequently processed by a specially developed post-processor code, POSTMCN. In the post-processing operation the neutron tally is converted to units of neutrons (sphere in) per MeV/total neutrons (sphere out) and the converted tally is then rebinned into the selected coarse mesh energy band structure. In addition, POSTMCN uses the law of propagation of errors to convert the Monte Carlo statistical errors from the fine mesh structure to the coarse-mesh structure.

Evaluation of Experimental Spectra. Experimental spectra and covariance matrices were derived from the measured time-of-arrival of leakage neutrons with a specially written code, TOFFEE. This code performs several tasks: 1) subtraction of background effects, 2) conversion of TOF data to energy spectra, and 3) integration of fine mesh

energy spectra and dispersion matrices to coarse mesh spectra and dispersion matrices. The processing of TOF data, and of TOF error data, are discussed in turn.

Background corrections of TOF data are of two kinds: 1) time independent and 2) time dependent. The source of the former consists of gamma rays emitted during the slowing down and capture of neutrons. This effect occurs on a time scale which is sufficiently long compared to the 17 MeV-2 MeV pulse that it may be considered constant in time. Its magnitude is determined by integrating the background during a suitable time interval between pulses and dividing by the corresponding time. The source of the time dependent background consists of several effects: 1) neutron scattering in the accelerator target and beam tube, 2) neutron scattering in the air, and 3) neutron scattering in the time-of-arrival detector and in the surrounding detector collimator.

Studies of the published TOF data and of the component of experimental error which is attributable to the uncertainty in the time-independent background correction, as performed in the course of the present work, uncovered a systematic error in the published data. Corrected raw time interval data were supplied by C. Wong,[5] and the appropriate systematic adjustments to the input TOF data and input experimental errors were added to the coding of TOFFEE.

The time dependent effects may be precisely corrected by a Monte Carlo simulation which more or less faithfully models the accelerator

structure, the air, and the collimator and detector structure. Thus, the actual experimental result may be corrected to the result that would have been obtained in an ideal experiment with massless supporting structures. The time dependent background itself for a bare target has been measured and the above components of the time dependent background also have been simulated for a bare target.[1] It is found that the target-assembly effect and the collimator effects alone account adequately for the observed time dependent background. Plechaty and Howerton have argued, however, that for sphere in/sphere out comparisons the time dependent background may often be ignored:

> The experiment consists of recording the ratio of counts with the sphere material in to counts with the sphere material out. With this differencing technique, the effects of the low-mass target assembly, the detector collimator, and the air in the flight path between the target and the detector essentially cancel out, and hence have no significant effect on the experimental data. In particular, with the sphere out, the counting rate from neutrons which are scattered from the target assembly and collimator is three orders of magnitude less than the counting rate from the uncollided neutron beam. Therefore, only the portions of the sphere-in neutron spectrum that have three-order-of-magnitude peak-to-valley changes in the counting rate will be affected. The largest effects are for the strongly-forward-peaked heavy elements - Pb, ^{235}U, ^{238}U, and ^{239}Pu.[4]

Other investigators have found, however, that for iron,[8] as well as for oxygen and nitrogen,[9] it is desirable to take into account the effect of the time independent background. Indeed, examination of the TOF data for spheres of ^{7}Li, especially the 0.5 mfp sphere, show that

peak-to-valley changes by a factor of at least several hundred occur. Consequently, correction for the effects of the time dependent background was considered in the present work.

The use of more exact,simulation corrections can be costly. To effect approximate, empirical corrections, bare source corrections previously have been substituted for sphere-in corrections.[8] In the present work, similar sphere-out corrections were explored. The following cases were analyzed: 1) no correction, 2) constant-in-time correction equal to the average contribution in the tail of the measured sphere-out spectrum, and 3) as in 2), except scaled to the magnitude of the transmitted peak. To the extent that the bare source time dependent background is modified in a complex way by spheres of various sizes, the above schemes provide only an order-of-magnitude estimate of the correction that would result from a precise simulation. These empirical corrections were applied in TOFFEE after adjustment of the time independent corrections but prior to the conversion to energy spectrum data.

Conversion of the input TOF spectrum, G(T), in counts/ns-source neutron, to a fine mesh neutron energy spectrum, F(E), in neutrons/MeV-source neutron, was implemented in TOFFEE with the formula:

$$F(E) * \frac{\eta(E)}{\eta(E_\theta)} = G(T) * \frac{T}{939.6 \times 10^9} \frac{(CT)^2}{R^2}\left[1 - \left(\frac{R}{CT}\right)^2\right]^{3/2}, \quad (1)$$

where $\eta(E)/\eta(E_\theta)$ is the ratio of detector efficiency at the energy bin

mid-point E to the efficiency at the neutron source energy along the detector line-of-sight (θ = 30° here), T is the measured time-of-arrival in ns, C is the velocity of light in units of R per unit T, and R is the flight path length to the detector. Here it is assumed that the neutrons are emitted as if from a point sphere. Monte Carlo comparison simulations confirm to first order the validity of this assumption. The actual energy spectrum value, F(I), is then obtained by dividing the left-hand side of Equation 1 by the average value of $\eta(E)/\eta(E_\theta)$ in the given fine mesh energy interval, I. It is then straightforward to integrate the fine mesh energy spectra, F(I), into coarse mesh spectra, CF(K):

$$CF(K) = \sum_{I \text{ in } K} F(I). \tag{2}$$

To determine the energy spectrum dispersion matrices, TOFFEE first calculates the fine mesh dispersion matrix and then uses the law of propagation of errors to calculate the coarse mesh dispersion matrix. From Equation 1:

$$\frac{\text{var } (F(E)}{[F(E)]^2} = \frac{\text{var } G(T)}{[G(T)]^2} + \frac{\text{var}[\eta(E_\theta)/\eta(E)]}{[\eta(E_\theta)/\eta(E)]^2} \tag{3}$$

The first relative variance on the right hand side is obtained from the corrected variance in the published TOF data[1] and the second relative

variance is taken as the quoted 4% uncertainty in the shape of the detector efficiency curve (quoted upper limit of 7%). The TOF variance, on an absolute scale, in turn may be shown to be of the form:

$$\text{var}\,(C_i,C_j) = C_{ij} + B\,(2 + .01B), \tag{4}$$

where C_{ij} represents the net raw counts per channel and B is the time-independent background.[1] Since the latter is obtained by averaging over a wide time interval and, as calculated, is identical for all narrow time intervals, the dispersion matrix contains a fully correlated off-diagonal component:

$$\text{cov}\,(C_i,C_j) = B(2 + .01B) \tag{5}$$

This off-diagonal component is converted to energy spectrum form exactly as the diagonal component is converted except that the off-diagonal contribution from the detector efficiency curve is zero since only the shape, and not the normalization, is involved in the ratio $n(E_\theta)/n(E)$.

Calculation of the coarse bin dispersion matrix is a straightforward application of the generalized law of propagation of errors. From the simple relation between coarse mesh and fine mesh spectra, Equation 2, it follows that:

$$\text{cov}[CF(K),CF(L)] = \sum_{I \text{ in } K} \sum_{J \text{ in } L} \text{cov}[F(I),F(J)]\ . \tag{6}$$

Construction of Relative Discrepancy Vector and Relative Dispersion Matrix of Integral Data. The form of the dimensionless dispersion matrix element of integral data is, from Equation 2-29:

$$\operatorname{cov}\left(\frac{Y_k - Y_k^\circ}{Y_k^\circ} \ , \ \frac{Y_\ell - Y_\ell^\circ}{Y_\ell^\circ}\right) . \tag{7}$$

If the reference values X_i°, and the integral quantities Y_i° calculated therefrom, are considered as arbitrary normalization constants and not as random variables,as was done in Chapter II, then Equation 2-32 follows:

$$\operatorname{cov}\ (Y_k, Y_\ell) = \frac{\operatorname{cov}\ (Y_k, Y_\ell)}{Y_k^\circ Y_\ell^\circ} \tag{8}$$

The integral data dispersion matrix, as used in the calculation of the initial chi-square, was taken in the tritium production experiment of the main text to be of the form of Equation 2-32, with allowance for the fact that in the ALVIN codes the normalization basis is slightly different (See Chapter III). In the case that Y_k° is obtained by a Monte Carlo calculation, however, the statistical variance in the calculation requires that Y_k° be considered as a random variable and not merely as an arbitrary normalization constant.

When the generalized law of propagation of errors is used to account for the variance in the transport calculation, one readily obtains the following result:

$$\operatorname{cov}\ (Y_k, Y_\ell) = \frac{\operatorname{cov}(Y_k, Y_\ell)}{Y_k^\circ Y_\ell^\circ} \ \frac{Y_k Y_\ell}{Y_k^\circ Y_\ell^\circ} \cdot \frac{\operatorname{cov}(Y_k^\circ, Y_\ell^\circ)}{Y_k^\circ Y_\ell^\circ} \tag{9}$$

A similar expression results for the particular normalization employed

in the ALVIN codes. The initial consistency may then be calculated as before, using on input a generalized dispersion matrix constructed from the POSTMCN and TOFFEE output. For this purpose the auxiliary code CBYE, cited in Appendix I, may be used.

Consistency of the Data After Adjustment

The principal features of the preparation of input data used to determine the consistency of the data after adjustment are the evaluation of cross section error matrices and the calculation of sensitivity matrices. In the present investigation it was apparent from the beginning that the pulsed sphere experiments, particularly in the case of the smaller spheres, where two dimensional effects are more pronounced, might not readily admit of the one dimensional, discrete ordinates sensitivity calculations that were used for the tritium production experiment described in the main text. On the other hand, the evaluation of cross section dispersion matrices, including an extension to secondary-energy and -angle uncertainties, would follow the general procedures set forth earlier. Accordingly, primary interest in the calculational procedure revolves around the method of sensitivity matrix calculation. This feature of the calculational procedure is treated next.

Calculation of Sensitivity Matrices. Effects of Dimensionality. To determine, in a preliminary way, the applicability of one dimensional sensitivity theory and of one dimensional models in general, the ^{7}Li 0.5 mfp sphere was calculated for two cases. Case One: As in the

section "Calculation of Spectra" in this appendix. Here the experiment is more or less faithfully simulated with the exception of the details of the accelerator structure, the ambient air, and the detector and collimator structure. (These effects were taken into account by correction not of calculated but of experimental results.) Case Two: As in Case One, except a) the void previously used to represent the accelerator structure is replaced with solid material of the same density as the rest of the sphere, and b) the disc-shaped anisotropic-in-energy and anisotropic-in-yield neutron source is replaced with a point, isotropic, monoenergetic neutron source. Thus a fictitious, one dimensional Gedankenexperiment is constructed. By comparing the results of the two dimensional and one dimensional cases, using Monte Carlo simulation, the general significance of the two dimensional features of the sphere is assessed, using the 0.5 mfp sphere as a worst case. As discussed in the section just below, the evidence for strong two dimensional effects was sufficiently persuasive as to discourage the casual use of one dimensional sensitivity models for the ^{7}Li pulsed-sphere experiments considered as a set.

Numerical Results

In this section are presented preliminary results which treat the consistency of the pulsed sphere data prior to and after adjustment.

Consistency of the Data Prior to Adjustment

Figure 1 presents fine mesh calculated (DTF, MCNG) and experimental energy spectra for the ^{7}Li 0.5 mfp 30° sphere, as normalized to the standard LLL format. Vertical bars of the experimental spectrum are standard deviations centered about the means. The experimental curve in Figure 1 was generated with no time dependent background correction.

Experimental leakage spectra in coarse mesh structure with Monte Carlo C/E ratios are shown in Table 1 for 0.5 mfp, 1.0 mfp, and 1.6 mfp ^{7}Li 30° spheres as a function of the particular time dependent background subtraction which was applied to the experimental TOF spectra. As indicated previously, the fixed correction is a subtraction of the average value of the time dependent background as measured for the sphere-out or bare target condition, namely $1.0 * 10^{-4}$ counts/ns. The scaled correction scales down the above subtraction by the ratio of the measured peak (determined on a per channel basis) for the sphere-in condition to the measured peak for the sphere-out condition. Also shown in Table 1 is the initial chi-square per degree of freedom for each case, where a 4% value for the uncertainty in the shape of the detector efficiency curve is used.

Consistency of the Data After Adjustment

As discussed previously, primary attention in this appendix is focused on the suitability of one dimensional sensitivity theory for the

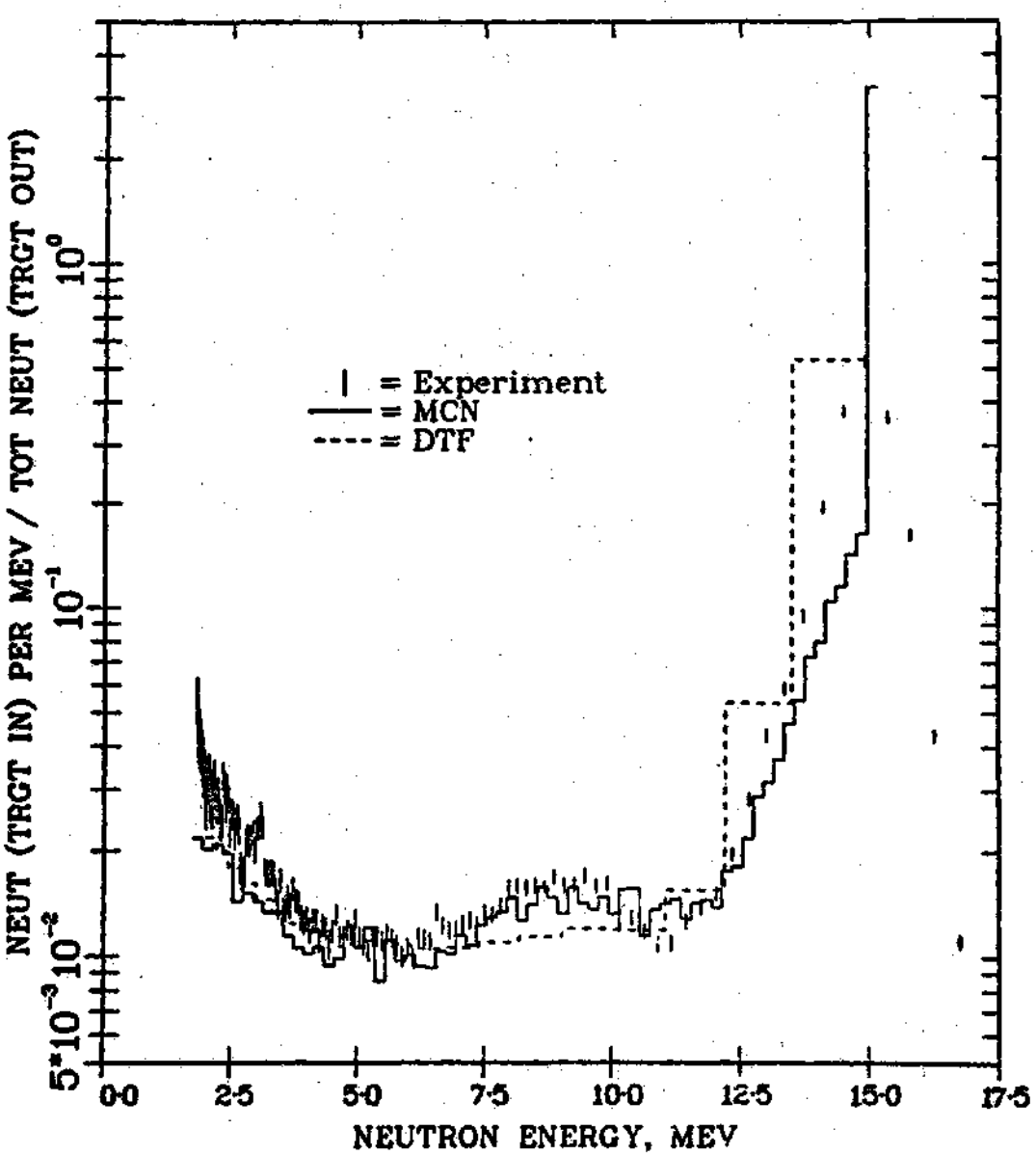

Figure 1. Comparison of Monte Carlo and Sn Calculations with 0.5 mfp ^{7}Li Pulsed Sphere Experiment. Fine Mesh. No Correction for Time-Dependent Background.

Table 1. Calculated vs. Experimental Leakage Spectra for ^{7}Li Spheres at 30°.

Time-dependent background subtraction		None			Fixed			Scaled to Elastic Peak		
Radius (mfp)	Energy Band (MeV)	E	C/E	χ^2/DF	E	C/E	χ^2/DF	E	C/E	χ^2/DF
0.5	17-10	.826	1.04	13.1	.821	1.05	2.7	.860	1.04	4.5
	10- 5	.069	.90		.063	.98		.062	.94	
	5- 2	.053	.75		.039	1.03		.040	.88	
1.0	17-10	.690	1.02	10.4	.686	1.03	.92	.688	1.02	4.0
	10- 5	.101	.94		.095	1.00		.099	.97	
	5- 2	.090	.84		.077	1.00		.084	.90	
1.6	17-10	.538	1.01	3.0	.530	1.02	2.6	.533	1.02	1.5
	10- 5	.111	.96		.105	1.01		.110	.97	
	5- 2	.100	.94		.088	1.08		.098	.97	

calculation of sensitivity matrices. Table 2 presents the results of the ^{7}Li 0.5 mfp 30° one dimensional vs. two dimensional calculational comparison.

Discussion of Results

This section analyzes the consistency of the pulsed sphere data before adjustment in the light of the various time-dependent background corrections. The reduced chi-square statistic is used as an index of the overall consistency. The consistency after adjustment is dependent on the treatment of two dimensional effects in the sensitivity calculation. Here the results of one dimensional and two dimensional calculation comparisons are discussed.

Consistency Before Adjustment

The large values of the reduced chi-square for the smaller spheres are seen to be rectified to a considerable extent by the application of empirical time dependent background corrections to the experimental spectra. Note that, for all cases, agreement in the high energy region, 17-10 MeV, is relatively good. Independent calculations[9,10] show that the time dependent background attributable to the scattering of neutrons by the real accelerator structure is effective predominantly below 10 MeV, while the collimator and detector structure effects operate predominantly in the region 10-12 MeV. In view of the relatively good agreement at 17-10 MeV compared to 10-5 MeV, and especially 5-2 MeV, it appears that, insofar as the time dependent background is concerned,

Table 2. Dimensionality Effect for ^{7}Li 0.5 mfp 30° Sphere

Energy Band (MeV)	M.C. 1D / M.C. 2D
17-10	1.02
10-5	0.87
5-2	0.79

the component induced by the accelerator structure, in particular, should be taken into account. Note that the agreement is best for the larger spheres, as would be expected when the accelerator structure mass becomes a smaller fraction of the total mass.

Because the background induced by the accelerator structure for a bare source is modified in a complex way by the presence of the sphere material, it is apparent that such bare-source derived corrections will be a compromise at best. This hypothesis is confirmed by the pattern of change for the Fixed and Scaled to Elastic Peak cases. While the Fixed correction improves the consistency in every case, it is apparent that the subtraction overcorrects the discrepancy, especially for the largest sphere. The Scaled to Elastic Peak correction, on the other hand, gives a more satisfactory pattern of improvement. Since the magnitude of the elastic peak diminishes with increase of sphere radius and, hence, also diminishes roughly as the fraction of scattering material represented by the accelerator structure, it is reasonable that such a correction would give better results than the Fixed correction. Even for this case, however, the variation of chi-square with radius is somewhat uneven. For quantitative work some time dependent correction must be used even for the ^{7}Li spheres, and for purposes of cross section consistency analysis, the more costly but more accurate simulation method of correction should be used.

Consistency After Adjustment

The results of the simple one dimensional and two dimensional Monte Carlo comparison for the ^{7}Li 0.5 mfp 30° sphere, Table 2, indicate only a slight dimensionality effect in the 17-10 MeV leakage fluence band. But, since small relative changes in the dominant peak imply larger relative changes in the valley, rather pronounced effects exist below 10 MeV. Note that if the density of the true sphere had been adjusted downwards to reflect the average density in the sphere with the accelerator penetration, then the discrepancies would have been even larger. Since the dimensionality effects are at least comparable to C/E ratios (uncorrected time dependent background) or are even larger (corrected time dependent background), it is apparent that a straightforward one dimensional analysis is inadequate for cross-section consistency analysis purposes. Progressively smaller — but still significant — effects may be expected for the larger spheres.

In the light of the inadequacy of a straightforward one dimensional approach, three avenues may be explored:

1. Use one dimensional sensitivity analysis, where:
    a. the sensitivity matrix is an admitted approximation, and
    b. the two dimensional experimental spectra are corrected to spectra that would have been obtained in a perfect one dimensional experiment, by use of simulation calculations.

2. Use two dimensional sensitivity analysis.

Within the one dimensional framework, course 1a is rather questionable. There is no strong reason to believe that an increase in, say, the P_1 component of a given scattering reaction will affect the 30° leakage fluence in a sphere with an accelerator penetration in the same way as in a true sphere. To show the contrary, at least in a systematic way, would be tantamount to a one dimensional vs. two dimensional sensitivity comparison. Course 1b suffers from a similar fault: in order to correct two dimensional experiments to one dimensional experiments, using such calculated factors as are given in Table 2, it must be shown that the variation of the geometry factor with cross section is itself small over the range of cross-section adjustment which is contemplated. In a systematic framework, this is again tantamount to a two dimensional sensitivity analysis. Thus it would appear that the significant dimensionality effects that are found here, particularly for the smaller spheres, merit serious consideration of course 2 from the outset, namely, implementation of the more elaborate apparatus of two dimensional sensitivity analysis.

Conclusions and Recommendations

1) For purposes of quantitative, cross-section consistency analysis, the time dependent background effect observed in the ^{7}Li pulsed sphere experiments is significant and should be taken into account, preferably by simulation of the accelerator target structure, the collimator

structure and detector structure.

2) For purposes of quantitative, cross section consistency analysis, the two dimensional geometry effect observed in the ^{7}Li pulsed sphere experiments is significant and merits the serious consideration of two dimensional cross section sensitivity methodology.

REFERENCES

1. C. Wong, J.D. Anderson, P. Brown, L.F. Hansen, J.L. Kammerdiener, C. Logan, and B. Pohl, Livermore Pulsed Sphere Program: Program Summary through July 1971, UCRL-51144, Rev. 1, Lawrence Livermore Laboratory (1972).

2. C. Wong, J.D. Anderson, R.C. Haight, L.F. Hansen, and T. Komoto, Nuclear Cross Sections and Technology, Vol. 1, p. 704, NBS Special Publication 425, U.S. National Bureau of Standards (1975).

3. L.F. Hansen, C. Wong, T. Komoto, and J.D. Anderson, Nucl. Sci. Eng., 60, 27 (1976).

4. E.F. Plechaty and R.J. Howerton, Calculational Models for LLL Pulsed Spheres, CSEWG Shielding Benchmark Collection No. SDT 10, UCID-16372, Lawrence Livermore Laboratory (1973).

5. C. Wong, Lawrence Livermore Laboratory, Private Communication (1976).

6. R.J. LaBauve and D. George, in C.I. Baxman and P.G. Young, Applied Nuclear Data Research and Development, April 1-June 30, 1976, LA-6560-PR, Los Alamos Scientific Laboratory (1976).

7. C. Wong, Lawrence Livermore Laboratory, Private Communication (1976).

8. S.N. Cramer, R.W. Roussin, and E.M. Oblow, Monte Carlo Calculations and Sensitivity Studies of the Time-Dependent Neutron Spectra Measured in the LLL Pulsed Sphere Program, ORNL-TM-4072, Oak Ridge National Laboratory (1973).

9. D.R. Harris, D.R. Koenig, and W. Preeg, Proc. Sem. Radiation Transport in Air, Oak Ridge, Tennessee, November 1971, ORNL-RSIC-33, p. 209, Oak Ridge National Laboratory.

10. D.R. Koenig, Los Alamos Scientific Laboratory, Private Communication (1976).

VITA

William Albert Reupke was born January 22, 1940 in Chicago, Illinois. He attended public schools in Chicago and graduated from Wayland Academy, Beaver Dam, Wisconsin, in 1957. Mr. Reupke studied Engineering Science, Physics, and Philosophy at Northwestern University in Evanston, Illinois, where he received a Bachelor of Arts degree in Physics in 1961. While serving as an aerospace physicist in university, government, and industry circles, he obtained, in 1967, a Master of Arts degree, with thesis, in History and Philosophy of Science from Indiana University, Bloomington, Indiana. Mr. Reupke subsequently returned to graduate school, in 1972, after directing control room operations at the Stanford Linear Accelerator Center in Palo Alto, California. In 1973 he obtained the Master of Science degree in Nuclear Engineering at Georgia Institute of Technology and in 1977 he was awarded the Doctor of Philosophy degree in Nuclear Engineering from the Institute.